ROLE OF QUANTITATIVE NEUROIMAGING TECHNIQUES FOR THE MAPPING OF IN VIVO BRAIN CHANGES IN FRONTOTEMPORAL DEMENTIA

SHEELA KUMARI R

PhD THESIS

2016

SREE CHITRA TIRUNAL INSTITUTE FOR MEDICAL SCIENCES AND TECHNOLOGY, TRIVANDRUM

THIRUVANATHAPURAM

ROLE OF QUANTITATIVE NEUROIMAGING TECHNIQUES FOR THE MAPPING OF IN VIVO BRAIN CHANGES IN FRONTOTEMPORAL DEMENTIA

A THESIS PRESENTED BY

SHEELA KUMARI R

TO

SREE CHITRA TIRUNAL INSTITUTE FOR MEDICAL SCIENCES AND TECHNOLOGY, TRIVANDRUM

Thiruvananthapuram

IN PARTIAL FULFILLMENT OF THE REQUIREMENTS FOR THE DEGREE OF

DOCTOR OF PHILOSOPHY

2016

DECLARATION

I, Sheela Kumari R, hereby certify that I had personally carried out the work depicted in the thesis entitled **"Role of Quantitative Neuroimaging Techniques for the Mapping of In vivo Brain changes in Frontotemporal Dementia"**. No part of the thesis has been submitted for the award of any other degree or diploma prior to this date.

Date **Sheela Kumari R**

CERTIFICATE BY THE RESEARCH GUIDE

DR. P.S.MATHURANATH

Additional Professor,

Department of Neurology,

National Institute of Mental Health and Neurosciences (NIMHANS),
Bangalore, India

And

Former Additional Professor,

Department of Neurology,

Sree Chitra Tirunal Institute for Medical Sciences and Technology (SCTIMST),
Thiruvananthapuram.

This is to certify that **Mrs. Sheela Kumari R** in the department of **Neurology** of this Institute has fulfilled the requirements prescribed for the PhD degree of Sree Chitra Tirunal Institute for Medical Sciences and Technology, Thiruvananthapuram. The thesis entitled, **"Role of Quantitative Neuroimaging Techniques for the Mapping of In vivo Brain changes in Frontotemporal Dementia"** was carried out under my direct supervision. No part of the thesis was submitted for the award of any degree or diploma prior to this date. Clearance was obtained from the Institutional Ethics Committee for carrying out the study

CERTIFICATE BY THE RESEARCH CO-GUIDE

Dr. C.KESAVADAS, MD
Professor of Radiology,
Department of Imaging Science and Interventional Radiology,
Sree Chitra Tirunal Institute for Medical Sciences &Technology,
Medical College P.O, Trivandrum,
Kerala, India- 695 011

This is to certify that **Mrs. Sheela Kumari R** in the department of **Neurology** of this Institute has fulfilled the requirements prescribed for the PhD degree of Sree Chitra Tirunal Institute for Medical Sciences and Technology, Trivandrum.

The thesis entitled, **"Role of Quantitative Neuroimaging Techniques for the Mapping of In vivo Brain changes in Frontotemporal Dementia"** was carried out under my direct supervision. No part of the thesis was submitted for the award of any degree or diploma prior to this date.

* Clearance was obtained from the Institutional Ethics Committee for carrying out the study

Signature

The Thesis entitled

ROLE OF QUANTITATIVE NEUROIMAGING TECHNIQUES FOR THE MAPPING OF IN VIVO BRAIN CHANGES IN FRONTOTEMPORAL DEMENTIA

Submitted by

SHEELA KUMARI R

for the degree of

Doctor of Philosophy

of

SREE CHITRA TIRUNAL INSTITUTE

FOR

MEDICAL SCIENCES AND TECHNOLOGY

Thiruvananthapuram

Is evaluated and approved by

Dr. P S Mathuranath **Examiner**
(Guide)

Dr. C Kesavadas
(Co-Guide)

ACKNOWLEDGEMENTS

I would like to begin by thanking my supervisor and mentor, ***Dr. P.S. Mathuranath*** *for his enduring inspiration, guidance, patience and support over the years. I am blessed to have such a person as my supervisor, who is one of the eminent personalities in this field.*

I am also greatful to my co-guide ***Dr. C. Kesavadas*** *for his constant source of encouragement and intellectual academic guidance. I cannot thank him enough for his timely advices and it is my fortune to have him as my co supervisor who sparkle an interest of clinical research for my PhD career.*

I also express my special thanks to Doctoral Advisory Committee members: ***Dr. Asha Kishore*** *(Director) and* ***Dr. Sanjeev V Thomas****, Professor, Department of Neurology for their sacrificed time, valuable comments and suggestions to improve my work.*

It is a great privilege to have an opportunity to carry out my doctoral thesis in the Department of Neurology, SCTIMST, Thiruvananthapuram. I also thankful to the former directors Dr.K. Radhakrishnan and Dr. Jagan Mohan Tharakan for the excellent facilities provided in this institute during the entire thesis work. I extend my deepest gratitude to Dr. Sundar Jaisingh, Deputy Registrar and Dr. A.V. George, Registrar, SCTIMST. Thanks are extended to all staffs of Library and Medical illustration, SCTIMST.

I express my sincere thanks to ***Dr. Bejoy Thomas****, Addditional Professor, department of Imaging Science and Interventional Radiology, SCTIMST, for imparting his expertise in Susceptibility Weighted Imaging and Iron Quantification. Special thanks to* ***Dr. Ramshekhar Menon****, Associate professor, Department of Neurology for his immense support to complete the data collection. I would like to thank Dr. Himanshu Soni, former DM student, Department of neurology, for his helping hands that made me to understand clinical characteristics of patient groups.*

Many special thanks to all the present and past technical staffs and DAMIT students of Dept of IS&IR. In particular, I am greatful to my sister Sheeba, Mahesh, and Alex for their valuable help and support to acquire the imaging data throughout my study. Special thanks to team members from Cognition and Behavioural Neurology Section and Speech therapy, Annamma George, Neelima Ranjith, Lekha , Sunitha, Priyanka, Maneeta, Manju, and Geetha for their support and care.

I am debt to my fellow students, Tinu Varghese, Jija S James, Smitha K.A, Ruma Madhu Sreedharan, Anuvitha Chandran, Subromonian, Mahalekshmi, Mini, Anu Sundar, Rajesh, Arun K.M, Aswathy P.M, Jairani, Reema George, Soumya, Sini, Arya Saraswathi, Shaiju, and Saifudeen, Mahalaxmi Ganjoo for their encouragement, new ideas, emotional support, friend ship and fun.

Additionally, I am thankful to Department of Science and Technology (DST) for granting me the financial assistance. This thesis would not be possible without the cooperation of patients, caregivers and volunteers.

I would like to thank my parents, brother, sisters, in laws, my parents in law, my husband and my son for their endless love and constant support.

Finally, I would like to dedicate this dissertation to my husband Mr. Rajesh G and my son Daksh.

SHEELA KUMARI R

TABLE OF CONTENTS

LIST OF FIGURES

LIST OF TABLES

ABBREVIATIONS

AAL	Automated anatomic labelling
AC	Anterior cingulate
ACE	Addenbrooke's cognitive examination
AD	Alzheimer's disease
ALS	Amyotrophic lateral sclerosis
AMY	Amygdala
ANOVA	Analysis of variance
ARV	Automated regional volumetry
BA	Brodmaan area
BET	Brain extraction tool
CAU	Caudate
CBD	Corticobasal degeneration
CDR	Clinical dementia rating scale
CL	Calcarine
CSF	Cerebrospinal fluid
CT	Computed tomography
DFT	Diffusion fibre tractography
DLDH	Dementia lacking distinctive histopathology
DLPFC	Dorsolateral prefrontal cortex
DN	Dentate nucleus
DTI	Diffusion tensor imaging
EOD	Early onset dementia
EPI	Echoplanar imaging
FA	Fractional anisotropy

FBI	Frontal behavioural inventory
FDR	False discovery rate
FG	fusiform gyrus
fMRI	Functional magnetic resonance imaging
FNIRT	FMRIB's nonlinear registration tool
FRS	Frontotemporal dementia rating scale
FrSBe	Frontal system behavioural scale
FSL	FMRIB's software library
FTD	Frontotemporal dementia
FUS	Fused in sarcoma
fvFTD	Frontal variant FTD
FWE	Family-wise error
FWHM	Full width half maximum
FWM	Frontal white matter
GDB	Goal directed behaviour
GLM	General linear model
GM	Grey matter
HP	Hippocampus
IEC	Institutional ethics committee
IFG	Inferior frontal gyrus
IFOF	Inferior fronto-occipital fasciculus
IFOperG	Inferior frontal opercular gyrus
IFTriG	Inferior frontal triangular gyrus
ILF	Inferior longitudinal fasciculus
IN	Insula
IOFG	Inferior orbitofrontal gyrus
MAPT	Microtubule-associated protein tau
MC	Middle cingulate

MD	Mean diffusivity
MFG	Middle frontal gyrus
MMSE	Mini mental state examination
MND	Motor neuron disease
MNI	Montreal neurological institute
MOFG	Middle orbitofrontal gyrus
MRI	Magnetic resonance imaging
MRS	Magnetic resonance spectroscopy
MTP	Middle temporal pole
NPI	Neuropsychiatric inventory
OC	Olfactory cortex
OFC	Orbitofrontal cortex
PBMC	Precentral gyrus anterior to central sulcus
PC	Posterior cingulate
PD	Parkinson’s disease
PET	Positron emission tomography
PHP	Parahippocampus
PNFA	Progressive nonfluent aphasia
PPA	Primary progressive aphasia
PSP	Progressive supra nuclear palsy
PUT	Putamine
RECG	Gyrus rectus
RN	Red nucleus
ROI	Region of Interest
RoperG	Rolandic operculum
SD	Semantic dementia
SFG	Superior frontal gyrus
SLF	Superior longitudinal fasciculus

SMA	Supplementary motor area
SMedOFG	Superior medial orbito frontal Gyrus
SN	Substantia nigra
SPECT	Single photon emission tomography
SPM	Statistical parametric mapping
STG	Superior temporal gyrus
SWI	Susceptibilty weighted imaging
TBI	Traumatic brain injury
TBSS	Tract based spatial statistics
TE	Time of echo
TFCE	Threshold free cluster enhancement
TH	Thalamus
TIV	Total intracranial volume
TR	Time of repetition
UF	Uncinate fasciculus
VaD	Vascular dementia
VBM	Voxel based morphometry
VMFC	Ventromedial prefrontal cortex
WCST	Wisconsin card sorting test
WM	White matter

SYNOPSIS

Frontotemporal Dementia (FTD) or Pick's disease is the second most common cause of dementia after Alzheimer's disease (AD). Three main syndromic variants of FTD are frontal or behavioural variant FTD (fvFTD), progressive nonfluent aphasia (PNFA), and semantic dementia (SD). Among these, fvFTD is the commonest with profound changes in personality and behaviour and the other two conditions constitute the primary progressive aphasia (PPA) syndromes with language and speech difficulties. The paucity of obvious symptoms and psychiatric symptomatology in the initial stages may hinder the early and differential diagnosis of FTD from psychiatric problem, AD, Parkinson's disease (PD) or Vascular dementia (VaD).

Till now, post-mortem via autopsy of the brain is considered as the gold standard for the definite diagnosis of FTD. In recent years, role of neuroimaging has expanded and has opened up a new window into the living human brain. These innovations allowing us for the first time to identify distinct patterns of regional cortical atrophy in FTD patients during life and may facilitate early diagnosis before the onset of behavioural problems. Since there are no treatments to slow or stop the progression of this dread demending disease, the knowledge gathered from the research will result in a growing number of potential therapeautics in the near future.

Structural Magnetic resonance imaging (MRI) and Diffusion Tensor imaging (DTI) are the widely available candidate biomarkers for the detection of cerebral grey

matter (GM) and associated white matter (WM) degeneration underlying in FTD pathology. Despite marked behavioural changes, in the early course of disease, MRI in fvFTD appears normal on visual inspection. Quantitative MRI, such as automated region of interest (ROI) based volumetry and voxel based morphometry (VBM) have refined these observations and can relate the pattern of GM atrophy with neurocognitive and behavioural profiles examined within minutes of imaging study. Inaddition, tract specific diffusion measurement is a promising tool for the quantitation of damage to specific neuronal pathway which seems to correlate with corresponding GM atrophy. Furthermore, the dysregulation of iron metabolism detected by susceptibility weighted imaging (SWI) is considered as a sensitive marker for the diagnosis and staging of neurodegenerative disorders.

To date, no such study has investigated the combined assessment of patterns of grey and white matter damage and the abnormal cortical iron deposition in the subtypes of FTD using MRI, DTI and SWI respectively. Thus we hypothesized that *quantification of grey and white matter degeneration along with abnormal iron deposition can differentiate subtypes of FTD and can help in understanding the behavioural correlates*. Thus the aim of the study was to analyse the GM degeneration, WM integrity and abnormal iron deposition in patients with fvFTD and PPA by means of VBM, DTI and SWI and its associations with behavioural profiles.

Forty six patients with FTD (34 fvFTD, 12 PPA including 8 SD and 4 PNFA) and 34 healthy normal volunteers with no history of alcoholism, neurological, psychiatric or systemic diseases were included in the study. All the subjects underwent extensive historical, neurologic and neuropsychological examination, followed by MRI of brain. Participants were assessed on the Frontal System Behavioural scale (FrSBe) as a measure of behavioural abnormalities. In addition, tests of global cognitive ability (Mini Mental State Examination (MMSE), Addenbrooke's Cognitive Examination (ACE) and Clinical Dementia Rating Scale (CDR)), executive function (Trail Making test and Digits span test), language (Confronation naming, Phonemic and Semantic fluency) were administered.

The imaging data were obtained from a 1.5 Tesla Scanner (Avanto SQ engine, Siemens, Erlangen, Germany) equipped with a standard quadrature head coil. Anatomical scans acquired with T1-weighted 3D spoiled gradient echo sequence were used for VBM analysis. DTI data were obtained using single-shot spin-echo echo planar sequence in 30 diffusion encoding directions. In addition, SWI images were obtained with a 3D spoiled gradient recalled echo sequence. The study was performed after taking written informed consent, which was approved by the Institutional Ethics Committee (IEC).

The regional and whole brain GM loss (orbito basal cortex, dorsolateral prefrontal areas, medial prefrontal areas, basal ganglia and temporal neocortex) in patients was

explored using VBM and Statistical Parametric Mapping (SPM- Wellcome Trust Department of Cognitive Neurology, London, UK, www.fil.ion.ucl.ac.uk/spm/) software. The DTI data were analyzed by whole brain Tract Based Spatial Statistics (TBSS) (http://www.fmrib. Ox.ac.uk/fsl/) software and the corresponding Fractional Anisotropy (FA) and Mean Diffusivity (MD) values were derived by generating the masks of uncinate fasciculus (UF), inferior longitudinal fasciculus (ILF), superior longitudinal fasciculus (SLF), cingulum, genu and splenium of corpous callosum (CC). Finally, the quantitative analysis of regional iron deposition in the superior frontal gyrus (SFG) medial to superior frontal sulcus, precentral gyrus just anterior to central sulcus (PBMC), anterior part of superior temporal gyrus (STG), insula (IN), basal ganglia regions, substantia nigra (SN), red nucleus (RN), frontal WM (FWM), anterior cingulate (AC), hippocampus (HP) and dentate nucleus (DN) in both hemispheres was performed by Signal Processing in NMR (SPIN, MRI Institute for Biomedical Research Detroit, MI, USA) software. The statistical analysis of this entire study was performed using SPSS software.

Demographic, Clinical, Neuropsychological and Behavioural Assessment: The patients with fvFTD and PPA did not differ interms of age (P=0.50), age at onset (P=0.49), sex (P=0.33, and education (P=0.21) in comparison to controls. Patients with fvFTD and aphasia showed behavioural disturbances and revealed pathological scores on FrSBe apathy, disinhibition and executive dysfunction and significant differences between diagnostic groups on disinhibition and executive dysfunction

scores. A significant group effect was observed for MMSE, ACE, and CDR ($P<0.001$), with significantly lower scores for patients compared to controls.

Imaging findings: Both qualitative and quantitative volumetric analysis in fvFTD revealed widespread bilateral atrophy predominantly involving lateral orbitofrontal, inferior frontal, medial prefrontal, dorsolateral prefrontal and temporal lobes bilaterally extending into bilateral insula, striatum, limbic lobe and olfactory regions. An additional involvement of parietal and occipital regions was also observed at lower thresholds. While PPA showed left greater than right temporal lobe atrophy with significant impairement in bilateral insula, rolandic operculum (RoperG), inferior frontal gyrus (IFG), AC, STG, left inferior and middle temporal (ITG and MTG), and right middle temporal pole (MTP), and left middle frontal (MFG) regions. Also a spread to caudate (CAU), parahippocampal gyrus (PHP), fusiform gyrus (FG), lingual, precuneus, inferior and middle occipital regions in the left hemisphere was detected in severely affected groups. A direct comparison between patients resulted only small clusters in bilateral cerebellum in PPA compared to fvFTD. Whereas in fvFTD left hemisphere is greatly involved with more significant patterns of volume loss in superior and middle frontal areas, thalamus (TH), AC, CAU, and gyrus rectus (RECG).

An increased apathy score in fvFTD correlated with reduced GM density in dorsolateral prefrontal, medial prefrontal, orbitofrontal, limbic, temporal and

sublobar regions where as the increased disinhibition score correlated with reduced GM density in limbic lobe, temporal lobe and sublobar insula.

Analysis of DTI data revealed varying degrees of symmetrical white matter abnormalities in the forceps minor, forceps major, IFOF, ILF, UF, SLF and cingulum pathways bilaterally in fvFTD and PPA in comparison to controls. The degeneration of forceps minor, IFOF and SLF was more prominent in fvfTD which showed reduced FA and corresponding increased MD values. On the other hand, patients with PPA revealed prominent reduction in FA and increased MD in forceps minor, IFOF, ILF and UF and anterior thalamic radiations. A direct comparison between fvFTD and PPA revealed significantly reduced FA in genu, anterior parts of SLF and IFOF in fvFTD relative to PPA. Patients with PPA did not show any areas of significantly reduced FA relative to fvFTD. In fvFTD, an inverse correlation was observed between FrSBe apathy, disinhibition scores and FA in SLF whereas, the PPA failed to reveal any significant association.

Quantification of iron content demonstrated significantly elevated iron levels in bilateral SFG, STG, putamen (PUT), AC, right hemisphere PBMC, HP, IN and RN. In PPA, significant deposition is observed in left IN and STG. When patient groups were contrasted, significant atrophy noted in the right SFG in fvFTD. In fvfTD, FrSBe scores of apathy significantly associated with iron content in right SFG and

disinhibition with RPUT. The patients with PPA did not show any association between iron content and any of the behavioural scores.

Implication of findings: Volumetric and group analysis revealed widespread atrophy in frontal and temporal regions in fvfTD and more involvement of left temporal regions in PPA. Hence the pattern of atrophy will help to differentiate between each of the patient groups. The DTI results implicated that the connections between frontal and temporal GM regions is highly impaired in syndromic variants. A significant cortical iron deposition in each of the variants revealed a new dimension to the disease profile. So the combined analysis of these techniques will prove to be helpful in differentiating the subtypes of FTD. The study confirmed that the clinical variants of FTD are characterized by distinctive profile of GM and WM involvement. The findings highlight that eventhough, they have considerable overlap, the changes were specific to each variant. Based on these observations we concluded that this multi parametric approach can be served as a predictor of impending behavioural abnormalities in FTD.

I INTRODUCTION

Dementia is one of the most burdensome public health issue world- wide and has a great impact on the quality of life of patient and caregiver. The global prevalence of dementia estimated to be approximately 46.8 million in 2015 and these figures are expected to reach over 131.5 million in 2050 ("World Alzheimer Report 2015") Alzheimer's disease (AD) is the commonest and well known of dementias with major cognitive deficits and often seen in patients with more than sixty years. While age is an important factor for the increasing prevalence, there is evidence for early-onset dementia (EOD) affecting people in early life at <65 years of age (Ratnavalli et al., 2002). The EOD patients and families are more vulnerable to social and economic burden as they are still in the prime of life compared to those with late-onset dementia (Rossor et al., 2010).

Frontotemporal dementia (FTD) is the second most common cause of dementia leading to EOD. Mostly it is familial and occurs in the age range of 35-75 years. The incidence and prevalence rates are variable and the recent estimated point of incidence is 2.7-4.1/100,000 and prevalence is 15-22/100,000 (Onyike & Diehl-Schmid, 2013). FTD is a progressive heterogenous disorder associated with selective and progressive atrophy of the frontal and temporal lobes (Rabinovici & Miller, 2010; Rohrer & Warren, 2011) which results the hallmark features of behavioural and language impairments (Neary et al., 1998). These presentations often mimic schizophrenia, bipolar disorder, major depression in youth (Velakoulis et al., 2009) and other focal pathologies of stroke, brain tumour or traumatic brain injury in later life.

The efficacy of current treatment for FTD is not impressive as it is inefficient to offer a complete cure but only provides a symptomatic relief. There has been extensive research to develop disease modifying therapies to prevent or slow down the progression of pathogenic mechanism of FTD. There is immense hope that these one or more approaches will be effective at altering the course of FTD in the coming years.

The FTD subjects in their initial stages performed flawlessly on standard cognitive neuropsychological testing, even though they have marked changes in social behaviour which severely affects their working and family life. Such behavioural manifestations include apathy, disinhibition, loss of empathy, pathological sweet teeth, lack of insight etc (Snowden et al., 2001; Hodges et al., 1992). Hence attention has been focused on behavioural inventories that can discriminate FTD from AD and depression (Kertesz et al., 2000; Kertesz et al., 2003). However, although neuropsychological tasks and behavioural measures may be effective in discriminating group of patients with FTD and other dementias or between the subtypes of FTD, none of them serve as an ideal diagnostic tool on individual basis.

Over the past four decades, the advancement of physics, computing, mathematics and clinical imaging sciences has dramatically changed our ability to accurately diagnose dementia world-wide. Till now, the diagnostic confirmation of FTD is based on postmortem autopsy results. The role of noninvasive in-vivo neuroimaging methods is now expanded and it provides an ideal quantitative biomarker for research and early detection of FTD during life.

A variety of brain imaging techniques allows the examination of structure, biochemistry, metabolic state and functional changes of the brain so as to improve the diagnosis and follow disease progression. Primary neuroimaging techniques that are widely used clinically to understand different aspects of brain structures or functions are computed tomography (CT), conventional magnetic resonance imaging (MRI), positron emission tomography (PET), single photon emission tomography (SPECT), functional magnetic resonance imaging (fMRI), magnetic resonance spectroscopy (MRS), and diffusion tensor imaging (DTI) or diffusion fiber tractography (DFT). Although fMRI, MRS, and SPECT have tremendous applications, structural brain imaging methods especially CT or MRI are routinely performed to assist in the diagnosis of dementia and to specifically rule out treatable and reversible etiologies.

Previous evidences indicate the reliability of variety of neuroimaging modalities to classify AD and FTD (Davatzikos et al., 2008; Zhang et al., 2009). Also brain imaging has been used to explain the deterioration of socio-emotional function and language in FTD disease course. Recent investigations target the utility of imaging to study FTD over time as it can measure the brain structure and function precisely unlike cognitive tests which are found to be highly dependent on factors such as sleep quality and use of medications.

While searching for the plethora of imaging biomarkers to classify subtypes of FTD, a noninvasive volumetric structural MRI and PET remains the time honoured standard neuroimaging tool to identify the patterns of GM atrophy or

hypometabolism. But PET is expensive and involves the injection with a short lived radioactive tracer. Moreover, the visual inspection of both MRI and PET appears normal in early stages hence difficult to distinguish from normals (Mendez et al., 2007). However, the modern imaging modalities like Voxel Based Morphomtery (VBM) and DTI have been used to define the abnormalities in GM and WM structural integrity in FTD patients. VBM provides highly objective whole brain analysis between group of subjects on a voxel-by voxel basis using (Ashburner & Friston, 2000; Good et al., 2002) statistical tests across all voxels. It has been effectively used to study volumetric structural brain changes in healthy subjects (Good et al., 2001) and in dementia settings, especially in FTD subjects, Gorno-Tempini et al., 2004; Williams et al., 2005). In addition, DTI has opened up a new window to analyse the microstructural alterations in the white matter (WM) in the living human brain by measuring the directionality of molecular diffusion. This is based on the notion that well organized tracts have high fractional anisotropy (FA) and it decreases in diseases due to decreased anisotropic diffusion.

Earlier studies have shown symmetric or predominant right hemisphere GM atrophy in the ventromedial frontal cortex (VMFC), insula, anterior cingulate (AC), striatum, amygdala (AMY), temporal pole (TP) and subcortical regions (Rosen et al., 2002; Boccardi et al., 2005; Du et al., 2007; Seeley, 2008; Piguet et al., 2011; Whitwell & Josephs, 2012) as well as less investigated changes in WM bundles of anterior part of superior longitudinal fasciculus (SLF), genu of corpous callosum (GCC), uncinate fasciculus (UF), and inferior longitudinal fasciculus (ILF) (Zhang et al., 2009; Whitwell et al., 2010). In PPA, SD patients has been associated with bilateral GM

atrophy in the anterior temporal lobes (Mummery et al., 2000; Rosen et al., 2002; Gorno-Tempini et al., 2004) and significant WM damage in ILF, UF (Galantucci et al., 2011), anterior SLF, arcuate fasciculus (AF) and GCC (Whitwell et al., 2010) while, PNFA is characterized by GM loss in left premotor, inferior frontal cortex and insula as well as severe WM changes in SLF (Galantucci et al., 2011) and dysfunction of its components (Whitwell et al., 2010; Rogalski et al., 2011).

Also it has been reported that GM and WM damage in FTD are related to the different clinical and neuropsychological profiles (Borroni et al., 2007; Zamboni et al., 2008; Zhang et al., 2009; F. Agosta et al., 2012b). The pattern of degeneration and its neural correlates of behavioural measures were inconsistent across the studies and there was a need to replicate the findings in other populations. Recently, postmortem studies suggested that impaired iron homeostasis is a major culprit in the pathogenesis of FTD (Santillo et al., 2009; De Reuck et al., 2014). SWI has been proved to be a potential in vivo marker for the identification of susceptibility changes associated with tissue iron in the form of ferritin and transferrin (Thomas et al., 2007). In the light of these findings, the present study was conducted to unravel the efficacy of advanced multimodal neuroimaging techniques to distinguish between patients with FTD from controls, and between clinical subtypes, with the eventual aim of aiding the diagnosis of FTD.

Objectives

The main objectives of the study are-

1. To analyze the gray matter degeneration in the syndromic variants of FTD using VBM

2. To determine the WM integrity changes in the clinical subtypes of FTD using DTI

3. To assess whether the putative iron deposition seen with SWI can be used as a biomarker for the diagnosis of clinical subtypes of FTD

4. To determine if the cortical GM atrophy, WM degeneration and elevated iron levels in the specific regions of the brain can serve as a predictor of an impending behavioral manifestation in FTD

Hypothesis

We hypothesized that the each syndromic variant of FTD would be associated with distinct pattern of GM damage, severe WM integrity changes to tracts connecting GM atrophic regions and increased brain iron deposition that is critical to the behavioural manifestation in FTD.

The rest of the thesis is organized in five heads. **Chapter II,** presents a brief review of the historical background of FTD, its etiology, genetics and neuropsychological features. It also describes the background to the MRI techniques including MRI, DTI and SWI and underlying principles of qualitative and quantitative MRI analysis

methods including morphometry, tractography, and iron quantification. This chapter also explains the neuroimaging biomarkers relevant to diagnosis of subtypes of FTD patients. **Chapter III** describes the materials and methods used to fulfill the objectives of the study. The section also includes the statistical analysis methods used to analyze the research findings. **Chapter IV** provides the main findings of the study with the statistical significance. The results are presented as tables, figures and boxplot. **Chapter V** discusses and interprets the observations of the current study and also proposes the major implications. **Chapter VI** gives the summary and conclusion with future direction of research.

II REVIEW OF LITERATURE

II.1 Historical Background of FTD

FTD formerly called as “Pick’s disease”, in honor of Arnold Pick, head of the Department of Psychiatry, University of Prague, who first discovered this condition at the end of the nineteenth century (Pick, 1892). The clinical characterization of Pick’s patients relied on the cognitive decline associated with marked behavioral and language manifestations and has been recognized to be asymmetric focal- cortical involvement. Histopathologic analysis revealed a distinct pattern of FTD from AD, but heterogeneous, even among similar clinical variants. Postmortem studies often showed more severe frontal atrophy. Recent advancements in immunohistochemical stains and insights gained from molecular genetic analysis revealed an overlap of FTD with corticobasal ganglionic degeneration (CBD), progressive supranuclear palsy (PSP), and motor neuron disease (MND).

The microscopic abnormalities of Picks disease were first described by Alois Alzheimer in 1911 (Alzheimer, 1991). He and Altman in 1923 reported the pathologic picture of Pick’s disease interms of argyrophilic inclusions (Pick bodies), swollen cells (Pick cells) and the cortical spongiosis in the frontal and temporal regions of atrophic brains. In 1922, Gans introduced the denomination “Pick’s disease”, who accentuated a discernable frontal atrophy convoyed by aspontaneity and major complaints of attention, judgment, behavior and language. These atrophic brains were devoid of Plaques and neurofibrillary tangles (Onari & Spatz, 1926), which confirmed the non-Alzheimer Pathology (Alzheimer, 1991). In 1927, Schneider proposed the frontal and temporal involvement in which, the pathological

involvement of temporal lobe was associated with language deficit, while involvement of frontal lobe was associated with behavioural disturbances, especially apathy (Schneider, 1927). But the histopathological examination failed to observe the presence of Pick's bodies (Schneider, 1927). Another salient observation by Tissot and Constantinidis recognized and documented a tripartic classification of clinically defined Pick's disease: the first group with swollen neurons and Pick bodies, the second group with only swollen neurons and now be called as CBD, and third group describes a pattern similar to Picks disease but without swollen neurons or Pick bodies (Constantinidis et al., 1974). These cases are now known as *dementia lacking distinctive histopathology* (DLDH) or *frontotemporal dementia of the non-Alzheimer's type* (Mann et al., 1993). Meanwhile, Warrington (Warrington & Shallice, 1984) and Mesulam (Mesulam, 1982) described cases of progressive language disorders in Western literature. Warrington depicted patients with selective impairment of semantic memory. Mesulam depicted patients who were exhibiting progressive language impairment including both production and comprehension that he named as primary progressive aphasia (PPA). Then in 1994, Lund and Manchester consensus criteria for the clinical and pathological diagnoses of FTD were published (Lund & Manchester Groups., 1994). The core diagnostic features of FTD consisted of supportive features of clinical MND.

II.2 Epidemiology, clinical presentation and risk factors of FTD

II.2.1 Epidemiology

FTD is the frequent cause of EOD (below 65 years) and its prevalence in epidemiological studies varies between 2.7 (in Netherlands) to 15.1 (in Cambridge,

UK) per 100,000 (Rabinovici & Miller, 2010). FTD syndromes commonly seen in people in their sixties (Hodges et al., 2003; Harvey et al., 2003), eventhough it could start both early in thirties (Harvey et al., 2003) and very old age (Gislason et al., 2003; Pikkarainen et al., 2008). Postmortem studies provided a relative frequency of FTD of 3–10% (Kertesz & Munoz, 2002). Also, the prevalence of familial cases are more than sporadic cases, (Borroni et al., 2014), suggesting as a genetic disorder (Warren et al., 2013). Inaddition, the average age of onset does not differ greatly between familial and sporadic cases (Piguet et al., 2004). Moreover, no male or female preponderance has been described (Rosso et al., 2003, Chow et al.,2005, Borroni et al.,2011, Iaonnidis et al., 2012) although some studies which reported a mild (Harvey et al., 2003)) or even a high male predominance (Ratnavalli et al., 2002). In subgroups, certain studies reported a male predominance in fvFTD and SD cases but female predominance in PNFA cases (Roberson et al., 2005). It has been demonstrated a younger onset in fvFTD (mean=57 years) and SD (mean=59 years) than PNFA (mean=65 years) (Snowden et al., 2007). Further, the survival rate varies across subtypes; bvFTD has the shortest (median= 8.7 years from onset) and SD has the longest (median=11.9 years), while PNFA has an intermediate (median=9.4 years) survival rate. A lowest survival (1.3 years) was found in FTD-MND cases(Brodaty et al., 2012). The epidemiological studies from India are limited (Das et al., 2012). However, one study on early onset dementias (<65 years) from East India reported FTD (27%) as the second most common cause after possible AD (30%), which showed positive family history in 20% of FTD cases (Nandi et al., 2008). Later, a clinic-based study from South India found that FTD accounts for 18.7% of total dementia cases (Alladi et al., 2011).

II.2.2 Clinical presentation

The hallmark feature of FTD is the manifestation of focal disintegration of temperament, judgement, social behavior, and speech. These presentations mimic schizophrenia, bipolar disorder and major depression in youth (Velakoulis et al., 2009) and other focal pathologies of stroke, brain tumour or traumatic brain injury in later life. According to Neary and colleagues (Neary et al., 1998), the typical presentation of FTD consists of behavioural phenotype known as frontal or behavioural variant FTD (fvFTD) with gross decline in social conduct and language phenotype known as primary progressive aphasia (PPA) with decline in expressive and receptive language domains. fvFTD is the common subtype, accounting for 30-50% of all cases (Ikeda et al., 2004; Kertesz et al., 2007). Mendez and Collegues reported a lack sensitivity of Neary and Manchester-Lund criteria (Mendez et al., 2007; Mendez et al., 2008) in describing the certain behavioural terms such as emotional blunting which limited the diagnosis of fvFTD in early stages (Rascovsky et al., 2007). A new criterion by Rascovsky et al has replaced the older ones (Rascovsky et al., 2011). In recent years, PPA have been classified into three variants such as progressive nonfluent aphasia (PNFA) (Mesulam, 2003), semantic dementia(SD) (Davies et al., 2005; Hodges & Patterson, 2007) and logopenic/phonological variant of progressive aphasia(LPA) (Gorno-Tempini et al., 2008; Gorno-Tempini et al., 2011).

Patients with fvFTD affects predominantly frontal and anterior temporal lobes (Figure 1.A) and presents with progressive loss of interpersonal and executive skills,

with poor insight and altered emotional responsivity and emergence of a variety of personality differences including apathy or abulia, disinhibition, impulsivity, obsessions, rituals, changes in apetite and stereotyped behavior (Neary et al., 1998) . Language phenotypes of FTD features effortful non-fluent, and agrammatical speech are known as progressive nonfluent aphasia (PNFA) and has been associated with predominant atrophy of left perysylvian fissure (Figure 1.B) (Gorno-Tempini et al., 2004, Wilson et al., 2011). Patients with SD features impaired comprehension of sentences and fluent but vacuous, circumlocutory speech with anomia and agnosia and has been associated with atrophy in bilateral anterior temporal lobes (Figure1.C) (Mummery et al., 2000; Rosen et al., 2002; Gorno-Tempini et al., 2004)

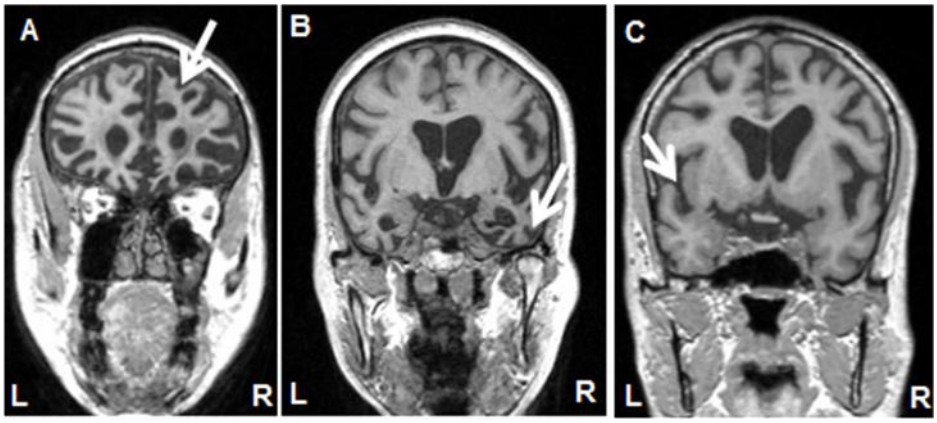

Figure 1: Structural MRI scans of typical FTD variants.

A) fvFTD B) SD and C) PNFA in our study group. Patterns of atrophy in fvFTD shows predominant atrophy in bilateral frontal lobe, SD shows atrophy in bilateral temporal lobe and PNFA shows atrophy in the perisylvian fissure.

II.2.3 Risk factors

There are very few studies concerning specific risk factors for FTD. The recognized risk factors include genetic susceptibility, personal history of head trauma and thyroid diseases. The prevalence of traumatic brain injury (TBI) was significantly higher in FTD patients as compared with the other dementias (Kalkonde et al., 2012). Specifically, the thyroid disease patients are associated with 2.5 times increased risk of FTD (Rosso et al., 2003).

II.3 Etiology

FTD is pathologically heterogeneous (Mackenzie et al., 2010; Premi et al., 2012). Currently three main types are recognized with buildup of abnormal proteins. Some FTD patients show tau- or ubiquitin- positive inclusions and some do not have any distinctive histological features.

FTD-Tau: Approximately, 40% of FTD patients show tau inclusions including most cases of PNFA, few cases of SD, and 45% of patients with fvFTD. Tauopathies present with either transcortical gliosis with tau reactive rounded intraneuronal inclusions (Pick bodies) or tau positive neurofibrillary tangles (NFT) in neurons and glial cells (Piguet et al., 2004)

FTD-TDP: In 2006, transactive DNA binding protein 43 kDa (TDP-43), a major component of the ubiquitously expressed DNA/RNA binding protein, has been identified in variants of tau-negative FTD (i.e. FTD-U and FTD-MND). Currently,

FTD-U outnumber FTD-tau in which around 50% of patients of FTD have TDP-43 inclusions, with mostly SD and PNFA, as well as 45% with fvFTD (Piguet et al., 2004; Goedert et al., 2012)

FTLD- FUS: Around 7-20% of the patients with FTD were clinically proved to be linked with TDP-43 pathology however a few cases do not follow the same pattern. Most of the cases had positive staining for fused sarcoma (FUS) protein, which is mainly concentrated in the nucleus and less in the cytoplasm of a normal brain tissue. In FTD, FUS protein cannot move into the nucleus, leading to FUS cytoplasmic accumulation. FUS-pathology is mainly linked with a frontal FTD phenotype, with behavioral changes and disinhibition among other manifestations (Mackenzie et al., 2008; Neumann et al., 2009).

II.4 Genetics

Up to 30-50% FTD cases have positive family history (Seelaar et al., 2011). The mostly known mutations are associated with microtubule associated protein tau (MAPT) gene (Hutton et al., 1998), progranulin gene (GRN) (Baker et al., 2006), Valosin containing protein (VCP) (Watts et al., 2004), Charged multivesicular body protein 2B (CHMP2B) (Skibinski et al., 2005)and C9ORF72(DeJesus-Hernandez et al., 2011; Renton et al., 2011). MAPT has been found to be associated with 5% of early onset fvFTD cases and PGRN with 5% of familial forms of FTD (Galimberti & Scarpini, 2012).

II.5 Diagnosis

II.5.1 Clinical Assessment

Clinical assessment of FTD involves a comprehensive and multifaceted evaluation including detailed history and demographics, a focused cognitive and physical examination, laboratory profiles and neuroimaging. A proper understanding of behavioural and cognitive features and its neuroanatomic correlates will help to understand the affected brain areas during the disease course which is necessary for the early diagnosis. Also the progressive nature of this disease can be properly evaluated by longitudinal studies with serial assessments, which is beyond the scope of this thesis.

II.5.2 Behavioural Assessment

As the first manifestations of FTD are behavioural abnormalities, behavioural inventories that focus on the unusual social behaviours and personality changes are more sensitive for the diagnosis (Barber et al., 1995; Kertesz et al., 1997). The Neuropsychiatric Inventory (NPI) (Cummings, 1997) and Frontal Behviour Inventory (FBI) (Kertesz et al., 2000) are the structured questionnaires for the comprehensive evaluation of behavioural changes. FBI is based on the caregiver interview that measures both positive and negative symptoms that has been found to be sensitive to discriminate FTD from other dementias (Marczinski et al., 2004). On the other hand, NPI evaluates hallucinations, delusions, disinhibition, apathy, anxiety, aberrant motor behavior, dysphoria, irritability, euphoria, sleep and apetite change. This is a very sensitive test to detect the behavioural changes in FTD and

PPA and may be useful in tracking the progression of behavioural symptoms over the period (Chow et al., 2002). Also, Frontotemporal Dementia Rating Scale (FRS) (Mioshi et al., 2010) is the test which measures the progression of illness. Recently developed Frontal System Behavioural scale (FrSBe) is a 46 item behavior scale that is intended to measure behavior syndromes associated with frontal sub-cortical brain deficits (Malloy et al., 2007).

II.5.3 Neuropsychological Evaluation

FTD is characterized by relative sparing of memory on cognitive testing. Although these patients experience memory problems, the Mini Mental State Examination (MMSE) (Folstein et al., 1975) and Clinical Dementia rating (CDR) (Hughes et al., 1982) are unreliable for the diagnosis of FTD, both developed initially for the diagnosis of AD. The memory deficits associated with these patients either may be due to the impulsive nature or may be due to the failure to monitor response. FTD subjects also have worse performance on word generation tasks and better performance on visuospatial ability tests than AD. They also exhibit marked impairment in working memory, attention, abstraction, and mental set shifting which indicates frontal lobe dysfunction. The tests such as the Wisconsin Card Sorting (WCST), Tower of London, Trail making etc are indicative of cognitive changes associated with frontal lobe dysfunction. The cognitive deficits varied within FTD subgroups in which subjects with more temporal atrophy have more semantic deficits while those with frontal lobe atrophy have more attention and executive deficits (Perry & Hodges, 2000). They perform poorly on semantic and fluency tasks but perform better on tasks involving picture naming, word-picture matching and

posterior language based tasks (Hodges et al., 1999; Perry and Hodges, 2000). The poor performance on the standard neuropsychological testing may be due to their inattention, poor organization, lack of self monitoring and less effort. The PPA perform poorly on tests of phonologic competence, reception of grammar, repetition, and Boston naming (Weintraub S et al., 1990; Hodges & Patterson, 1996). Phonemic verbal fluency is more impaired than semantic fluency whereas the word picture matching, synonym tasks and other semantic tasks, visuospatial perceptual function tests and orientation is well preserved (Weintraub S et al., 1990).

II.5.4 Neuroimaging

The role of neuroimaging in FTD diagnosis remains controversial. Structural imaging can be helpful for distinguishing FTD from other types of cognitive diseases. In early phases of disease, MRI in fvfTD appears normal. Functional imaging methods such as PET and SPECT have been shown to be more sensitive than structural MRI in FTD (Mendez et al., 2007), which respectively show hypometabolism and hypoperfusion in frontal and/or temporal cortices. Each clinical variants of FTD typifies hypometabolism and hypoperfusion and it correlate with the structural changes (Ishii et al., 1998; Diehl et al., 2004).

II.6 Neuroimaging and Analysis Techniques

As the focus of this thesis is neuroimaging analysis of FTD, this section discusses the details of the theoretical background of imaging techniques used in the study.

II.6.1 MRI

MRI also known as nuclear magnetic resonance imaging (NMR) is an advanced form of non invasive and non ionizing imaging technique. Recent advances in MRI technology presents it as the prime example of the significance of physical science in medicine in supporting clinical applications and developing new techniques. These advantages make MRI as the most promising instruments in medical imaging in diagnosis and research, especially in neurological, cardiovascular, musculoskeletal and oncological studies.

The phenomenon of MRI utilizes the quantum mechanical properties of the hydrogen protons in the human body. Usually, the tissue contrast in MRI is provided by unpaired protons (like hydrogen proton) with non-zero quantum of the nuclear spin. When a human body is placed in a scanner, the spins align either parallel (spin-up low energy) or antiparallel (spin down- high energy) to the field (B_0)(Zeeman effect), hence creating a net magnetistaion parallel to the applied field (Figure 2). In addition, the nuclear spins experience a torque by the external magnetic field and precess around the direction of external magnetic field. The angular frequency (Larmor frequency) of precession is given by Equation (1)

$$\omega_0 = \gamma B_0 \qquad 1$$

Where ω is the Larmor frequency, γ is the gyromagnetic ratio, a constant for specific

nuclei in a magnetic field (γ = 42.57 MHz/T for 1H) and B_0 is the magnetic field strength.

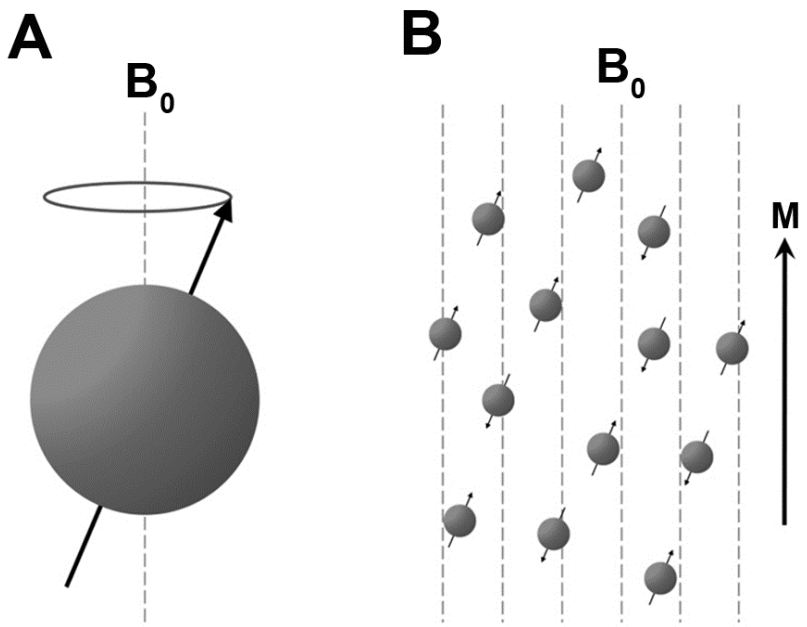

Figure 2: Spin precession in a magnetic field. Hydrogen protons possess spin, a quantum property that induces a molecular moment (A; black arrow) along the axis of rotation. When an external magnetic field is applied, spins precess about the field with frequency ω (A) and align parallel to it (B), producing a net magnetization vector M.

Applying a suitable RF pulse (B1 field), tuned to the Larmor frequency at right angles to Bo, excites the spins in an equilibrium state to a higher energy state thereby reducing longitudinal magnetization and increasing transverse magnetization. The radio frequency pulses also tips over the net magnetization to 90 degrees transverse to the applied field (B_1). The degree of rotation of magnetization vector is termed as flip angle.

Cessation of the transverse radio-frequency (RF) pulse causes the reversion of excited magnetization to energetic equilibrium. This process is known as relaxation. The process of reversion is characterized by two relaxation time constants T1 and T2, both of them can be modelled as exponential curves (Bloch, 1946). Longitudinal (T1) relaxation or spin-lattice relaxation is accomplished through energy exchange in the form of heat with the surrounding lattice and transverse (T2) relaxation or spin-spin relaxation is dominated by the exchange of energy between two susceptible nuclei with similar precession frequencies. These time constants together with the concentration of the magnetization spins can be adjusted to enhance the quality of MR images.

Both T1 and T2 are tissue-specific and hence used to form a contrast between different tissues in the MRI image. The image contrast in MR image depends on two key parameter repetition time (TR) and echo time (TE), measured in milliseconds. TR is the time between the application of an RF excitation pulse and the start of next RF pulse. TE is the time between the application of the RF pulse and the peak of the signal or echo detected.

Sometimes, transverse magnetization decays faster than T2 decay due to magnetic field inhomogeneities. The sources of differences may occur with the presence of metallic objects/dental implants, air, or calcium or may because of the limitations of the construction of the magnet. This decay is designated as T2* which finds common use in fMRI and SWI. According to the Faraday law of electromagnetic induction,

the net magnetization vector M after turning off the RF pulse can induce an electromotive force (EMF) in a receiver coil. This oscillating time signal is called free induction decay (FID), which is considered as MR signal.

II.6.2 MR Image formation

In order to reconstruct an image from the NMR signal, three spatially varying magnetic field gradients (G) are required (Lauterbur, 1973). The first gradient called slice selection gradient (Gz) is applied during the RF pulse to isolate a single slice or volume to be measured by exciting only those spins whose Larmor frequency is the same as the frequency of the applied RF pulse. The second gradient called phase encoding gradient (Gy) is applied to alter the phase of the precessing spins and spins will dephase faster with higher gradient strength. Finally, a gradient called frequency encoding gradient (Gx) is applied during read out to spatially encode the selected slice by altering the precession frequency based on field strength. Hence, it is necessary to be applying the gradient fields in a given order to relate the frequency and phase of the signal to their localization. The diagram displays the timing of the application of gradient and RF pulses is called pulse sequence diagram. After repeating this process for multiple read out, the received signal is processed using a Fourier transform that can assign signal intensities to the volume element in the slice that has the correct phase and frequency.

II.6.3 K space and Fourier Transform

K space is a spatial frequency domain where raw imaging data are stored in the MR imaging system (Twieg, 1983). Each point in K space contains a specific frequency,

phase and signal intensity information. The central regions of k-space encode tissue contrast information, whereas the peripheral regions (edges) encode spatial resolution. After obtaining samples of signal from all parts of K-space, Fourier transformation (2DFT) is applied to generate the image (Figure 3). Fourier transforms resolves the frequency- and phase-encoded MR signals that compose k-space. A single pixel in k-space, when inverse-transformed, contributes a single, specific spatial frequency (containing are alternating light and dark lines) to the entire image. The relative intensity of a pixel reflects its overall contribution to the image, with brighter pixels contributing more of a particular spatial frequency.

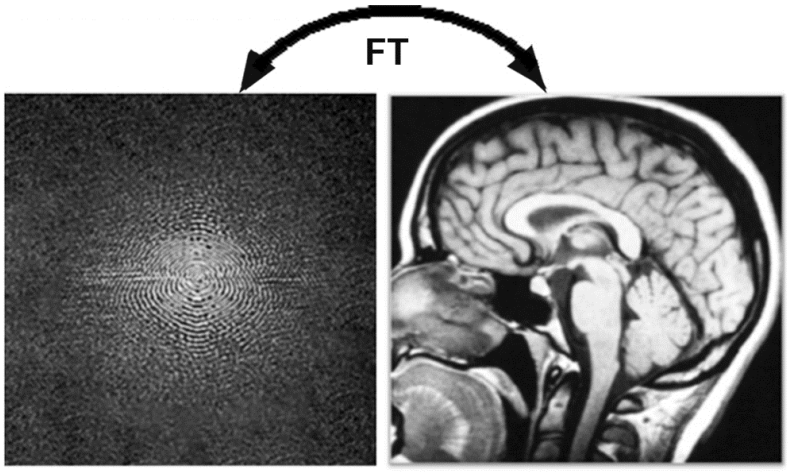

Figure 3: **The MR image formation of a human head and its K space representation.**

II.6.4 Pulse sequences

The basic pulse sequences are the Spin echo (SE) and Gradient echo (GRE).

II.6.4.1 Spin echo (SE) or Hahn echo sequence

It is the most commonly used one and sequence timing can be adjusted to produce T1-weighted, T2- weighted and proton density images. SE sequences include a 90° RF pulse to excite the magnetization followed by one or more 180 degree refocusing pulses. The 90° RF pulse flips the net magnetization in transverse plane and the 180° pulse at a time equal to one-half of TE rephase the spinning nuclei and thereby recovering the transverse magnetization, producing an echo (Figure 4).

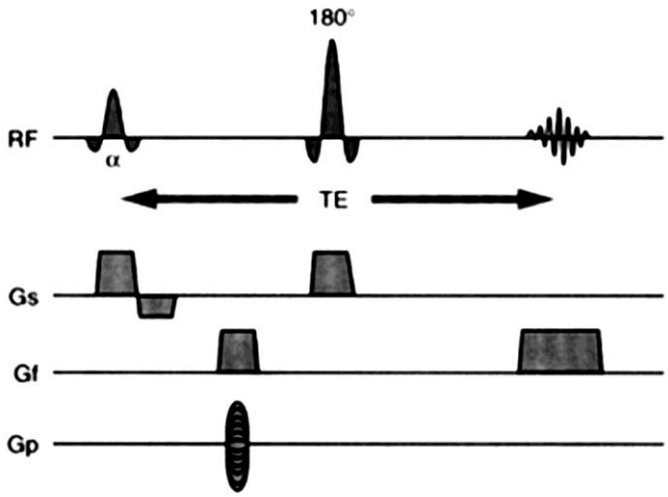

Figure 4 : **Pulse sequence for Spin echo imaging**

II.6.4.2 Gradient echo Sequence

Gradient echo sequences uses flip angle less than 90°. The applied RF pulse causes the partial flipping of the net magnetization vector into the transverse plane. After the RF pulse, the dephasing and rephasing gradients with opposite polarity are used to dephase and rephase the magnetic moments in transverse magnetization (Figure 5) (Bitar et al., 2006).

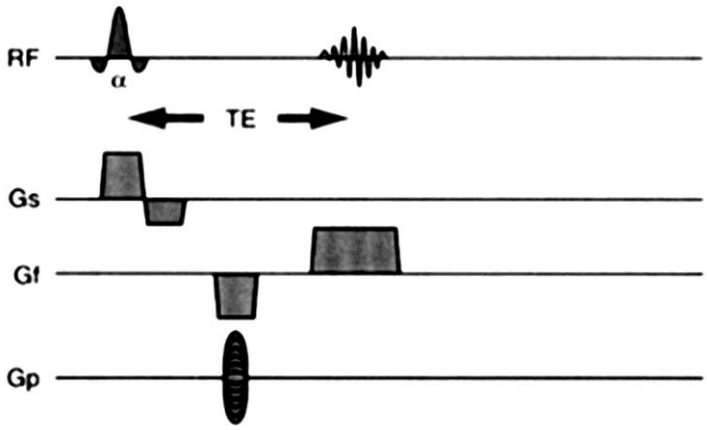

Figure 5: Pulse sequence for Gradient echo imaging

The lack of 180^0 RF pulse makes this sequence very sensitive to T2* decay, which have found application in SWI. Since GRE sequences are very fast, the whole brain volumetric images can be acquired in a shorter time. The widely used sequence for acquiring structural data is Spoiled Gradient Recalled Echo (SPGR) by GE or Fast Low Angle Shot (FLASH) by Siemens (Figure 6).

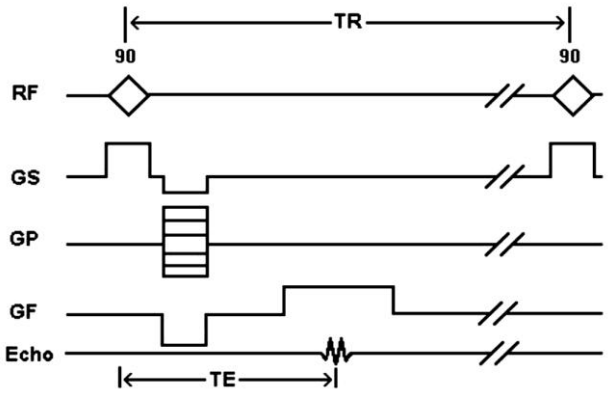

Figure 6: Pulse sequence for FLASH imaging

In FLASH technique, the residual steady-state transverse magnetization is spoiled after signal acquisition so that it will not interfere with the next cycle. This is usually achieved by applying RF spoiling, by applying variable gradient spoilers and by lengthening TR. As a result, only the longitudinal component affects the FLASH signal which can reduce T2* weighting and increases T1 weighting. For acquisition of gradient echo signal, Flash combines low flip angle ($<90^0$) and RF excitation pulses with rapid repetition of the basic sequence. The low flip angle pulses create equilibrium of longitudinal magnetization and results in the elimination of transverse magnetization. In this sequence, the fluid appears as dark, GM as grey and WM as white.

II.6.4.3 Echo planar Imaging Sequence

Echo-planar imaging (EPI) (Mansfield, 1977), is capable of shortening MR acquisition time substantially about 20–100 msec. In EPI, multiple lines of k- space data are collected after a single RF excitation. EPI is classified as single shot and multishot EPI. In a single shot, all the lines of k- space are filled in a single TR whereas, in multishot, entire k space is filled in two or more TRs. The rapid filling of k-space is accomplished by very rapid turned on and off of phase-encoding gradient and the frequency-encoding gradient (Stehling et al., 1991) (Figure 7). Each oscillation of the frequency encoding gradient corresponds to one line of imaging data in k space and each phase encoding blips corresponds to a transition from one line to the next in k space. Also, single-shot EPI is commonly of poorer contrast and lower resolution than other forms of MRI, but allows the capture of rapidly changing dynamic processes, most notably changes in blood oxygenation in fMRI and the

diffusion of water molecules in diffusion MRI, that have wide application as a clinical and research tool.

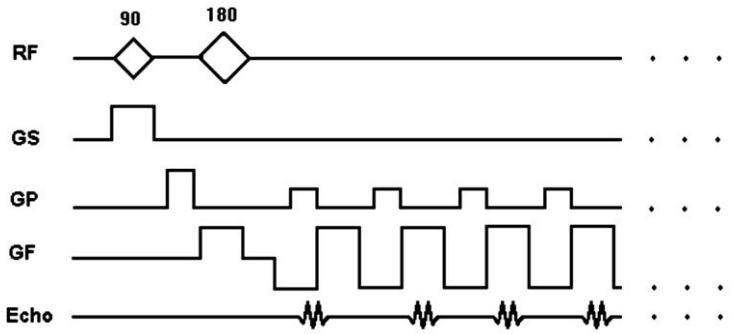

Figure 7 : Pulse sequence for Echoplanar imaging

II.7 Diffusion MRI

Diffusion is a physical process that represents random motion, also called Brownian motion resulting from the thermal motion of molecules, whose temperature is greater than absolute zero (0 Kelvin). According to Fick's law, random diffusion of water molecules over time may also occur in response to differences in pressure or temperature, caused either by ion-ion interactions or in response to other factors. This process was formalized by Albert Einstein in 1905, demonstrating that (Einstein, 1956).

$$D = \frac{<\Delta r2>}{2n\Delta t} \qquad 2$$

The diffusion coefficient, D (in mm^2/s), is proportional to the mean squared-displacement, $\langle \Delta r^2 \rangle$ divided by the number of dimensions, n, and the diffusion time, Dt. The diffusion coefficient is a scalar and for pure water at 20°C the value is roughly $2.0 \times 10^{-3} mm^2/s$, and increases at higher temperatures. In the absence of physical barriers to impede the motion, the molecular water displacement is described by a Gaussian probability density.

$$P(\Delta r, \Delta t) = \frac{1}{\sqrt{(2\pi D \Delta t)^3 exp\{-\Delta r^2 | 4D\Delta t\}}} \quad 3$$

Diffusion of water throughout the biological tissues is delimited by all the cell membranes and myelin sheaths, causing water to take more tortuous paths, thereby reducing their mean squared displacement over time (Beaulieu, 2002). Moreover, the calculated diffusion coefficient is known as the so-called apparent diffusion coefficient (ADC). The diffusion tortuosity and corresponding apparent diffusivity may be increased by either cellular swelling or increased cellular density. Conversely, certain conditions like necrosis decreases tortuosity and increases the apparent diffusivity.

A similar process happens in the brain is clearly not a homogeneous medium and the presence of various cellular compartments within the parenchyma creates barriers to diffusing water molecules, reducing their mean displacement over time (Beaulieu, 2002) . The coherent organization of long neuronal axons and their myelin sheets of

the cerebral white matter facilitated diffusion along axonal fibers, and hindered in the direction perpendicular to the fibers. However, in free medium like, CSF and GM, which lacks any coherent linear structure, the water diffuse isotropically.

II.7.1 Diffusion Weighted Imaging (DWI)

DWI is the imaging technique which is based on the physical principles of diffusion NMR. The most successful application of diffusion anisotropy of water protons within the brain was first demonstrated by Moseley et al. (Moseley et al., 1990), which forms the basis of clinical diffusion MRI. DWI is especially useful for measuring diffusion (eg: GM of the cerebral cortex or subcortical nuclei), where the diffusion rate appears to be constant regardless of the axis of measurement (Lansberg et al., 2001).

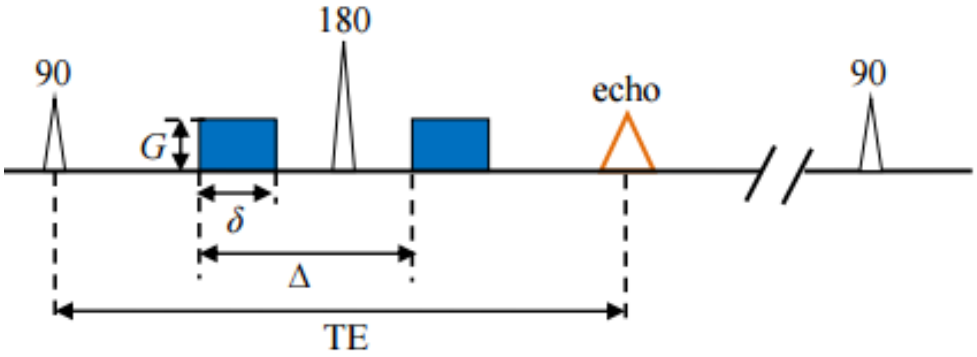

Figure 8: Timing diagram of a PGSE sequence. The bipolar diffusion pulses (blue squares) with magnitude G, duration δ, and separation interval Δ are placed on either side of the 180˚ refocusing pulse

It provides the opportunity to receive suitable treatment at a stage when brain tissue might still be salvageable in patients with acute stroke (Kesavadas et al., 2003). A DWI image can be generated by the use of a pair of strong diffusion gradient pulses which can estimate a relative amount of water diffusion in the form the image contrast (Figure 8).

This sequence was initially developed by Stejskal and Tanner in 1965 and its simplest configuration uses a pair of matched large gradient pulses (blue squares) placed on either side of the 180° refocusing pulse. The first gradient pulse dephases the magnetization across the sample (or voxel in imaging); and the second pulse rephases the magnetization. Hence, the degree of diffusion weighting is determined by a parameter called b value, which is determined by the strength of the diffusion gradients(G), the duration of the gradients(δ), and time interval between the two diffusion weighting gradient (Δ) (Hanyu et al., 1999) and is given by

$$b = \gamma^2 G^2 \delta^2 (\Delta - \delta/3) \qquad 4$$

Where, γ is the gyromagnetic ratio of hydrogen protons. Therefore, in the presence of diffusion gradients, water molecules will accumulates in different phases and hence, the measured signal will be attenuated. The signal attenuation for the diffusion gradient pulses in isotropic Gaussian diffusion is described by

$$S = S_{0\,e^{-bD}} \qquad 5$$

Where S is the DW signal, So is the signal without any DW gradients (but otherwise identical imaging parameters), b is the diffusion-weighting described by the properties of the pulse pair, and D is the apparent diffusion coefficient, calculated from the attenuation of the diffusion weighted signal intensity compared with the one without diffusion gradient at the same voxel. The most commonly used b value for human brain diffusion imaging is in between 900 and 1,500 s mm^{-2} and when considering acquisition time and noise-independent measurements (Armitage & Bastin, 2001) the most suited is 1,000 s mm^{-2}.

II.7.2 Diffusion Tensor Imaging (DTI)

Diffusion tensor imaging (DTI) is a promising method for characterizing the three-dimensional diffusion of water in biological tissue (Basser et al., 1994; Beaulieu, 2002). The major aspects that render this modality as a powerful tool are the microscopic length scale and orientation information. The microscopic length scale of water diffusion in tissue gives DTI microscopic spatial sensitivity, whereas the orientation information can be used to differentiate apparently homogenous WM on conventional MRI into its constituent fiber tracts. Advancements in these two aspects over the past decades have led to the use of DTI to characterize the structural integrity of neural tissue and noninvasively trace neuronal tracts in the brain and spine. DTI has aided surgical planning for brain and spinal cord tumors and increased the diagnostic potential in a variety of neurodegenerative disorders, including multiple sclerosis, AD (Hanyu et al., 1999), and FTD (Borroni et al., 2007). Hence, the appreciation of its clinical applications requires a brief

understanding of its basic underlying principles as well as the richer understanding of brain white matter pathways. In DTI, diffusion is measured in a series of different spatial directions and uses magnetic gradients to infer information about water diffusion in living tissue (Basser et al., 1994). However, with the existence of anisotropy in tissue, the diffusion cannot be characterized by a single scalar coefficient, but requires a second-order symmetric diffusion tensor $\overline{D}$

$$\overline{D} = \begin{bmatrix} D_{xx} & D_{xy} & D_{xz} \\ D_{yx} & D_{yy} & D_{yz} \\ D_{zx} & D_{zy} & D_{zz} \end{bmatrix} \quad 6$$

Where Dxx, Dyy and Dzz correspond to diffusivities along three orthogonal axes, and Dxy, Dxz and Dyz correspond to the correlations between the displacements along the orthogonal axes. Moreover, the diffusion tensor has the property to describe the molecular mobility along any direction which can be represented as a 3D ellipsoid. The ellipsoid represents the probability of diffusion from the origin. Diagonalisation of diffusion tensor D yields three eigen-values ($\lambda1$, $\lambda2$, $\lambda3$; $\lambda1 \geq \lambda2 \geq \lambda3$) and the corresponding eigen-vectors (e1, e2, e3) (Figure 9). The eigenvectors identify the symmetry axes of diffusion while the eigen values identify the diffusion coefficients along the axes. The first eigen vector e1 describes the predominant diffusion direction and is known as Principal Diffusion Vector (PDV) or Principal Diffusivity (PD). For an isotropic tensor, the probability of diffusion is equal in all directions and the surface describes a sphere ($\lambda1 = \lambda2 = \lambda3$). While in anisotropic medium like cerebral white matter, the orientation of tensor ellipsoid is

assumed to be along the predominant fiber orientation (Basser et al., 1994; Basser & Pierpaoli, 1996) and the eigenvalues are significantly different in magnitude (eg: $\lambda 1 > \lambda 2 > \lambda 3$).

Since D is characterized by six degrees of freedom, at least six diffusion-weighted measurements along with a reference image acquired without diffusion weighting are needed to fully determine a diffusion tensor.

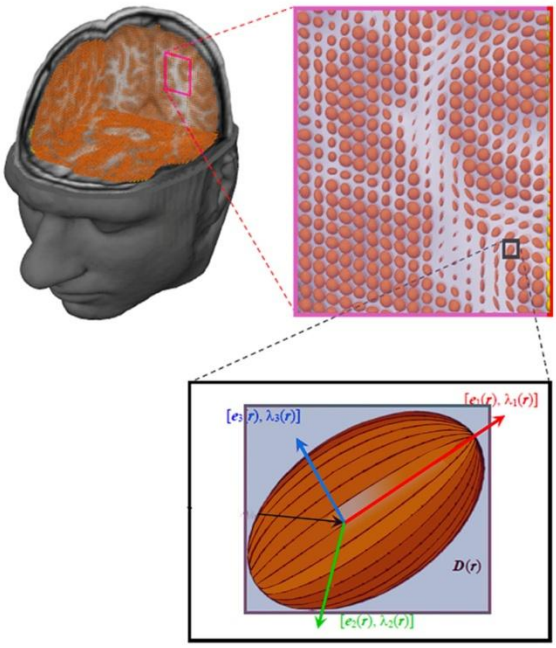

Figure 9: **The geometrical representation of diffusion tensor field in the form of an ellipsoid with a background T1-weighted image**. The spectral component of diffusion tensor D(r) at every voxel (position r) of the data set is defined by the eigenvectors ei(r) and eigenvalues λi(r).

Moreover, the magnitudes of eigen values highly depend on changes in local tissue microstructure due to tissue injury, disease or normal physiological changes like

aging. Thus, the diffusion tensor can be used as a sensitive probe for characterizing both normal and abnormal tissue microstructure.

II.7.2.1 Diffusion tensor derived measures

The diffusion tensor is proportional to the Gaussian covariance matrix that fully characterizes diffusion in 3D space. Inorder to make a meaningful measurement of diffusion matrix at each voxel, it is important to distill the information contained in the image into simpler scalar maps. Several indices derived from diffusion tensor can be used to reflect the diffusion characteristics. The most commonly used indices are the Mean Diffusivity (MD) and fractional Anisotropy (FA), both are rotationally invariant. MD is also known as the apparent diffusion coefficient or ADC is defined as the average of three eigen values which is defined by

$$\mathrm{MD} = \left(\frac{\lambda_1 + \lambda_2 + \lambda_3}{3}\right) \qquad 7$$

MD is a measure of directionally-averaged tissue diffusivity and is affected by cellular size and integrity (Basser et al., 1994). However, FA describes the deviation of diffusion from isotropy (Basser & Pierpaoli, 1996) and reflects the structural integrity of white matter fibre tracts. More specifically, it gives the directionality of diffusion and is computed as below:

$$FA = \frac{\sqrt{(\lambda_1 - \langle\lambda\rangle)^2 + (\lambda_2 - \langle\lambda\rangle)^2 + (\lambda_3 - \langle\lambda\rangle)^2}}{\sqrt{\lambda_1{}^2 + \lambda_2{}^2 + \lambda_3{}^2}} \quad 8$$

where <λ> is the mean diffusivity. It is an absolute dimensionless value ranges between 0 (perfectly isotropic) and 1 (limit of infinite anisotropy). It is widely accepted that, in various brain pathologies, the FA is reduced and MD is increased. In addition, eigenvalue amplitudes or combinations of the eigenvalues (radial diffusivity = (λ2 + λ3)/2)) and an estimated magnitude of diffusion parallel to fibre direction (axial diffusivity, λ1) can demonstrate more specific white matter pathology.

The tensor orientation distribution function described by the major eigenvector ellipsoid is an important measure for visualizing the diffusion tensor data. The practical way of visualization is the color map, which can be generated by calculating diffusion tensor derived indices on a voxel-by-voxel basis and is often represented as RGB (red-green-blue) with intensity proportional to the level of anisotropy. In color coded FA map, red indicates diffusion along right to left direction, green indicates diffusion along anterior-posterior direction and blue represents diffusion along the superior-inferior direction (Alexander et al., 2007).

The DTI derived maps of MD, FA, Eigen vector with color orientation and eigen values are shown in Figure 10. The identification of specific white matter tracts on the eigenvector color maps has proven useful for fibre tractography approach. Fibre tractography allows the visualization of cerebral axonal bundles based on DTI

measurements (Le Bihan et al., 2001). Several fibre tracking algorithms have been developed in recent years such as probabilistic (Parker et al., 2003) and deterministic tractography (Mori et al., 1999). The probabilistic tractography is capable of drawing all possible orientations instead of providing single tractectory in deterministic tractography.

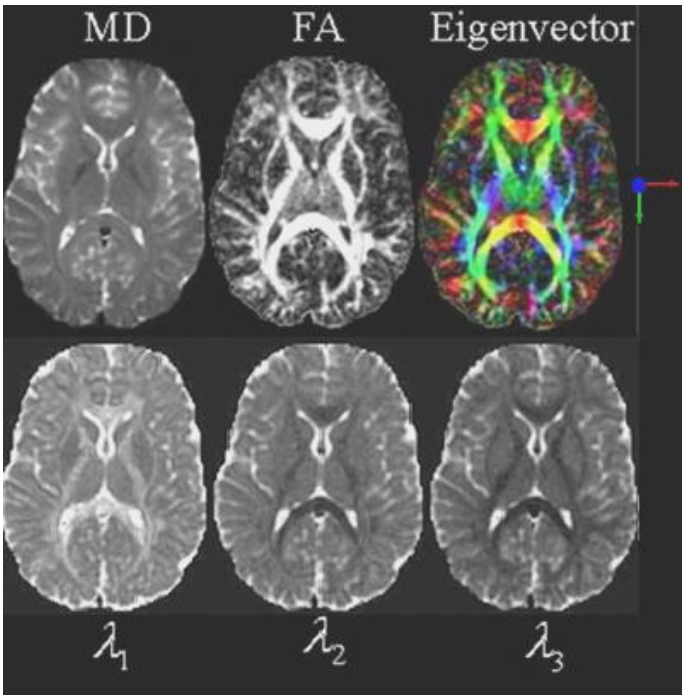

Figure 10: Maps of diffusion tensor data. Amongst, MD is mean diffusivity (describes average diffusivity in each voxel, CSF appears hyper intense due to the presence of free water in that region); FA is fractional anisotropy (describes degree of diffusion anisotropy in the brain; white matter appears hyper intense due to high anisotropy while the intensity for gray matter is low); the colour coded eigen vector (displays the orientation of white matter tracts, red = R/L, green = A/P, blue = S/I);

λ1, λ2 and λ3 are the eigen value corresponding to magnitude of diffusion along the major, intermediate and minor axis respectively.

II.8 Susceptibility Weighted Imaging

SWI is a novel MR imaging technique that exploits magnetic susceptibility differences between various tissues, such as blood, iron, copper and calcification in the brain to study pathologic conditions. It is a three-dimensional high spatial resolution fully velocity compensated gradient echo sequence which offers a unique contrast (Reichenbach et al., 1997; Haacke et al., 2007). Similar to T2* imaging, it relies on spin dephasing caused by local field inhomogeneities and uses phase information in addition to magnitude information. Phase images are used to map the field changes independent of the magnitude response, and hence becomes a robust means to measure iron content (Hackkee et al., 2005) and other substances that can make local changes in susceptibility. In SWI, the corrected phase image is used as a phase mask to enhance the novel contrast of the magnitude image (Haacke et al., 2004). Recently, SWI has been shown to be very sensitive in vivo marker of paramagnetic non- heme iron in the form of ferritin, hemosiderin, deoxyhemoglobin and transferrin (Reichenbach et al., 1997) and offers information about iron in the order of µg /g of tissue.

II.9 Structural MRI Analysis

Morphometric analysis of structural MR is widely used in neuroimaging to detect alterations in structural shape, volume and tissue density without a priori selection of

regions-of-interest. The most commonly used techniques are VBM (Ashburner & Friston, 2000), deformation or tensor-based morphometry (DBM/TBM) (Ashburner et al., 1998). Among these, DBM and TBM in reference to methods for studying brain shapes and VBM to identify volume differences between groups.

II.9.1 VBM

VBM techniques are developed to identify the brain morphometry and structural effect of neuroplasticity in the human brain. VBM is an automated and unbiased neuroimaging analysis technique that allows investigation of focal differences in brain anatomy, using the statistical approach known as statistical parametric mapping (SPM) (Ashburner & Friston, 2000). It involves a voxel-wise statistical comparison of the local concentration of gray and white matter density within or between two groups of subjects with minimal operator dependence. It has several advantages over traditional manual tracing and ROI based approach, which is laborious and time consuming. Since it is a whole-brain approach there is no need for a priori specification of relevant structures that should emerge from the analyses irrespective of the expectations of the investigators (Ashburner & Friston, 2000; Timmann et al., 2009). In essence, VBM analysis involves spatial normalistion of all the images to the same standard stereotactic space, extracting the GM, WM, and CSF, smoothing of the segmented GM and WM with an isotropic Guassian kernel to reduce the image noise, and finally performing a statistical analysis to obtain a statistical parametric map and make inferences about, group differences.

II.9.2 Processing steps in VBM

The processing steps include spatial normalization, segmentation, smoothing, and statistical analysis using VBM tool box of SPM (Statistical Parametric Mapping, Wellcome Trust Center for Neuroimaging, London; (Ashburner & Friston, 200) running in MATLAB (Mathworks, Natrick, MA).

II.9.2.1 Spatial Normalisation

Spatial normalization involves warping all the individual MR images to the same template image by minimizing the residual sum of squared differences between them. An ideal template is an average of a large number of MR images that have been registered in the same stereotactic space. The registration greatly adjusts for differences in head position or orientation in scanner and global brain shape differences. The registration utilizes different algorithms (Ashburner & Friston, 200; (Davatzikos et al., 2001) for transformation. The most commonly used is the 12-parameter affine transformation (3 translation, 3 rotation, shearing and zooming) followed by a nonlinear registration using a mean squared difference matching function (Ashburner & Friston, 2000). Hence the spatially normalized image should have a relatively high resolution and will free from partial volume effects during the segmentation of GM and WM.

II.9.2.2 Segmentation

Spatial normalization is then followed by segmentation into its tissue compartments (GM, WM and CSF) based on tissue probability maps (TPM) (Ashburner & Friston, 2000) as well as voxel intensity of each tissue type at individual voxels. During this

process, voxel intensity distributions that match with specific tissue types are identified and continuous probability maps are created. Further, a step called modulation is often applied to ensure that the total amount of specific tissue type in each voxel was conserved before and after spatial normalization. This is achieved by, multiplying the spatially normalized images by its relative volume before and after spatial normalization.

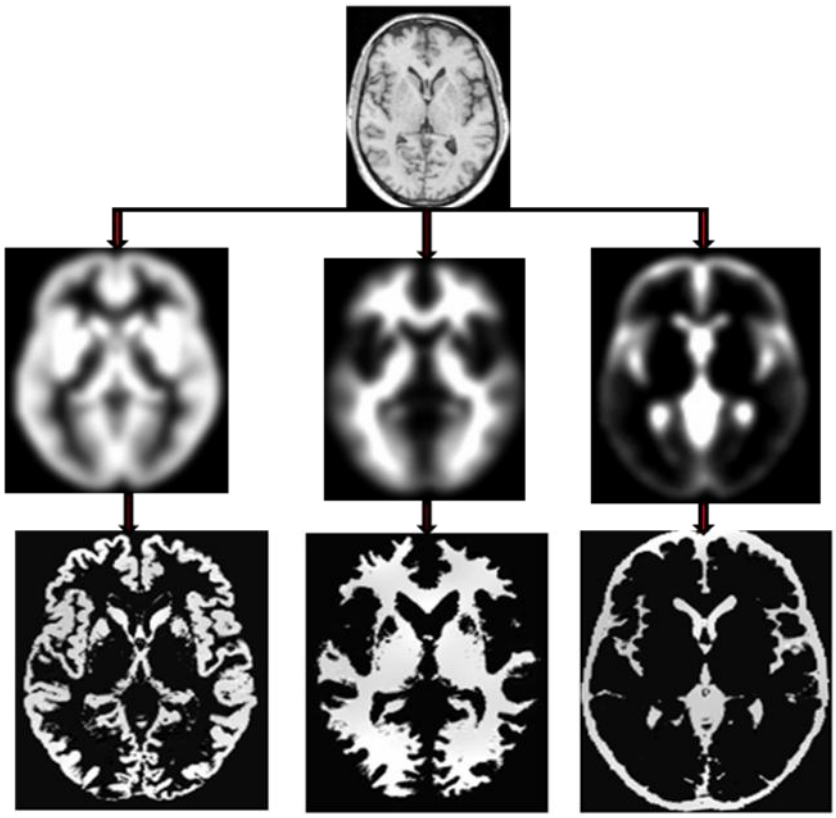

Figure 11: Segmentation of T1 weighted image into GM, WM and CSF. The top row shows a warped T1 image. The middle row shows the tissue probability maps of ICBM GM, WM and CSF. The bottom row shows the each segmented image of GM, WM and CSF.

II.9.2.3 Smoothing

The segmented and modulated tissue segments are then smoothed with an isotropic Guassian Kernel to improve the signal-to-noise ratio whereby the intensity of each voxel is replaced by the weighted average of the surrounding voxels. This resulted the blurring of segmented image and enable the data to be more normally distributed by the central limit theorem. The size of the smoothing kernel (8 mm or 12 mm FWHM) (Ashburner & Friston, 2001) should be comparable to the size of the expected regional differences between the groups of brains and its regional density. Smoothing increases the sensitivity to detect changes by reducing the variance across subjects, although excessive smoothing will diminish the ability to accurately localize change in the brain. Smoothing also has the effect of reducing the effective number of statistical comparisons, thus making the correction for multiple comparisons less severe.

II.9.2.4 Voxel wise statistical analysis

The final step of a VBM analysis involves a voxel-wise statistical analysis of tissue densities using SPM. This employs the general linear model (GLM) and the theory of Gaussian random fields that allows a variety of different statistical tests such as group comparisons and correlations with covariates of interest. The standard parametric statistical tests (T-test and F-test) are performed at every voxel in the image and the significance of any differences is ascertained using the theory of Gaussian random fields. If the statistical model is appropriate, the residuals are most

likely to be normally distributed once the segmented images have been smoothed. These analyses generate statistical parametric maps showing all voxels of the brain that refute the null hypothesis and show regions of significant change to a certain, user-selected, *p* value. Because of many voxel-wise statistical tests are performed, it is important to correct for multiple comparisons to prevent the occurrence of false positives. A couple of methods such as the family-wise error (FWE) (Friston et al., 1993) and false discovery rate (FDR) are used to perform such corrections, by which we can reduce the chance of false-positive results. The FWE correction controls the chance of any false positives across the entire volume, whereas the FDR correction controls the expected proportion of false positives among supra-threshold voxels.

II.10 Diffusion MRI Analysis

The structural connectivity of the human brain is fundamental to understanding the organization of the brain and its response to disease and injury. Multi-subject DTI analyses are developed to examine differences in anisotropic diffusion along specific white matter tracts. The directional information available through the DTI can be used to examine the routes of cerebral fibre pathways by voxel based analysis or tractography (Catani et al., 2002).

VBM style analyses are fully automated method adapted for the comparison of voxel-wise maps of Diffusion MRI derived parameters such as FA between subjects without pre-specifying regions/features of interest. As discussed in section (II.9),
VBM allows nonlinear registration of scalar images derived from diffusion datasets (most commonly FA maps) to a common target space, smoothing and mass

univariate analysis. The major limitations are the problems caused by registration accuracy of FA maps to a standard space, and the lack of a principled way to choose smoothing extent. These limitations led to the recent development of TBSS by Smith et al (Smith et al., 2006). It has the advantages of voxelwise character of VBM and tractography methods. TBSS is an open source tool available online as a free software download via the FMRIB Software Library (FSL) (http://www.fmrib.ox.ac.uk/fsl/) (Jenkinson et al., 2012). The methodological advances are made by solving alignment and smoothing issues and by being fully automated and covering the whole brain without prespecifying tracts.

In contrast to VBM, TBSS does not require precise spatial alignment and does not require smoothing (Smith et al., 2006). It is primarily defined by an approximate non-linear registration that is followed by generation of a skeletonised dataset by morphological thinning of the inter-subject mean FA. Essentially, the skeleton represents the centres of all fibre bundles that are common to the subjects involved in a study and over which paired voxel-wise statistics are performed. After this, each individual subject's FA image is projected onto the mean FA skeleton, by filling the skeleton with FA values from the nearest relevant tract centre. The final step is the voxelwise statistical analysis of skeleton space data. The more detailed steps involved in TBSS are given below.

II.10.1 Pre processing

Preprocessing involves both corrections for head motion during scanning and to reduce eddy current distortion effects created by the gradient coils of MRI. Head motion causes rigid-body image motion while eddy current appears as first order linear image transformation. *Eddy current correction* option in FSL corrects these distortions by using affine registration to a reference volume. After preprocessing, diffusion tensors can be calculated by a simple least squares fit of the tensor model for the diffusion data. The diffusion tensor eigen values (primary, secondary and tertiary) can be extracted from these diffusion tensors and then FA and MD values can be calculated. Finally, BET (brain extraction tool) is applied to exclude nondiffusion brain voxels (Smith, 2002).

II.10.2 Nonlinear alignment

This step for aligning multiple FA images to each other uses nonlinear alignment with intermediate degrees of freedom (DOF). The alignment preserves the fundamental nature of the image and keeps the general structure intact. The different ways to complete nonlinear registration are (a) Registering FA images to FMRIB58_FA standard-space image(software package) (b) Registering FA images to a user defined target image and (c) Registering to "most representative" target image selected from the subject data. Among these, first one is recommended as it involves only one registration for each subject. While the third one takes higher computation and longer time.

II.10.3 Creating a Mean FA Image and Skeletonisation

After selecting the most typical subject for the target, all FA images are aligned to this and the entire data is affine transformed into $1mm^3$ MNI152 space. The space is chosen for convenience to interpret and display the analysis result. The selection of higher resolution is to avoid significant interpolation blurring (increase in partial volume) with a slight decrease in processing speed. Then the transformed FA images are averaged to create a mean FA image. The resulting image is smoothed both due to averaging and resolution upsampling. The mean FA image fed for generating the skeleton image that represents the tracts 'common' to all individuals and its look like a single line running down the centre of the tract. The most contiguous set of tracts appears to be curved sheets with certain thickness, or tubes (Figure 12.A) and identifies voxels of the highest intensity, or FA.

The skeletonisation is started by estimating a local surface perpendicular direction in every voxel in the image, and then performing non-maximum suppression in this direction. This identifies the single voxel with the highest FA in the centre of the tract. After defining the perpendiculars, the skeleton is formed. In every voxel, its FA value is compared with the two neighboring voxels on each side. If the voxel has higher FA than neighbouring one, it is considered to be in the skeleton. This process can be repeated for all voxels to construct the skeleton tract. The FA skeleton formed is then thresholded to disregard tract areas with large intersubject variations. An optimum value of threshold between 0.2 and 0.3 has been shown to result in an appropriate skeleton (Smith et al., 2006). The topology of the skeleton can contain

disconnections in the tract structure due to the tract perpendicular direction is notwell-defined at junctions.

II.10.4 Projection of FA on to the skeleton

After skeletonisation, individual subject FA images are projected into the mean FA skeleton. This step aimed to compensate for residual misalignments after the initial registrations. Then a local search method is employed in perpendicular directions to find the maximum FA value of the individual subjects and assigned to the skeleton voxel (Figure 12.C). The perpendicular search strategy is constrained both in search length (up to the midpoint in between two tracts) and in probability function which deweights the potential center voxels if they are most distant from the skeleton position (a guassian kernel of 20 mm FWHM) .

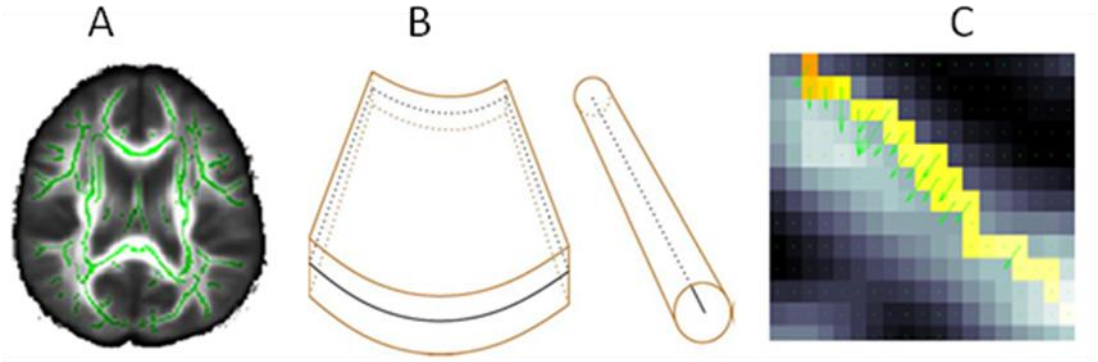

Figure 12 : Skeletonisation in TBSS. A) Mean FA image thinned to form FA skeleton B) Examples of white matter fibre bundles comprising a set of thick sheets with thin surface as skeleton or tubes with line as skeleton C) FA values projected onto the group skeleton to reduce the effect of mis-registration (Adapted from Smith 2006).

II.10.5 Statistics and Thresholding

The final step is the feeding of 4D skeletonised FA image into voxelwise cross subject statistical analysis. The simplest way to achieve this is univariate linear modeling, which is to analyse each skeleton voxel independently by generating the GLM across subjects. In order to find the local FA skeleton voxels which are significantly different between two groups, a two sample t test is preferred. Since the cross-subject null distribution of FA values is in Gaussian form, a simple parametric regression and inference can be used. Alternatively, group analysis can be done by multiple comparison permutation-based approach (Nichols & Holmes, 2002) by testing voxel t-value, cluster size or cluster mass against null distribution of maximum values of test statistics. This approach gives a strong control over family wise error.

II.11 Neuroimaging in FTD

II.11.1 Structural MRI studies

Structural imaging preferably with MRI is an essential tool for the diagnosis of FTD with focal degeneration. FTD encompasses a heterogeneous group of patients sharing unique patterns of brain atrophy with focal degeneration within the anterior frontal, temporal, and insular regions. The high resolution T1-weighted MRI images can be routinely used to exclude other diagnoses such as cancer and cerebrovascular disease and the pattern of atrophy which can differentiate FTD from other dementias. The first description regarding its potential value was in 1993 by Filley and Cullum in which they reported a single case of “putative FTD” with neuropsychological

evidence of extensive frontal system dysfunction with mild memory, language and visuospatial deficits. They reported that MR images were nonspecific in early course and revealed bilateral frontal and temporal atrophy with ventricular enlargement in later stages (Filley & Cullum, 1993). Later, Kitagaki et al analysed the MR images of FTD and AD and have confirmed the asymmentric pattern of frontal and anterior temporal atrophy in FTD patient (Kitagaki et al., 1998). Some studies in FTD have found frontal and asymmetrical atrophy (Miller & Gearhart, 1999; Duara et al., 1999) while others could not find any evidence for frontal and temporal atrophy in the early stages (Hokoishi et al., 1999; Gregory et al., 1999). Further, a lot of studies were conduted in which most of them aimed the differential diagnosis of AD, FTD and controls, and others look for an association between specific brain regions and specific cognitive deficits. Recently, there has been intensive research to identify biomarkers for disease progression, or to identify pathological phenotypes inaddition to clinical phenotypes.

The early imaging signatures in fvFTD often revealed consistent patterns of atrophy on MRI in the frontal lobes, involving medial, dorsolateral and orbitofrontal regions, as well as the anterior temporal lobes with relative sparing of posterior cortical regions, such as occipital lobe (Rosen et al., 2002; Boccardi et al., 2005). Rosen et al studied the patterns of atrophy in 20 controls, 8 fvfTD patients and 12 SD patients using VBM. They found a consistent pattern of atrophy in the bilateral frontal and left AC in both groups. Boccardi et al used VBM to study 26 control and 9 FTD subjects. They reported that the areas of loss correlated to rostral limbic system including AC, VMPFC, ventral striatum, AMYG, anterior insula and periaqueductal

gray. A scattered loss was found in the left frontal gyrus, including Brocas area and ITG. They highlighted the importance of rostral limbic system in the fine tuning of behavior and damage to this system may be responsible for the behavioural disturbances in fvFTD. A similar observation of involvement of anterior insula, AC and frontal lobes has found, although atrophy has also been observed in left anterior and medial temporal areas (Grossman et al., 2004).

Eventhough, the frontotemporal atrophy is supportive of the diagnosis of FTD, an associated variable pattern at the individual level and non affected posterior cortical involvement is reported (Seelaar et al., 2008). Atrophy in fvFTD is progressive in nature with rate of whole brain loss can be as fast as 3% in each year (Chan et al., 2001; Knopman et al., 2005). In the later stages, which have a high CDR score, in addition to anterior temporal and frontal lobe, the lateral and medial parietal lobes become affected (Whitwell et al., 2009a). Several studies have found asymmetrical patterns (Rosen et al., 2002; Boccardi et al., 2004; Du et al., 2007; Seeley et al., 2008; Whitwell et al., 2009a) often with right side predominance, which can help to differentiate fvFTD from AD and SD; where the left temporal lobe affection is predominant (Boccardi et al., 2003). In some fvFTD cases, a remarkable atrophy in anterior temporal lobe than frontal regions has been displayed (Whitwell et al., 2009b). Some studies have indicated the GM loss in other structure such as thalamus (Boccardi et al., 2005; Borroni et al., 2007; Seeley et al., 2008), striatum (Boccardi et al., 2005; Seeley et al., 2008) and hypothalamus (Piguet et al., 2011). Earlier VBM studies in fvFTD have demonstrated hippocampal atrophy (Boccardi et al., 2005; Seeley et al 2008). Pan P et al in 2012 performed a Meta analysis of VBM studies of

fvFTD patients and healthy controls from 2000 to June 2011 (Pan et al., 2012). They have analysed 11 VBM studies involving 237 fvFTD patients and 297 controls and detected GM volume loss in the anterior medial frontal cortex (BA 9), extending to other frontal areas (BA 8, 10, 46, 24, 32), and other areas, such as the insula cortex, as well as the subcortical striatal regions in patients with fvFTD. The meta-analysis provided the evidence of GM changes in the frontal-striatal-limbic, fronto-insular cortex and AC. A recent study in 80 fvFTD subjects has been showed symmetric patterns in majority of fvFTD patients (65%), although some have left (20%) or right (15%) dominant patterns (Whitwell et al., 2013).

In the typical variant of SD, a characteristic 'knife- edge' atrophy of anterior posterior gradient is observed with marked degeneration in anterior temporal lobes. Mummery et al was the first to study the anatomical damage in SD using VBM (Mummery et al., 2000). Mummery et al described a study involving 6 SD patients and 14 controls using VBM and identified a most consistent damage in temporal pole in correlation with semantic memory impairement. They also found an extended atrophy to anterior, lateral and medial temporal lobe with left-greater-than (L>R) asymmetry, with lesser involvement of right temporal pole and amygdala. A severe degeneration is observed in FG, HP, TP, AMYG, ITG, entorhinal cortex (EC) and MTG (Mummery et al., 2000; Chan et al., 2001). The bilateral pattern in SD has been detected, although the severity usually greater on the left side (Rosen et al., 2002; Gornotempini et al., 2004). However, patients with greater right hemisphere (Thompson et al., 2003; Chan et al., 2009; Josephs et al., 2009) are also observed in

which they experienced problems in recognizing familiar faces and showed more behavioural abnormalities than leftsided SD (Thompson et al., 2003; Josephs et al., 2009). Longitudinal neuroimaging studies have shown a spread of atrophy throughout both temporal lobes (Whitwell et al., 2004; Rohrer et al., 2008; Frings et al., 2012) and the least affected lobe at baseline progresses faster and 'catch up' with most affected, resulting a bilatteral temporal patterns in later course. Although, the anterior temporal atrophy is common in fvfTD and SD, the greater degree of frontal lobe and therefore, the ratio of temporal to frontal atrophy may be the most diagnostically useful measure to distinguish fvFTD and SD (Frings et al., 2012).

Patients with PNFA associated with GM loss target the Broca's area in the inferior frontal gyrus and the superior premotor cortex (Nestor et al., 2003; Gorno-Tempini et al., 2004). In MRI, it usually appeared as widening of perisylvian fissure along with inferior frontal gyrus atrophy. Rohrer et al studied cortical thickness measurement in PNFA and described the involvement of left frontal, lateral temporal and anterior parietal lobes in severe group (Rohrer et al., 2009). Gunawardena and colleagues provided evidence that deficits with grammatical processing associated with left inferior frontal and anterior-superior temporal thinning which is the probable reason for non-fluent speech in PNFA (Gunawardena et al., 2010). In contrast to other variants, a relative sparing of anterio temporal lobe was seen in PNFA. Atrophy is often progressive with faster progression in frontal lobes (Whitwell et al., 2004).

II.11.2 Diffusion MRI

To date, fewer diffusion imaging studies in FTD in comparison to structural MRI. One of first studies by Larsson et al reported reduced anisotropy in the frontal lobes of an FTD brain which had been preserved in formalin (Larsson et al., 2004). Later, Yoshiura et al have found abnormal MD elevation in frontal and temporal lobes of FTD patients using visual rating scales (Yoshiura et al., 2006).

White matter degeneration is specific to variants also. Borroni et al carried out a VBM analysis of FA maps in a group of 28 fvFTD, 8 temporal variant (tvFTD) and 23 controls (Borroni et al., 2007). They showed a selective WM reduction in SLF of fvFTD and ILF of tvFTD patients respectively. Group studies have shown bilatteral and widespread WM integrity changes in tracts connecting frontal and temporal lobes including SLF, anterior cingulum, GCC, UF, and ILF (Borroni et al., 2007; Zhang et al., 2009; Whitwell et al., 2010; Agosta et al., 2012a). Eventhough the most severe changes observed in anterior portions of the frontal and temporal lobes, involvement of PC and posterior part of SLF has been demonstrated. This fact may reflect the involvement of lateral and medial parietal lobe early in some fvFTD patients, but can also detect the progression of disease in others. Studies demonstrated that reduced diffusivity in the anterior CC can differentiate fvFTD from other variants (Zhang et al., 2009; Agosta et al., 2012a).

In SD patients, disintegeration of temporal lobe WM tracts particularly has been reported (Whitwell et al., 2010; Acosta-Cabronero et al., 2011). Whitwell et al

demonstrated WM tract diffusivity changes in the left anterior and posterior ILF and left UF of SD patients (Whitwell et al., 2010). Studies have shown that the greater degeneration of ILF in SD can differentiate it from other variants (Whitwell et al., 2010; Agosta et al., 2012a). The WM tract pathologies in PNFA has been observed throughout the left SLF (Whitwell et al., 2010; Galantucci et al., 2011) particularly the arcuate fasciculus that projects into the inferior frontal lobe. Galantucci et al analysed the PPA syndromes using probabilistic tractography. They compared the mean FA, axial and radial diffusivities in 48 patients and 21 controls. They reported greatest changes in all metrics in PNFA; severe changes in SD and least in logopenic variant.

II.11.3 Grey and white matter degeneration contribute to apathy and disinhibition

Previous studies have refined the association between behavioral abnormalities and neuroimaging features in fvFTD. In addition, the role of right temporal lobe in behavioural features have been described previously (Thompson et al., 2003; Zamboni et al., 2008) and suggest that variability in behavioural presentation may mirror anatomic variability. It has also been demonstrated that fvFTD can show differing patterns of atrophy according to behavioural profile and pathology (Liu et al., 2004). Similarly a high frequency of apathy in cohorts of fvFTD subjects noted previously (Levy & Dubois, 2006; Rosen et al., 2005). VBM study by Rosen et al in a heterogeneous cohort of dementia patients related apathy to atrophy in ventromedial frontal regions (Rosen et al., 2005). Specifically, studies have found

that apathetic patients associated with dorsolateral and medial frontal changes, while disinhibited patients associated with orbitofrontal and temporal lobe changes (Massimo et al., 2009). VBM studies in fvFTD identified an association between disease in bilateral medial, orbital, inferior, and dorsolateral frontal areas, as well as bilateral anterior temporal and right caudate regions and apathy (Zamboni et al., 2008; Massimo et al., 2009). VBM analyses have also related disinhibition to atrophy in these orbitofrontal, dorsolateral, and medial prefrontal gray matter regions, as well as anterior and medial temporal gray matter regions (Liu et al., 2004; Zamboni et al., 2008; Hornberger et al., 2011). Some previous findings have also demonstrated associations between disinhibition and the temporal lobes (Liu et al., 2004; Zamboni et al., 2008).

WM disease has also been implicated in the apathy and disinhibitory profile in fvFTD patients. A recent study by Power et al found that damage in left UF associated with apathy (Powers et al., 2014). A previous study using ROI analysis has shown a relationship between FA in the right SLF and disinhibition measured by FBI (Borroni et al., 2007). Hornberger et al, using TBSS found that FA in the UF, cingulum and forceps minor correlated with disinhibition measured by hayling test (Hornberger et al., 2011). Power et al also found that disruption in right corona radiata related to disinhibition. The above observations provide the notion that the neuroanatomical correlates of these behavioural profiles have been more variable and less clear. The variability across studies may be due to different populations and different analysis methods hence need to be verified in a homogenous patient group with sophisticated measures.

II.11.4 Quantitative iron measurement using MRI

Several neurodegenerative brain disorders including Alzheimer's disease (Bartzokis and Tishler, 2000), Parkinson's disease (Wallis et al., 2008; Gupta et al., 2010), multiple sclerosis (Bagnato et al., 2011) and ALS (Kwan et al., 2012) have been associated with region-specific iron accumulation. Neuroimaging techniques which can invivo quantify this tissue iron include T2, T2*, magnetic field correlation (MFC), field-dependent relaxation rate increase (FDRI) and SWI (Péran et al., 2007; Bartzokis et al., 2007; Harder et al., 2008; Sheelakumari et al., 2015). Recently, studies involved the in vivo quantitative estimation of iron in AD has been increased (Wang et al., 2013; Raven et al., 2013). However, only postmortem findings reported in Pick disease (Ehmann et al., 1984) and FTD-ALS (Santillo et al., 2009).

The previous detection of micro-bleeds in the basal ganglia regions using postmortem study in FTD demonstrated a trend of increase in iron levels. Recently, another postmortem by the same investigator using 7T MRI identified significant iron deposition (De Reuck et al., 2014). They have examined one hundred and fifty two postmortem brains including AD (46), FTD (37), ALS (11), Lewy body dementia (LBD, 13), PSP (14), VaD (16) and controls (15). They identified significantly increased iron load in the claustrum, caudate nucleus and putamen of FTLD brains and to a lesser degree in the globus pallidus, thalamus and subthalamic nucleus. However, invivo quantitative estimation in FTD is still unknown.

III DESIGN OF THE STUDY

III.1 Subjects

A case control study design was followed to meet the objectives of the study. Patients were selected from the decade old well-established Dementia Clinic in the Department Of Neurology, Sree Chitra Tirunal Institute for Medical Sciences and Technology (SCTIMST), Thiruvananthapuram, Kerala during the period 2010- 2014. The diagnosis of FTD was established using published diagnostic criteria (Neary et al., 1998). All fvFTD patients met recent clinical criteria (Rascovsky et al., 2011). PPA patients were then diagnosed (Mesulam 2001) and classified (nonfluent and semantic) based on diagnostic guidelines by an international group of PPA investigators (Gornotempini et al., 2011).

Participants underwent a detailed historic and neurological examination, neuropsychological evaluation, behavioural assessment and a high quality MRI scan. All these evaluations were repeated at 1 year follow up. Patients were included if they had a history of progressive change in personality and behavior such as apathy, disinhibition, loss of empathy, lack of insight and foresight, reduced verbal output, poor planning and judgment, perseveration, distractibility and impulsiveness. Also we excluded patients who had a past history of cerebral ischemic infraction or hemorrhage, head trauma, alcohol abuse, cardio vascular and major psychiatric diseases, past history of depressive illness and epilepsy or other neurological disorders. After the screening the subjects were stratified into fvFTD, SD and PNFA.

For all the patients, duration of illness was defined as the estimated onset of behavioural symptoms to the date of MR imaging. Assessment was conducted to get information on activities of daily living (self care, using domestic appliances, concentration, communication, orientation, using public transport, participation in social activities, taking medications and handling finances), Age of onset, education and occupational history, family history of dementia or other neurological diseases, and substance abuse from proxy informant. For all the patients, duration of illness was defined as the estimated onset of behavioural symptoms to the date of MR imaging.

Normal healthy age matched controls with no past history of neurological and psychiatric diseases, and no contraindications of neuroimaging were recruited from the first degree relatives (mostly spouses) of patients and the SCTIMST control cohort. The study was approved by the Institutional Ethics committee of SCTIMST and written informed consent was obtained from all subjects and patient relative and care-giver.

The original data set of current study included a total of 90 subjects: 55 patients with FTD (39 with fvFTD, 16 with PPA= 10 SD and 6 PNFA)) and 35 normal controls. Out of these patients, 5 fvFTD and 4 PPA (two from each group) were excluded due to poor MRI quality and movement artifacts. As well, during the study period, one control subject developed memory complaints and hence excluded from further

analysis. The final set consisted of 34 fvFTD, 12 PPA and 34 controls. The flow diagram of proposed study is given below (Figure 13).

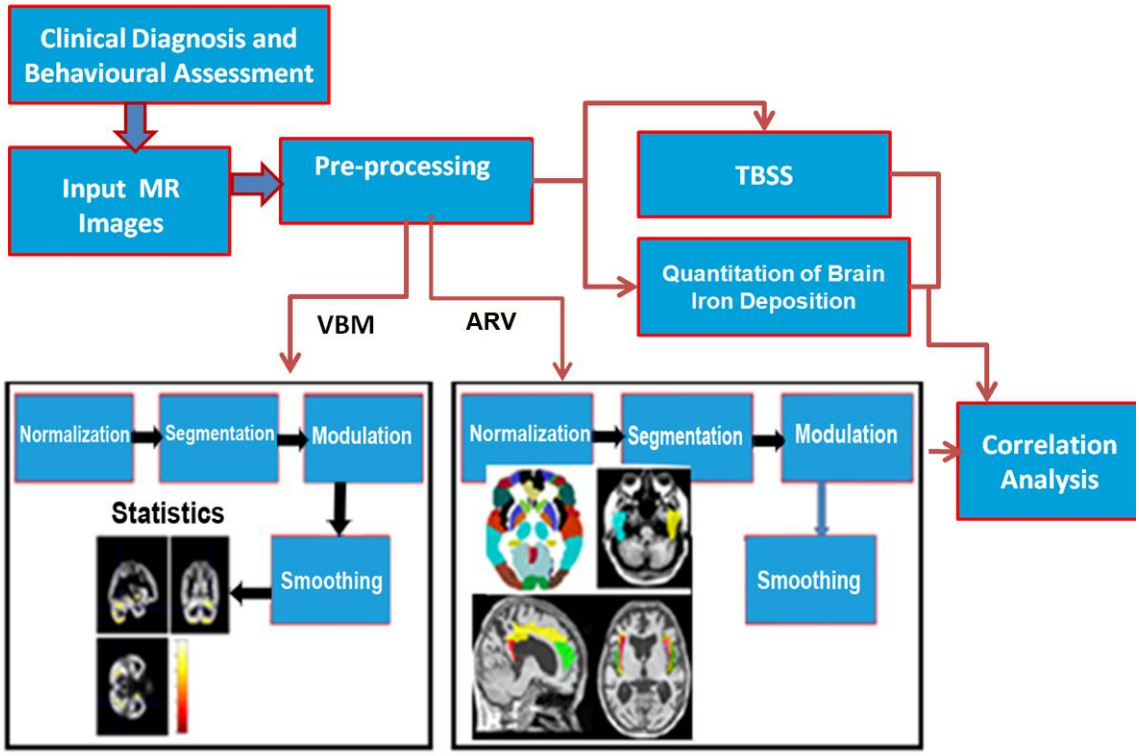

Figure 13: Workflow of Proposed study

III.2 Neuropsychological evaluation

All patients were administered neuropsychological test battery (Table 1).

Table 1: A brief description of neuropsychological tests used in the study

Test	Description of test
Mini Mental State Examination,(MMSE, (Folstein et al., 1975)	A brief test that measures orientation to time and place, registration of three words, attention and calculation, recall language and visual construction.
Malayalam adaptation of the Addenbrooke's Cognitive Examination (ACE)(Mathuranath et al., 2004)	It comprised of component scores to assess six cognitive domains, including orientation, attention, memory, verbal fluency, language, and visuospatial skills
Clinical Dementia Rating scale	A global scale developed to note the disease stage and severity. It mainly comprises six domains: memory, orientation, judgment and problem solving, community affairs, home and hobbies, and personal care.
Semantic Battery- Confrontaion Naming (Mathuranath and George, 2005)	Tested using 55 item version of the semantic battery naming test. The participants were presented with visual stimuli of black-and-white line drawings.
Semantic battery- Verbal Fluency (Mickanin et al., 1994)	Letter (Phonemic) fluency test to generate words beginning with |P|,|K| and |S|, other than people or places. Responses were recorded for 1 minute each for each phoneme. Category (semantic fluency) fluency test to generate semantic categories: animals, fruits-vegetables and household objects without repetition. The responses were recorded for 1 minute each for each category.

Weschler Memory Scale Digit span (Wechsler, 1981)	It is the subtest of Weschler scales, comprised of digits span forward (DF) and digits span back ward (DB). DF primarily taps short-term auditory memory, sequencing, and simple verbal expression while DB measures deficits in working memory
Hospital Anxiety and depression scale (Zigmond and Snaith, 1983)	It is a self-report screening scale that intend to measure depression and anxiety in patients within and outside hospital and community settings, avoiding any evident physical problems. Both anxiety and depression consists of 7-item subscale and are rated from 0 to 3.
Trail making Test A,B(Reitan, 1958)	It is a measure of attention, visual searching, mental processing speed, and mental flexibility. Part A measures processing speed (to draw lines to connect consecutive numbers) and Part B measures the ability to flexibly shift the course of an ongoing activity (to draw lines alternating between numbers and letters). Part A tests requires visual searching, numeric sequencing, and motor coordination while Part B tests,cognitive task performance which requires motivation, problem solving, visual motor and visual spatial abilities and mental flexibility.The part B is considered as sensitive test for frontal lobe dysfunction. Both are timed and scores are represented interms of time taken and errors.

III.3 Behavioral assessments

FrSBe, a 46 item behavior scale was administered to measure behavior syndromes associated with frontal sub-cortical brain deficits (Malloy et al., 2007). Each of the 46 items on the FrSBe deals with a specific behavior and its frequency rated from 1(Almost never) to 5(Almost always). The subscales are apathy/abulia (14 items), Disinhibition (15 items) and executive dysfunction (17 items). Hence it gives a total and a component score. FrSBe consists of a Self assessment form (to be completed by patient) and carer assessment form (to be completed by spouses or other family members) which were administered at the same time. After completing the scoring, T scores-on each subscale were obtained by the normative data supplied by the publisher (Stout et al., 2003). A score of 65 or greater is considered as clinically relevant and severity of disease/ insult increases with increase in score.

III.4 Image Acquisition

MRI data acquisition was performed on a 1.5 Tesla Scanner (Avanto SQ engine, Siemens, Erlangen, Germany) using transmit receive head coil array with 12 elements. During scanning, foam padding was used to limit head motion and ear plugs were used to reduce scanner noise. All patients and controls underwent same scanning protocol. The protocol included a whole-brain high resolution structural imaging, multi slice diffusion tensor imaging, and susceptibility weighted imaging. The 3D T1 weighted anatomical scans were acquired using a spoiled gradient recalled Echo Sequence((3-D FLASH (Fast Low Angle Shot) with following

parameters TR 11 ms , TE 4.95 ms, flip angle 15^0 and a matrix size of 256x256, slice thickness 1mm, voxel size 1x1x1mm and 176 sagittal slices.

Then diffusion tensor images were acquired using a single-shot spin echo echo-planar sequence. For the acquisition, diffusion sensitizing gradients were applied in 30 non-collinear directions with the following imaging parameters TR 5400 ms, TE 88 ms, matrix 112 × 108, field of view 220 mm, 3mm slice thickness with 1.5 mm gap averaged twice and with b values of 0 and 1000 s/mm^2.

SWI images were obtained with a 3D spoiled gradient recalled echo sequence (TR/TE: 49 ms/40 ms, flip angle: 200, slice thickness: 2.1 mm, no of slices: 56, matrix: 260x 320). All the MR images were stored in Digital Imaging and Communications in Medicine (DICOM) format.

III.5 Image Analysis

III.5.1 Analysis of GM atrophy

III.5.1.1 Voxel Based Morphometry

All the structural images were checked for artifacts and images with poor resolution and low contrast were eliminated. The volumetric DICOM data were first converted to '.dcm 'format using BRAIN VOYAGER licensed software and then to 'nifti' format using 'MRICONVERT'. Then the cortical GM changes across the entire brain was analysed using the VBM8 toolbox (version 435; University of Jena,

Department of Psychiatry) in SPM 8 (Functional imaging laboratory, University College of London, UK) implemented in Matlab 7.4 (Mathworks Inc., Sherborn, Mass., USA). A detailed description of the steps involved in SPM processing is explained in section (II.9.1).

All the images were oriented in the AC-PC line and were normalized into Montreal Neurological Institute (MNI) template using "Estimate and Write"estimation option in VBM (Figure 14). After Dartel normalization, the images were segmented into GM, WM, and CSF using an automated Bayesian algorithm (Ashburner & Friston, 2000). Image intensity non-uniformity correction is incorporated to account for the smooth intensity variation caused by different positions of cranial structures within the MRI coil. The tissue classification based on a posteriori probability values between zero and one. Segmentation was performed by the default settings, except for 'clean up' in which 'light-clean up' was used to remove any remaining non-brain tissue as advocated by the VBM-8 manual. The segmentation is then followed by modulation, for preserving the volume of a particular tissue in a fixed voxel and the volumes of GM, WM, CSF and TIV were calculated. The segmented and modulated normalized gray matter images were smoothed with an isotropic Guassian kernel of 12 mm full width a half-maximum (FWHM) filter, which minimizes the error related to inter-subject variability in local gyral anatomy and the risk of false positives (Salmond et al., 2002). This smoothed image was further used for volumetric analysis and statistical comparison.

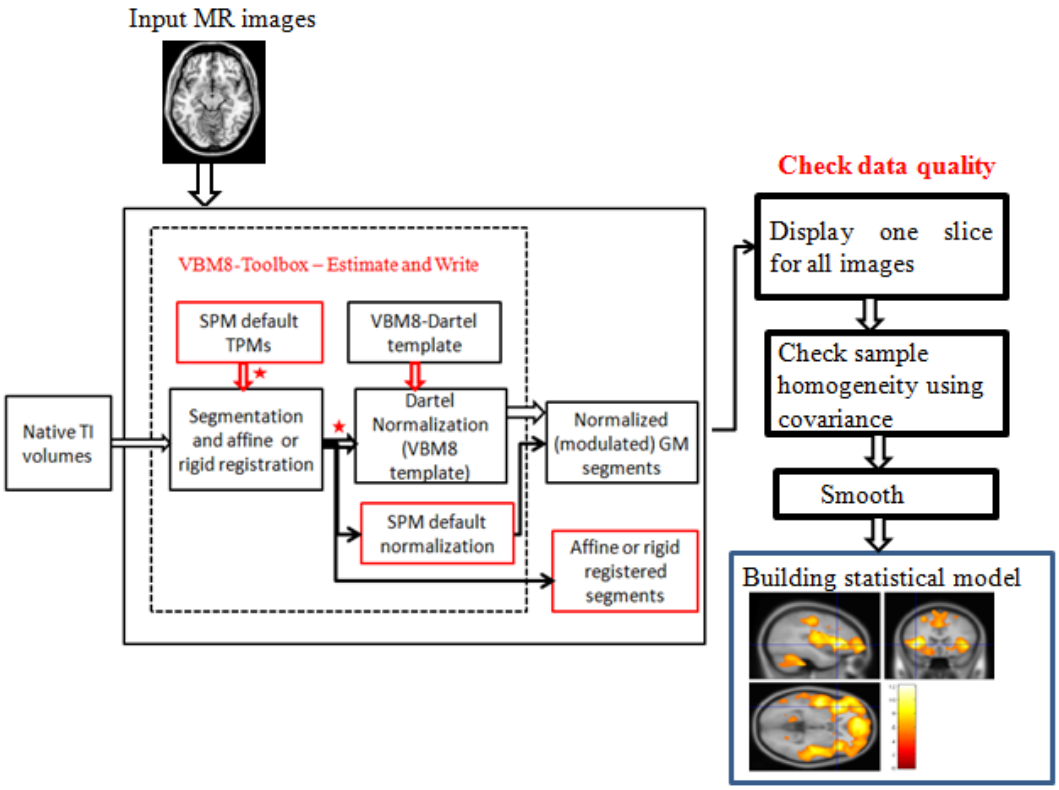

Figure 14 : Block diagram of VBM processing steps

The voxel wise statistical comparison between patients and controls were performed using ANOVA within the SPM8 general linear model. For group comparisons, age and sex were entered into the design matrix as nuisance variables and TIV was entered as a global correction factor. Posthoc comparisons were made using four separate contrasts (a) fvfTD < Controls, (b) PPA< Controls, (c) fvFTD<PPA and (d) PPA< fvFTD. The statistical threshold for significance was initially set to P<0.05, FDR corrected with an additional cluster extent threshold of 30 contiguous voxels. In those contrasts that did not survive for multiple comparisons, results were obtained at an uncorrected threshold of P<0.001.

The significant atrophic regions were overlaid on T1 weighted standard brain images, allowing the localization of areas of significant GM loss. The atrophic regions are reported in MNI coordinates with the help of xjview toolbox (http://www.alivelearn.net/xjview/). Subsequently, a multiple regression analysis was performed to determine the correlation between specific behavioural manifestation in fvFTD and reduced gray matter density. For that, the FrSBe T scores of subscales A, and D were entered as regressors in to the design matrix with age, sex and TIV as confounding covariates. The analysis were conducted at a significance level of $P<0.001$, uncorrected with an additional cluster extent threshold of 30 contiguous voxels.

III.5.1.2 Automated Regional Volumetry (ARV)

The volumetric analysis of cortical GM structures was performed by using segmentation algorithm in SPM8 and masks derived from Automated Anatomic Labelling (AAL)(Tzourio-Mazoyer et al., 2002), a digital brain atlas provided by the Neurofunctional Imaging Group (GIN, UMR6095, CYCERON, Caen, France, http://www.cyceron.fr/web/aal) (Figure 15) .

Based on the whole brain findings in the FTD subjects, the target structures were chosen apriori in ARV. The current study included 30 ROI's (Frontal Lobe; Middle frontal Gyrus (MFG), Middle orbitofrontal Gyrus (MOFG), Inferior Orbitofrontal Gyrus (IOFG), Superior frontal Gyrus (SFG), Superior Orbitofrontal Gyrus (SOFG),

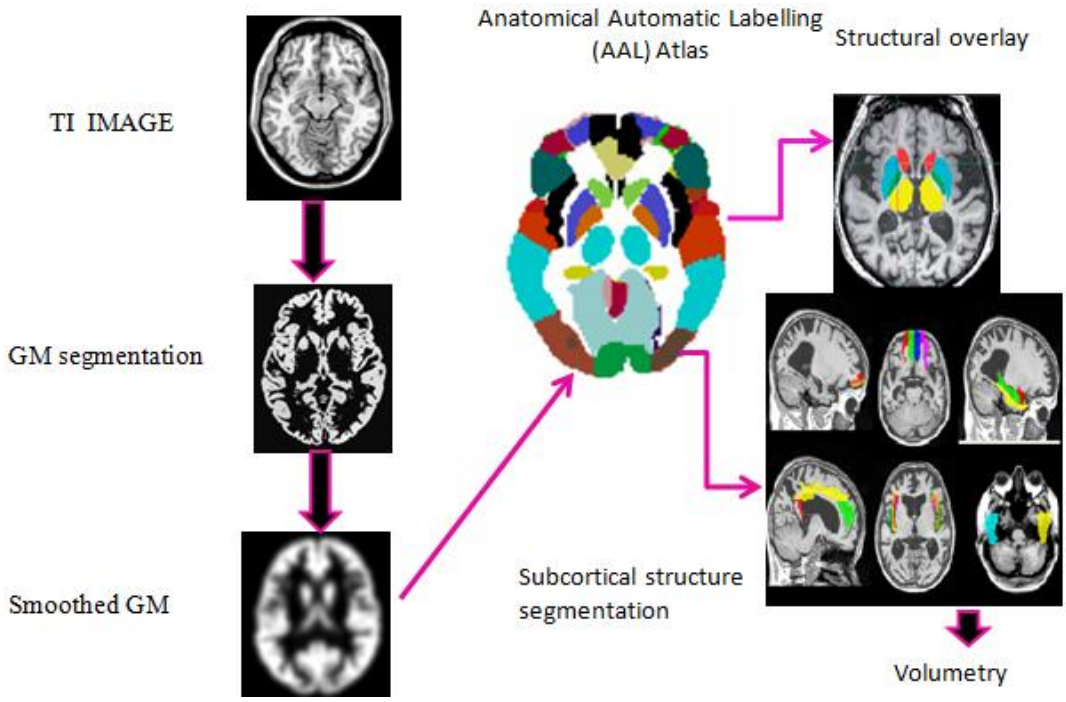

Figure 15: Flow Diagram of Automated Regional Segmentation

Inferior frontal Opercular Gyrus (IFOperG), Inferior frontal Triangular Gyrus (IFTriG), Rolandic operular Gyrus (RoperG), Supplementary Motor Area (SMA), Olfactory cortex (OC), Superior Medial Orbito frontal Gyrus (SMedOFG), Gyrus Rectus (RECG), **Insula and Cingulate Gyri**: Insula (IN), Anterior Cingulate (AC), Middle Cingulate (MC), Posterior Cingulate (PC), **Subcortical structures:** Caudate (CAU), Putamine (PUT), Thalamus(TH), **Temporal Lobe:** Hippocampus (HP) , Para Hippocampus (PHP), Amygdala(AMY), Fusiform Gyrus (FG), Heschyl Gyrus (HG), Superior Temporal Gyrus (STG) , Middle Temporal Gyrus (MTG), Inferior Temporal Gyrus (ITG), Superior Temporal pole (STP), Middle Temporal pole (MTP), **Occipital Lobe:** Calcarine (CL)) (Figure 16) of the AAL atlas for analyses of group differences in volume.

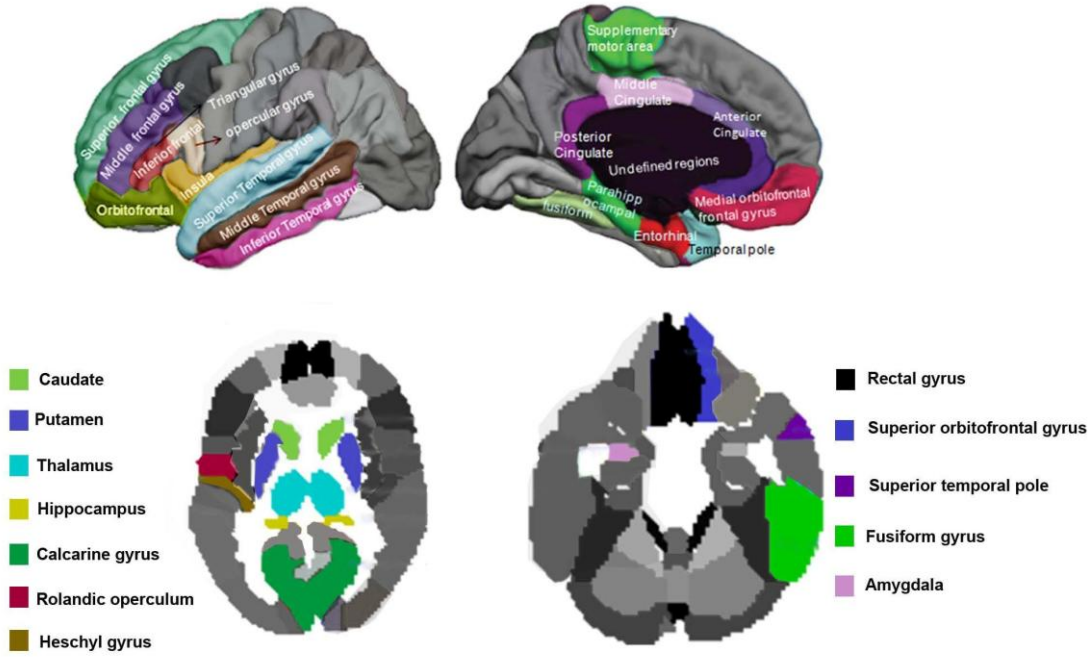

Figure 16: ROI's selected for the Volumetric Analysis

In order to obtain the volume of a specific brain structure of interest, the binary mask of corresponding structure derived from the AAL atlas was multiplied with the smoothed image of GM tissue using the image calculator (ImCalc) of SPM8. The total volume of the investigated gray matter structures in milliliter units were obtained by summing up the values of all voxels, and then dividing by 1,000.

III.5.2 WM Structural Integrity

III.5.2.1 Voxel-wise Analysis

Prior to analysis, all diffusion images were visually inspected for artifacts. The raw DICOM images were converted into nifti format using the 'dcm2nii' program found at "www.sph.sc.edu/comd/rorden/dicom.html". Then data analysis was carried out offline by using FSL 5.0 (FMRIB Software Library tools, www.fmrib. ox.ac.uk/fsl).

The images were preprocessed using 'Eddy Current correction' by registering all the images to a b=0 s/mm2 diffusion image which is to correct for distortions due to the gradient directions applied (Figure 17). The diffusion tensor model for each voxel was calculated by DTI Fit in FSL software (http://www.fmrib.ox.ac.uk/fsl/fdt) that generates eigenvectors (v1, v2, v3), eigenvalues (λ1, λ2, λ3), mean diffusivity, FA, and S0 (raw T2 signal with no diffusion weighting).

Whole brain voxel wise statistical analysis of the FA and MD data were performed by TBSS (Smith et al., 2006), part of FSL tool box. FA and MD maps of individual subject brain was registered to a common space (MNI152) using FMRIB's Non-linear Image Registration Tool (FNIRT). The mean FA image was then generated and thinned to create a mean FA skeleton. The mean FA skeleton represents the centers of all of the tracts that are common to all the subjects. The FA skeleton was thresholded at 0.2 to exclude voxels with GM or CSF. Finally, each subject's aligned FA data were projected onto this mean FA skeleton and the final skeletonised data were fed into voxel wise cross-subject statistical modeling. A voxel by voxel permutation nonparametric test was built up over 5000 permutations to assess group-related differences using thresholdfree cluster enhancement (TFCE), controlling for age, sex, and total brain volume. The results were observed significant at $p<0.05$, TFCE, corrected for multiple comparisons across space ((Family wise Error Rate, FWE). Moreover, a multiple regression analysis was performed using the FrSBe subscale scores and age and gender as nuisance variables in the GLM to study the relationship between behavior score and FA values.

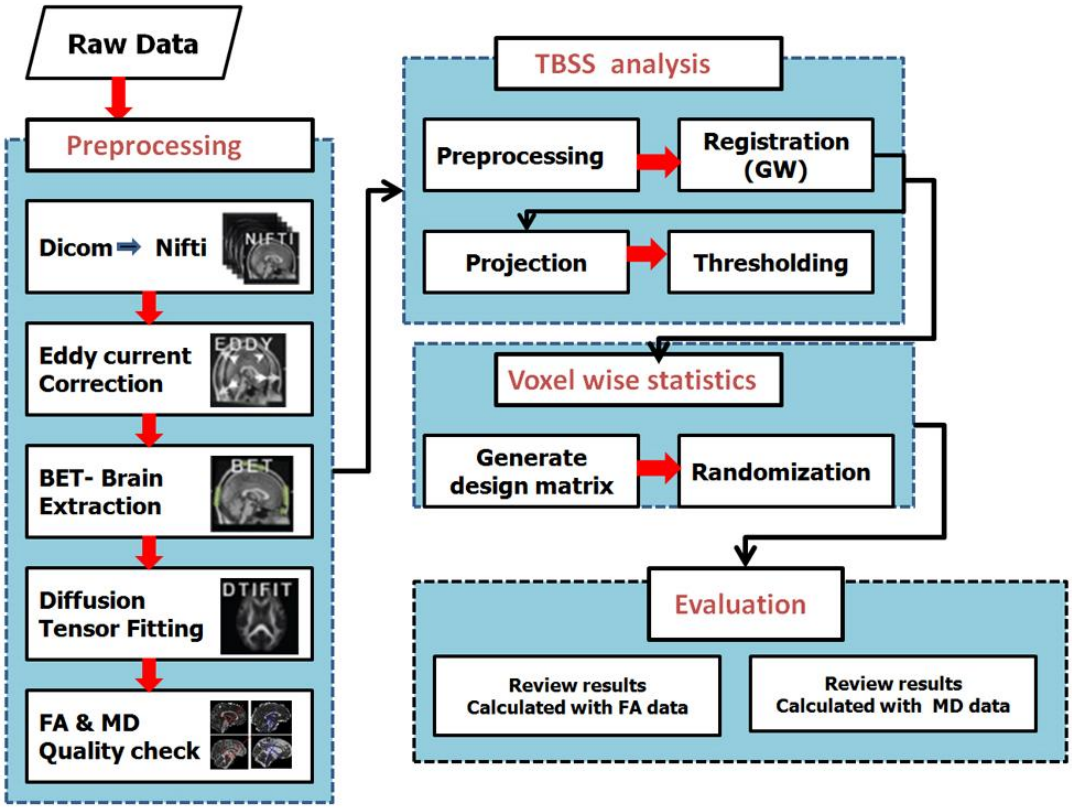

Figure 17: Pipe line of Tract based Spatial Statistics

III.5.2.2 White matter Tract of Interest Measurements

Voxel-wise analysis in patients with FTD have shown significant WM degenerations in UF (interconnecting limbic system in temporal lobe with OFC), ILF (interconnecting anterior temporal lobe and posterior occipital pole), SLF (interconnecting dorsolateral frontal lobe and posterior associative areas including occipital, parietal, and temporal lobes), cingulum (tracts inter connecting the precuneus/PC and medial frontal cortex), genu (tracts connecting frontal poles through the anterior corpous callosum) and splenum of corpus callosum. So in the present study, an ROI analysis was done by creating the masks of above mentioned

tracts from the two white matter atlases within FSL, Johns Hopkins University, White-Matter tractography atlas and ICBM-DTI-81 labels (Wakana et al., 2007). The ROI masks were loaded onto the skeletonised DTI data and corresponding FA and MD values were derived bilaterally.

III.5.3 Quantitative Analysis of Cortical Brain Iron deposition

All the SWI mages were visually examined in the regular clinical settings by two experienced neuroradiologists and a neurologist with more than 15 years of experience in their respective fields. ROI based quantitative analysis of regional Fe content was performed using SPIN (Signal processing In Nmri, MRI Institute for Biomedical Research Detroit, MI, USA) software. The SWI images were magnified two times and the ROIs were drawn manually on respective slices with extreme care to minimize partial volume effects. The ROIs drawn on both hemispheres included: the GM at the precentral gyrus just anterior to central sulcus (PBMC), adjacent subcortical WM and CSF in the central sulcus, superior frontal gyrus medial to superior frontal sulcus (SFG), anterior pat of superior temporal gyrus, basal ganglia regions, substantia nigra, red nucleus, frontal WM, anterior cingulate, hippocampus and dentate nucleus (Figure 18). The ROIs were copied to phase images for obtaining the mean phase shift values within. For all the subjects, phase values were measured by the two observers to determine the inter-observer agreement.

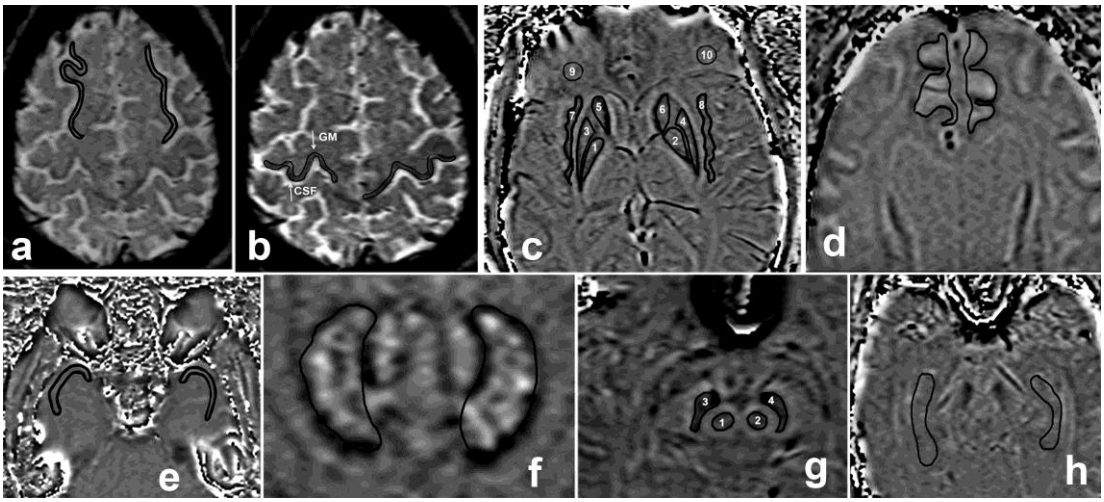

Figure 18: Representative slice in fvFTD subject showing regions of interest where phase is measured in a) superior frontal gyrus medial to superior frontal sulcus (SFG) b) the precentral gyrus just anterior to central sulcus GM, and central sulcus CSF(PCG) c) the globus pallidus(GP:1,2), putamen(PUT:3,4) and caudate nucleus(CAU: 5,6) , insula (IN:7,8), and frontal white matter(FWM:9,10) d) anterior cingulate (AC) e) anterior part of superior temporal gyrus (STG) f) dentate nucleus(DN) g) red nucleus (RN: 1,2), substantia nigra (SN:3,4) and h)hippocampus(HP).

In the corrected phase images there is a direct correlation between the phase and iron content of the tissue. For a left hand system, phase is given by the relation

$$\varphi(phase) = \gamma.\Delta B.T_E \qquad 10$$

Whereγ, ΔB , $.T_E$ represents the gyromagnetic ratio, the magnetic field change between tissues and echo time (millisec)respectively. Iron is a paramagnetic element

it aligns with the main magnetic field and thus creates a positive ΔB. Thus the larger the iron content in the tissue the larger will be the value of ΔB and thus larger the phase change φ relative to its surroundings.

$$\Delta B = \Delta_\chi B_0 \qquad 11$$

$$\Delta_\chi \propto c \qquad 12$$

Where Δ_χ, the change in susceptibility and c is the concentration of iron.

Our MRI processing uses the phase convention

$$\emptyset = 2048\left[\left(\frac{\phi}{\pi}\right) + 1\right] \qquad 13$$

Where ϕvaries from $-\pi$ to π and $\emptyset$ varies from 0 to 4096.We take 180 units of (0.276 radians) of phase to be equivalent to 60 µg Fe/g tissue(Haacke et al., 2007). The iron content is then given by the relation

$$\text{Iron concentration (µg Fe/g tissue)} = \frac{(\phi - 2048)\pi}{2048 \times 0.276} \times \frac{60\mu g\ Fe}{Gram\ tissue} \qquad 14$$

A simplification of the above equation shows that 3 Siemens phase units is equal to 1 µg Fe/g tissue (Haacke et al., 2007, Haacke et al., 2009). The phase images obtained were high pass filtered by a 64x64 size k space filters and resulted a SWI filtered phase image. In order to compare data across patients, the CSF in each patient was

assumed to contain zero iron (Haacke et al., 2007). Thus the iron content in an ROI is directly proportional to the shift in phase between the CSF and the particular ROI.

III.6 Statistical Analysis

The statistical analysis of this entire study was performed using IBM SPSS Statistics for Windows version 21 (Armonk, NY, USA). One way ANOVA and Chi square test was used to determine the group differences between subjects in age and gender respectively. One way ANOVA analysis with posthoc- Bonferroni correction was applied to compare means of volumes of cortical GM structures, FA and MD values, iron deposition in various ROI's between the different diagnostic groups. Subsequently, a linear regression analysis was performed between means and behavioural scores. In all the analysis, the significant threshold was set at $p<0.05$.

IV RESULTS

IV.1 Demographic and Clinical features of patients and controls

The demographic and clinical characteristics of subjects are summarized in Table 2. The patients with fvFTD and PPA did not differ in terms of age (P=0.50), sex (P=0. 33), and education (P=0. 21) in comparison to controls. Age at onset (P=0. 49), age at diagnosis (P= 0.43) and duration of illness (P=0. 8) was also comparable between fvFTD and PPA patients. The behavioural variants were relatively younger with more men than language variant and control groups.

Table 2: Demographics and Clinical characterestics of FTD patients

	Controls	**fvFTD**	**PPA**	**Group effect**
N	34	34	12	
Sex (M/F) [a]	18/16	23/11	8/4	0.33
Mean Age(Mean± SD in years)[b]	61.07±6.15	61.18±11.9	64.64±3.98	0.5
Age at diagnosis (years)	-	60.85±11.81	62.85±3.64	-
Age of onset (years)	-	58.29±11.86	63.1±3.81	-
Duration of illness (years)	-	2.85±1.71	1.9±1.19	-
Education[b] (years)	12.27±4.61	10.12±5.25	10.78±3.27	0.21
Global function				
MMSE	28.66±1.11	18.9±7.71	22.82±5.51	<0.001

ACE total Score	92.45±7.03	53.29±24.9	55.9±20.59	<0.001
CDR Total	0±0	1.43±0.99	0.50±0.35	<0.001
Behaviourl Assessment				
FrSBe Apathy	19.36±10.55	30.26±11.72	27.58±13.16	0.003
FrSBe Disinhibition	15.86±2.12	33.74±9.27	24±8.07	<0.001
FrSBe Executive dysfunction	20.41±5.68	56.65±16.93	34±9.73	<0.001
FrSBe Total score	51.23±6.02	125.21±27.53	83.33±27.84	<0.001

[a]Chisquare test [b]Posthoc Oneway ANOVA

The cognitive screening test data MMSE and ACE was not available in 8 out of 34 fvfTD patients and 2 out of 12 PPA patients. The mean MMSE score of the fvFTD was 18.9 (2- 27) whereas that of PPA was 22.82 (4-29). The posthoc one way ANOVA analysis showed that both patients were significantly impaired on the MMSE (fvFTD: P<0.001, PPA: P=0. 007) and ACE (P<0.001) in comparison to controls, but did not differ from each other. With respect to CDR, the patients were significantly differed between each other with higher score in fvFTD (P=0.02).

Comparisons of the behavioural assessment scores on FrSBe revealed a significant group effect on the FrSBe total T score (P<0.001), apathy (P=0. 003), disinhibition (P<0.001) and executive dysfunction (P<0.001). Posthoc bonferroni correction and comparison indicated significant differences between behavioural variant and controls in all the FrSBe sub scores and total score, whereas the aphasic was more impaired than controls on a Total (P<0.001), disinhibition (P=0.023) and executive dysfunction(P=0.016) score. Nevertheless, significant impairment was not observed

in the PPA for apathy (P=0.159). Post hoc test also revealed that two subgroups differ significantly in the presence of disinhibition (P=0.003), executive dysfunction (P<0.001) and total score (P<0.001).

IV.2 Correlations between behavioural assessment scores

Among the patient groups, the FrSBe apathy did not correlate with disinhibition and executive dysfunction profiles. Whereas, the executive dysfunction showed a significant correlation with disinhibition profile (Pearson r =0.772, P<0.001). The correlation between subscales in fvFTD group showed that apathy was significantly correlated with both disinhibition (Pearson r = 0.271, P=0.027) and executive dysfunction (Pearson r = 0.368, P=0.002). In PPA, executive dysfunction only revealed significant association with disinhibition and the other scores failed to reach statistical significance. However, no significant correlation was found between any of the subscales and age at diagnosis, age at onset in years and disease duration (Pearson r <0.2, N.S).

IV.3 VBM analysis of cortical GM degeneration in patients

IV.3.1 Patterns of GM loss in fvFTD compared to controls

The voxel by voxel analysis of GM between fvfTD and healthy volunteers with covariates of age, sex and TIV revealed widespread atrophy in bilateral frontal, temporal and occipital regions (P<0.05, FDR corrected, Figure 19, Table 3).

Significant voxels were also found bilaterally in insula, rolandic operculum, dorsal anterior cingulate, caudate head, thalamus, and putamen regions.

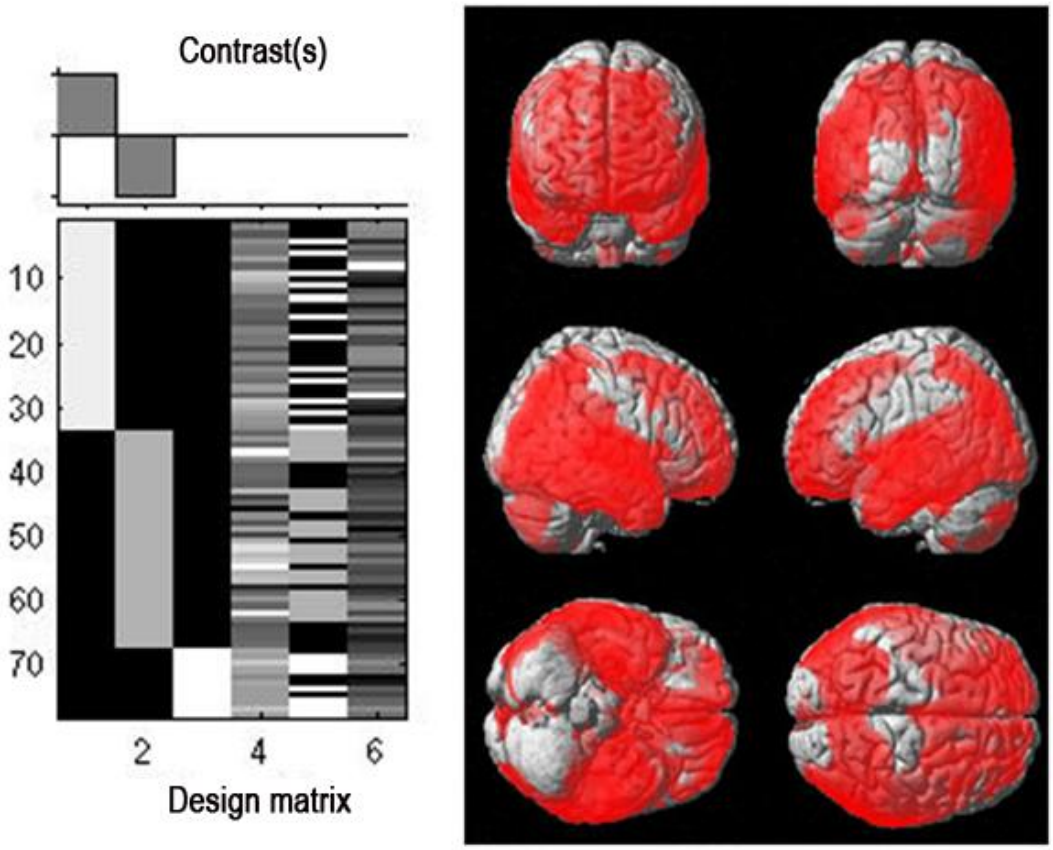

Figure 19: Pattern of gray matter loss in fvFTD compared to controls with age, sex and TIV as covariates. SPM T- maps were rendered on the single subject brain. All regions surviving P<0.05, FDR corrected, 30 minimum cluster size in the whole brain analysis is presented. The results are displayed in neurological convention.

Table 3: Regional gray matter reduction in fvFTD patients compared with controls

Anatomical Localization	(Brodmaan area, BA)	Side	MNI Co-ordinate areas X	Y	Z	Cluster size (mm3)	Z score
Middle orbital frontal gyrus	BA11	L	-30	58	-14	2874	5.98
		R	32	38	-16	5479	6.04
Middle frontal gyrus	BA 10	L	-28	32	47	10134	5.01
		R	41	51	23	14300	5.39
Medial orbital frontal gyrus	BA11	L	-4	43	-11	4143	6.11
		R	3	41	-11	5479	6.15
Superior orbital frontal gyrus	BA 11	L	-10	41	-25	4121	5.98
		R	16	21	-26	4168	5.63
Superior frontal gyrus	BA8	L	-20	42	39	8993	4.64
		R	20	36	46	9446	4.5
Inferior orbital frontal gyrus	BA 47	L	-45	25	-10	8197	4.52
		R	43	27	-10	6981	4.27
Inferior frontal opercular gyrus	BA47	L	-52	18	2	2952	4.65
		R	36	-28	-18	3045	4.91
	BA 45	L	-56	12	12	2643	4.82
		R	47	18	6	3016	3.80
Inferior frontal triangular gyrus	BA47	L	-47	47	-2	3482	3.71
		R	47	20	2	4182	5.22
		L	-54	16	13	280	4.63
	BA46	R	51	39	2	500	4.22
Gyrus rectus		L	-3	21	-18	5012	6.11
	BA 11	R	8	20	-26	4484	8.52

Olfactory	BA 25	L R	-3 3	11 15	-15 -7	2037 2067	6.25 5.87
Anterior cingulate	BA 32	L R	-2 2	43 42	-2 3	7706 5665	6.45 6.66
Middle cingulate	BA 32	L R	-2 5	24 25	35 35	3575 3352	5.05 4.66
Supplementary motor area	BA8 BA 32	L R	-5 3	15 6	47 47	7153 3679	4.53 5.64
Rolandic operculum	BA13 BA22 BA 43	L R R R	-42 42 58 54	-11 -13 2 -10	13 15 4 11	5339 6551 2123 4512	6.68 6.87 6.91 5.91
Insula	BA 13	L R	-39 43	-12 -10	6 6	9177 9974	6.21 7.34
Fuisform gyrus	BA 20	L R	-34 33	-16 -16	-34 -34	7720 7356	5.58 4.54
Heschyl gyrus	BA 13 BA 6	L R	-39 50	-20 -7	6 6	1444 1659	6.08 6.25
Inferior temporal gyrus	BA 37	L R	-64 64	-30 -29	-18 -18	16058 16025	5.43 5.98
Middle temporal gyrus	BA21	L R	-65 65	-29 -16	-14 -18	20565 15681	6.63 7.22
Middle temporal pole	BA 38	L R	-41 50	15 14	-37 -28	1489 3633	6.08 4.95
Superior temporal gyrus	BA 22 BA41	L R	-55 51	-10 -20	6 11	11025 17384	6.15 6.11
Caudate/caudate head		L R	-5 5	12 7	-5 -3	1392 1186	6.35 6.18

Putamen/lentiform nucleus		L R	-19 20	14 16	2 2	214 243	4.33 4.46
Thalamus/Medial Dorsal nucleus		L R	-5 3	-16 -16	12 12	694 524	4.43 3.89
Hippocampus/Limbic lobe		L R	-29 30	-13 -15	-16 -16	5133 5541	8.14 7.66
Amygdala/Limbic lobe		L R	-24 24	-8 -8	-14 -14	1548 1600	6.63 6.46
Parahippocampal gyrus/Limbic lobe	BA34	L R	-20 19	-6 3	-30 -20	6203 7049	4.84 5.19
Lingual gyrus	BA30	L R	-14 15	-35 -32	-6	1539 873	4.19 4.6
Supramarginal gyrus	BA40	L R	-60 65	-56 -25	24 24	922 2639	3.95 3.43
Angular gyrus	BA39 BA40	L R	-48 59	-69 -59	30 30	3467 4207	4.19 4.6
Precuneus	BA7	L R	-7 8	-64 -64	54 54	6468 5199	3.8 3.6
Middle occipital gyrus	BA19 BA39	L R	-41 8	-82 -64	24 54	3585 2374	4.06 4.81

IV.3.2 Patterns of GM loss in PPA compared to controls

The VBM analysis of GM between PPA and controls showed significant atrophy in the bilateral temporal, occipital and frontal regions with severity in left temporal regions (Figure 20, Table 4). The atrophic patterns also observed in insula, limbic structures and extended patterns into super and middle temporal regions, angular gyrus, supramarginal gyrus, precuneus and middle and inferior occipital gyrus.

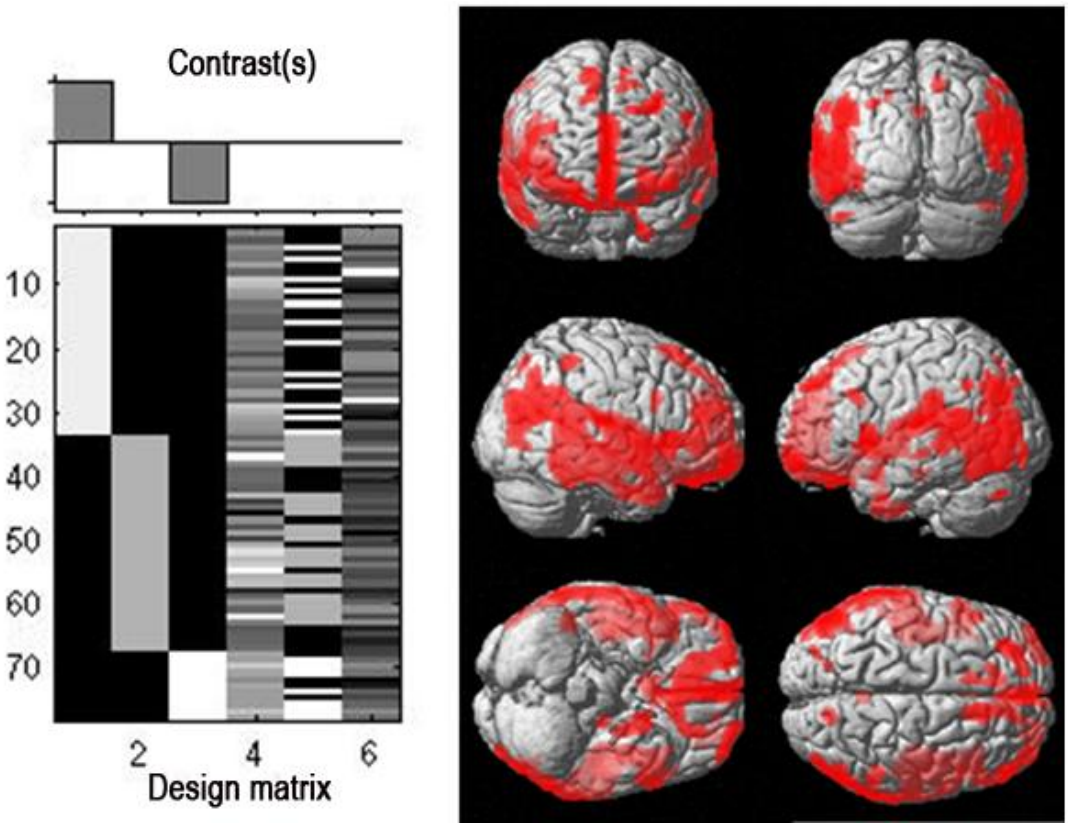

Figure 20: Pattern of gray matter loss in PPA compared to controls with age, sex and TIV as covariates. SPM T- maps were rendered on the single subject brain. All regions surviving P<0.001, FDR corrected, 30 minimum cluster size in the whole brain analysis is presented. The results are displayed in neurological convention.

Table 4: Regional gray matter reduction in PPA patients compared with controls

Anatomical Localization	(Brodmaan area, BA)	Side	MNI Co-ordinate areas			Cluster size(mm3)	Z score
			X	Y	Z		
Middle orbital frontal gyrus	BA11	L R	-26 42	34 54	-22 -12	190 418	4.99 5.38
Middle frontal gyrus	BA 9 BA10	L L R	-40 -46 30	34 50 52	38 6 22	334 579 1266	4.28 4.43 3.32
Medial orbital frontal gyrus	BA10	L R	-2 4	54 52	-4 -8	330 371	5.81 5.62
Superior medial frontal gyrus	BA11 BA 32	L R	-2 4	54 48	10 6	666 592	5.57 5.43
Superior frontal gyrus	BA9	L R	-18 18	48 54	36 38	301 102	4.51 4.14
Superior orbital frontal gyrus	BA10	L R	-18 28	64 64	-11 -8	108 263	4.51 4.65
Inferior orbital frontal gyrus	BA 47	L R	-52 54	38 36	-8 -4	62 277	4.73 4.76
Inferior frontal opercular gyrus	BA44 BA45	L R	-56 58	14 12	12 20	244 337	4.62 4.54

Inferior frontal triangular gyrus	BA45 BA46 BA47	L L R L R	-56 -48 54 -52 52	26 40 26 22 22	14 14 14 0 0	84 875 1030 280 500	3.52 3.62 3.51 3.34 5.28
Rectal gyrus	BA 11	L R	-2 4	26 40	-22 -22	468 345	5.50 5.28
Olfactory	BA 25	L R	-2 4	18 18	-8 -8	39 59	5.44 3.84
Anterior Cingulate	BA 32	L R	-2 6	42 44	10 7	412 260	6.13 5.43
Supplementary motor area	BA 6	L R	-8 14	6 22	64 60	80 141	3.29 4.39
Rolandic operculum	BA13 BA43	L R L R	-46 48 -48 52	-20 -12 -18 -14	14 10 14 14	445 620 681 858	6.68 6.87 6.91 5.91
Insula	BA 13	L R	-44 44	8 0	-4 2	869 1176	6.72 7.22
Fusiform gyrus	BA 38 BA20	L R	-22 40	4 -18	44 -30	2778 2860	5.58 3.21
Heschl gyrus	BA 13	L R	-42 44	-18 -20	8 8	167 213	5.80 7.02
Inferior temporal gyrus	BA 37	L R	-58 64	-62 -50	-12 -14	320 783	4.95 5.32
Middle temporal gyrus	**BA21** **BA22**	L R L	-62 68 -66	-58 -18 -44	0 -12 8	3310 2231 1443	5.72 5.24 6.07

		R	66	-48	8	1304	6.50
Middle temporal pole	BA38 BA 21	L R	-22 52	12 8	-38 -32	61 168	3.95 4.76
Superior temporal gyrus	BA 22	L R	-64 66	-46 -42	18 14	1037 1392	6.35 5.54
Superior temporal pole	BA22 BA38	L R	-50 58	8 8	-2 -8	178 271	6.54 4.99
Caudate/caudate body		L R	-4 6	14 12	0 2	146 52	4.51 3.91
Hippocampus/Limbiclobe	BA34/35 BA28	L R	-20 18	-12/-20 -14	-18 -18	125 85	4.25/4.76 4.14
Amygdala/Limbic lobe	BA34	L R	-18 22	2 4	20 -18	37 28	4.26 4.46
Parahippocampal gyrus/Limbic lobe	BA28	L R	-14 20	0 -18	-22 -22	281 57	4.40 4.32
Angular gyrus	BA39	L R	-50 56	-66 -64	24 28	441 477	5.06 5.98
Precuneus	BA7	L R	-2 4	-54 -54	36 34	50 90	4.62 4.95
Supramarginal gyrus	BA40	L R	-66 66	-30 -44	26 28	242 167	6.43 4.73
Middle occipital gyrus	BA39	L R	-48 48	-78 -78	32 26	657 359	5.91 6.28

IV.3.3 Patterns of GM loss in fvFTD compared to PPA

The direct comparison between fvFTD and PPA revealed predominant atrophic patterns in bilateral lfrontal, subcortical and limbic regions along with left insula as shown in Figure 21 and Table 5.

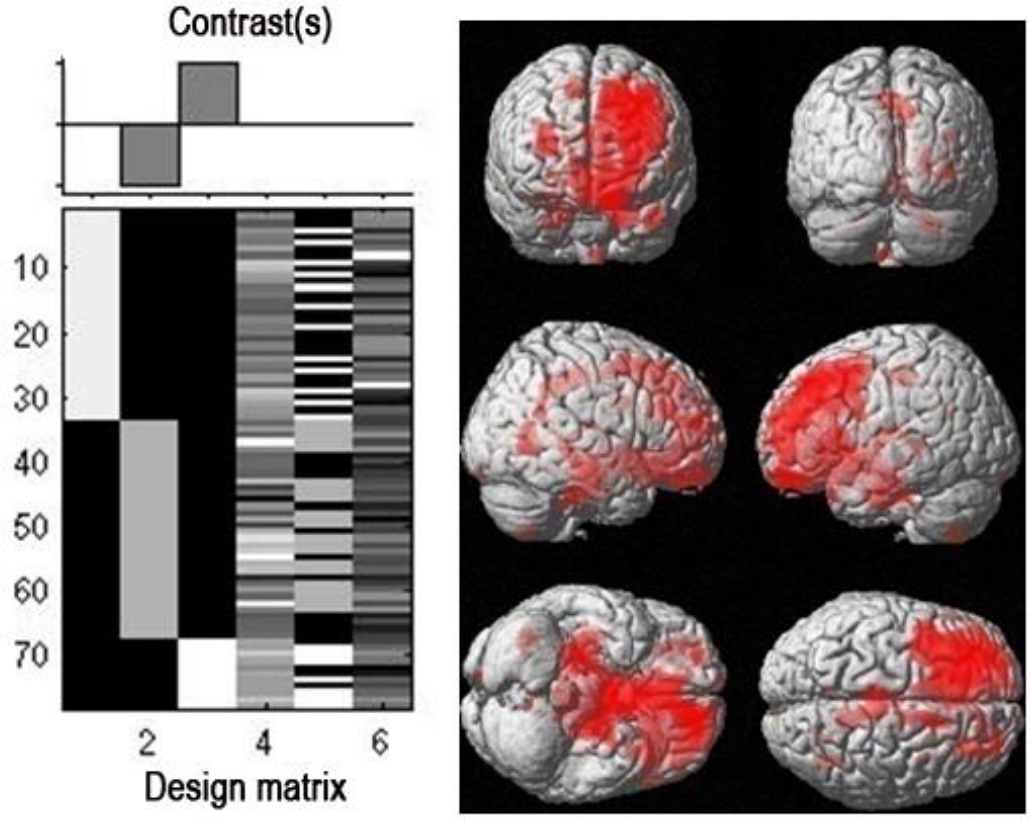

Figure 21: Pattern of gray matter loss in fvFTD compared to PPA with age, sex and TIV as covariates. SPM T- maps were rendered on the single subject brain. All regions surviving P<0.001, uncorrected in the whole brain analysis were presented. The results are displayed in neurological convention.

Table 5: Regional gray matter reduction in fvFTD compared with PPA patients

Anatomical Localization	(Brodmaan area, BA)	Side	MNI Co-ordinate areas (X Y Z)			Cluster size(mm^3)	Z score
Middle frontal gyrus	BA 9	L	-30	32	42	19326	3.10
Middle orbital frontal gyrus	BA11	L R	-17 28	54 53	-16 -18	863 223	2.95 3.1
Superior frontal gyrus	BA8	L	-20	25	46	9552	4.14
Medial orbital frontal gyrus	BA 11	L R	-3 6	30 28	-12 -11	1455 1495	2.44 2.37
Precentral gyrus	BA9	L	-46	3	30	3166	2.13
Gyrus rectus	BA25	L R	-3 6	25 6	-16 -19	2279 1410	2.35 2.16
Supplementary motor area	BA24	L R	-10 10	6 -6	50 50	1403 990	2.85 3.02
Olfactory	BA 25	L R	-4 3	15 14	-12 -12	1252 1197	2.78 2.85
Caudate/caudate head		L R	-8 6	15 10	-5 -6	1900 872	2.56 2.74
Thalamus/Medial Dorsal Nucleus		L R	-6 3	-16 -17	11 12	3022 334	3.25 2.98
Insula	BA13	L	-32	21	8	2470	2.16

Anterior cingulate	BA32	L R	-5 8	34 43	-3 2	5044 1846	2.56 2.29
Middle cingulate	BA31	L R	-2 3	-25 -28	46 46	1613 532	2.56 2.65
Hippocampus	BA27	L R	-16 23	-10 -33	-14 -3	1648 2493	2.26 2.65
Parahippocampus	BA28 BA 35	L R	-24 20	-12 -24	-30 -18	2078 1200	2.35 2.35
Fusiform gyrus	BA28	L	-28	-11	-34	434	2.43

IV.3.4 Patterns of GM loss in PPA compared to fvFTD

When PPA is compared to fvFTD, only small clusters were found in bilateral cerebellum. No other clusters were noted in any of the frontal and temporal regions (Figure 22).

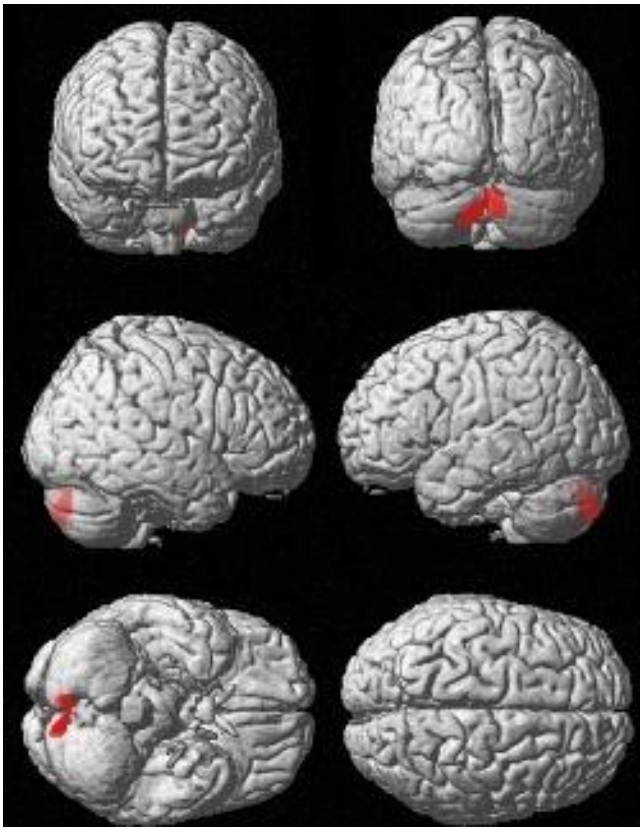

Figure 22: Pattern of gray matter loss in PPA compared to fvFTD with age, sex and TIV as covariates. SPM T- maps were rendered on the single subject brain. All regions surviving P<0.001, FDR corrected, 30 minimum cluster size in the whole brain analysis is presented. The results are displayed in neurological convention.

IV.3.5 Patterns of GM loss associated with apathy and disinhibition in fvFTD

Analysis of individual behaviours associated with tissue loss in focal brain regions revealed significant clusters in the frontal and temporal lobe for apathy and disinhibition (Figure 23) in fvfTD at an uncorrected threshold. However, the analysis did not reveal any significant clusters at a corrected threshold.

IV.3.5.1 Apathy

The increased apathy score was associated with reduced GM volume in several distinct brain areas located in the dorsolateral prefrontal cortex, medial prefrontal cortex, orbitofrontal cortex, limbic lobe, insula, superior and middle temporal gyrus and inferior parietal lobule with greater involvement of right hemisphere ($P<0.001$, uncorrected) (Figure 23, Table 6). The atrophied network contained most significant clusters in the right middle frontal gyrus, right superior frontal gyrus, left rectal gyrus, bilateral anterior cingulate, left inferior frontal gyrus, right supplementary motor area and bilateral insula.

IV.3.5.2 Disinhibition

The increased disinhibition score was associated with GM volume loss in the limbic lobe including parahippocampus, hippocampus and amygdale, temporal lobe including bilateral middle temporal gyrus, right superior temporal gyrus, bilateral middle and superior temporal pole, bilateral fusiform gyrus and right insular cortex as represented in Figure 23 and Table 6.

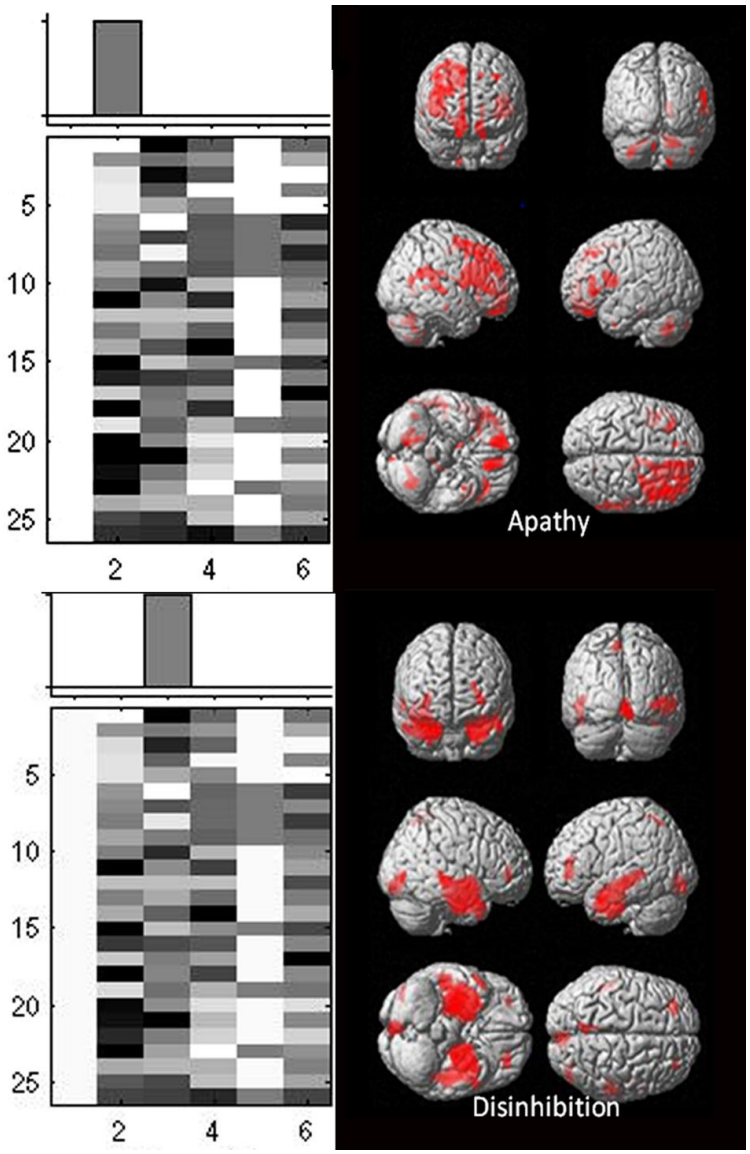

Figure 23: Regions of reduced gray matter density associated with apathy and disinhibition in frontal variant FTD (P<0.001, uncorrected, 30 minimum cluster size in the whole brain analysis are presented. The results are displayed in neurological convention.

Table 6: Regions of reduced gray matter tissue density correlated with apathy and disinhibition in frontal variant FTD

Anatomical Localization	(Brodmaan area, BA)	Side	MNI Co-ordinate areas			Cluster size(mm^3)	Z score
			X	Y	Z		
APATHY							
Dorsolateral Prefrontal cortex							
Middle frontal gyrus	BA10 BA9	R R	34 41	43 23	26 39	1612 10687	2.55 3.2
Inferior frontal gyrus	BA45	L	-50	25	3	369	2.28
Superior frontal gyrus	BA	L	-12	48		305	
Middle frontal gyrus	BA8	L	-32	28	43	897	2.8
Sublobar							
Insula	BA13	L R	-36 36	7 12	13 12	283 1219	2.83 2.45
Medial prefrontal cortex							
Anterior cingulate	BA10	L R	-14 12	47 47	10 10	245 305	2.47 2.78
Medial orbital frontal gyrus	BA10	R	11	51	-2	2281	2.34
Gyrus rectus	BA25	L	-12	30	-20	1071	2.61
Superior frontal gyrus	BA8	R	10	30	46	1117	2.94
Limbic Lobe							

Anterior cingulated	BA32	R L	11 -14	43 47	6 -3	1415 238	2.51 2.23
Supplementary motor area	BA24	R	8	-4	50	2237	2.85
Orbitofrontal cortex							
Superior frontal gyrus	BA11	R	17	43	-21	1983	2.62
Gyrus rectus	BA11	R L	12 -11	38 37	-21 -20	651 351	2.32 3.08
Inferior frontal gyrus	BA47 BA45	L L L R	-15 -36 -50 51	29 30 25 36	-20 -2 3 3	117 501 2258 60	2.46 2.51 2.18 2.52
Temporal lobe							
Superior temporal gyrus	BA22	R	61	-28	3	3453	2.44
Middle temporal gyrus	BA21 BA39	R R	55 59	-46 -46	3 16	1030 254	2.66 2.32
Inferior Parietal lobule	BA40	R	59	-44	23	963	2.4
DISINHIBITION							
Limbic lobe							
Parahippocampus	BA34 BA28	L R	-16 24	-4 -18	-26 -26	318 640	2.00 2.88
Hippocampus		L R	-34 30	-16 -10	-12 -26	45 186	2.10 3.14
Amygdala		L R	-24 30	-2 0	-26 -22	69 169	2.00 2.94
Temporal Lobe							

Middle temporal gyrus	BA21	L R	-48 56	-32 8	-2 -26	378 288	2.21 1.87
Superior temporal gyrus	BA21	R	44	-8	-12	197	2.48
Superior temporal pole	BA38	L R	-32 34	-6 6	-22 -26	76 127	2.18 2.28
Middle temporal pole	BA38	L R	-38 56	8 8	-32 -30	58 69	2.01 1.92
Fusiform	BA28 BA20	L R	-26 38	-10 -18	-36 -26	260 359	2.44 2.71
Sublobar							
Insula	BA13	R	42	-6	-8	127	2.56

IV.4 Automated Volumetric findings

IV.4.1 Global volume measures

The one way ANOVA analysis revealed a significant group effect for the global measures of GM (P<0.001), WM (P=0.011), and CSF (P=0.005) volume. While TIV demonstrated a trend towards significance (P=0.068). The volume comparison in the patients and controls were displayed as a box plot (Figure 24).

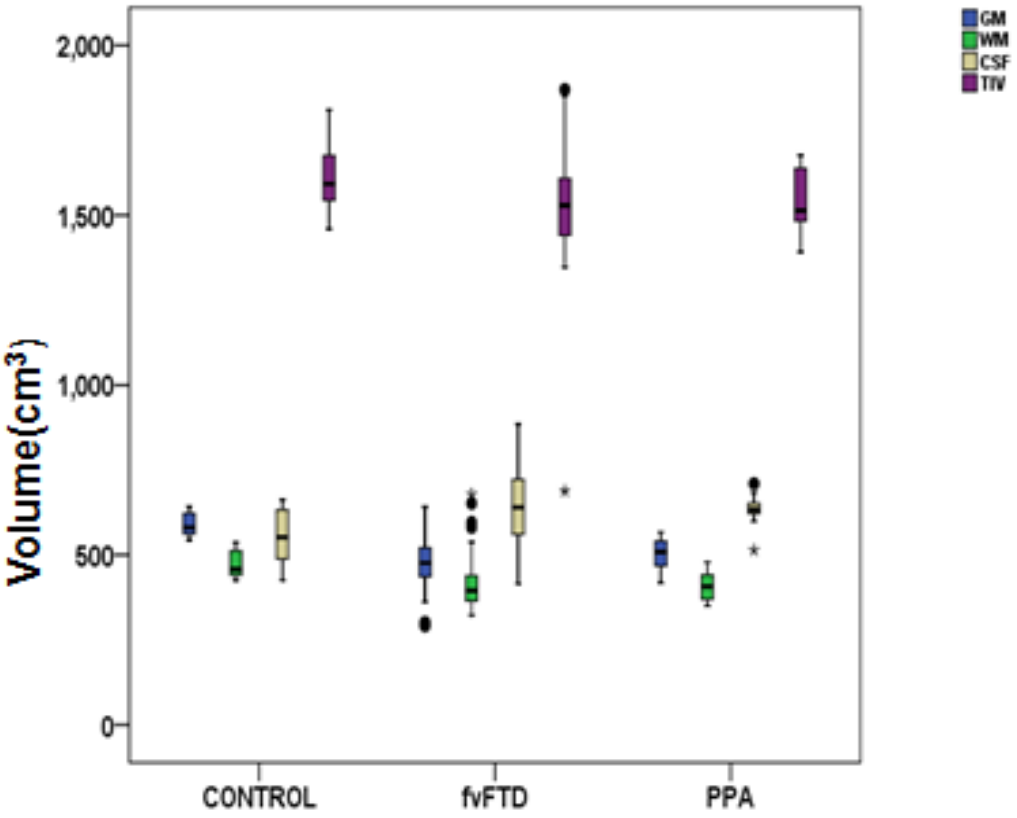

Figure 24: Box plot representation of global brain volumes in patients and controls.

Post hoc Bonferroni comparisons revealed that fvfTD group had significantly reduced volumes of GM (P<0.001), WM (P=0.01) and corresponding increased CSF volume (P=0.005) compared to healthy controls. Similarly the patients with PPA had significant reduction in GM (P<0.001) and WM (P=0.031) volume in comparison to controls. In contrast, no statistically significant increase in CSF volume (P=0.084) and decrease in TIV volume (0.557) was noted in PPA compared to healthy controls. A direct comparison between the patients failed to reveal any significant change in any of the global measures.

IV.4.2 Regional GM volumes

In order to find the regional GM volume reduction in FTD patients, an automated parcellation of GM structures in frontal, temporal, subcortical and occipital regions was performed. The volumetric results are summarized in Table 7. The ANOVA analysis of regional brain volumes demonstrated significant group effect for most of the analysed structures. However, bilateral PC failed to reveal any significant main effect. Post hoc Bonferroni comparison revealed significantly reduced frontal, temporal, subcortical, insular, anterior and middle cingulate, and calcarine volumes in fvFTD compared to controls. Similarly, the PPA group, compared to controls, had reduced volumes of all the analyzed structures except for the bilateral CM, PC and RTH. Furthermore, the fvFTD group showed reduced volumes of the LMFG (P=0.043), LSFG (P=0.039), bilateral AC (LAC= 0.04, and RAC, P=0.038), bilateral RECG (LRECG, P=0.025 and RRECG, P=0.026), CAU (LCAU, P=0.037 and RCAU, P=0.027) and bilateral TH (LTH=0.021 and RTH=0.032) than PPA.

Table 7: Group comparison of regional volumes between Controls, fvFTD and PPA

Dependent Variable	Controls	fvFTD	PPA	Bonferroni corrected P value			
				Group effect	*fvFTDVs Controls	*PPA Vs Controls	*fvFTD Vs PPA
Frontal Lobe							
LMFG	15.69±0.88	11.98±2.65	13.73±1.63	<0.001	<0.001	0.03	0.043
RMFG	15.78±1.18	11. 91±2.72	13.61±2.13	<0.001	<0.001	0.026	0.08
LMOFG	2.6±0.20	1.86±0.49	2.13±0.21	<0.001	<0.001	0.003	0.115
RMOFG	2.61±0.25	1.91±0.51	2.11±0.19	<0.001	<0.001	0.006	0.376
LSFG	11.08±0.71	8.52±1.91	9.67±0.73	<0.001	<0.001	0.026	0.064
RSFG	10.50±0.71	7.89±1.91	9.15±0.92	<0.001	<0.001	0.038	0.039
LSOFG	2.84±0.275	2.15±0.55	2.44±0.236	<0.001	<0.001	0.035	0.150
RSOFG	2.77±0.24	2.14±0.55	2.39±0.22	<0.001	<0.001	0.053	0.250
LIOFG	5.09±0.6	3.45±1.06	3.83±0.77	<0.001	<0.001	<0.001	0.588
RIOFG	4.72±0.59	3.35±0.95	3.79±0.62	<0.001	<0.001	0.003	0.137
LIFoperG	3.27±0.31	2.47±0.61	2.6±0.38	<0.001	<0.001	0.001	0.98
RIFoperG	4.04±0.45	3.0±0.74	3.21±0.34	<0.001	<0.001	0.001	0.899

LIFTriG	7.54±0.76	5.78±1.5	6.21±0.73	<0.001	<0.001	0.002	0.55
RIFTriG	5.73±0.51	4.29±1.2	4.69±0.6	<0.001	<0.001	0.009	0.610
LRoperG	3.35±0.37	2.51±0.58	2.63±0.43	<0.001	<0.001	<0.001	1.00
RRoperG	4.33±0.59	3.24±0.57	3.35±0.47	<0.001	<0.001	<0.001	1.00
LSMA	6.26±0.75	4.82±1.14	5.17±0.56	<0.001	<0.001	0.006	0.823
RSMA	6.80±0.92	5.27±1.13	5.68±0.54	<0.001	<0.001	0.008	0.66
LOC	1.2±0.1	0.89±0.23	1.02±0.16	<0.001	<0.001	0.037	0.11
ROC	1.22±0.09	0.86±0.25	1.03±0.11	<0.001	<0.001	0.02	0.026
LSMedOFG	2.61±0.22	2.06±0.51	2.20±0.17	<0.001	<0.001	0.017	0.927
RSMedOFG	3.30±0.33	2.55±0.66	2.78±0.23	<0.001	<0.001	0.021	0.605
LRECG	2.99±0.33	2.16±0.56	2.55±0.11	<0.001	<0.001	0.014	0.025
RRECG	2.73±0.29	2.05±0.4	2.36±0.08	<0.001	<0.001	0.016	0.026
Insula and Cingulate Gyrus							
LIN	`7.03±0.78	4.9±1.17	5.16±1.19	<0.001	<0.001	<0.001	0.67
RIN	6.54±0.74	4.75±1.50	4.81±0.86	<0.001	<0.001	<0.001	1.00
LAC	5.16±0.40	3.69±0.92	4.31±0.39	<0.001	<0.001	0.004	0.04
RAC	4.85±0.362	3.50±0.92	4.12±0.359	<0.001	<0.001	0.015	0.038

LCM	6.55±0.47	5.78±1.04	6.22±0.45	0.004	0.003	0.805	0.339
RCM	7.57±0.77	6.55±1.14	7.15±0.65	0.001	0.001	0.67	0.217
LPC	1.33±0.14	1.24±0.25	1.25±0.123	0.222	0.284	0.731	1.00
RPC	0.82±0.10	0.77±0.16	0.78±0.08	0.342	0.469	0.996	1.00
Subcortical structures							
LCAU	2.75±0.176	1.91±0.626	2.30±0.23	<0.001	<0.001	0.034	0.027
RCAU	2.74±0.27	1.87±0.613	2.32±0.34	<0.001	<0.001	0.042	0.037
LPUT	3.57±0.63	3.02±0.474	3.17±0.57	<0.001	<0.001	0.041	0.914
RPUT	3.80±0.279	3.30±0.446	3.44±0.47	<0.001	<0.001	0.043	0.998
LTH	2.63±0.45	1.98±0.46	2.44±0.70	<0.001	<0.001	0.806	0.021
RTH	2.69±0.26	2.22±0.50	2.58±0.29	<0.001	<0.001	0.819	0.032
Temporal Lobe							
LHP	3.76±0.22	2.52±0.63	2.97±0.62	<0.001	<0.001	0.000	0.075
RHP	3.78±0.32	2.53±0.64	2.98±0.55	<0.001	<0.001	0.000	0.072
LPHP	4.72±0.54	3.30±0.71	3.71±0.44	<0.001	<0.001	0.000	0.545
RPHP	4.69±0.61	3.59±0.85	3.65±0.52	<0.001	<0.001	0.001	0.214
LAMY	1.12±0.09	0.82±0.2	0.91±0.23	<0.001	<0.001	0.005	0.451
RAMY	1.22±0.12	0.94±0.20	1.01±0.15	<0.001	<0.001	0.005	0.655
LFG	9.71±0.74	7.13±1.7	8.45±1.34	<0.001	<0.001	0.008	0.061

RFG	10.25±0.68	8.99±1.3	9.02±0.828	<0.001	<0.001	0.007	0.304
LHG	0.64±0.07	0.47±0.10	0.48±0.09	<0.001	<0.001	0.000	1.00
RHG	0.86±0.09	0.56±0.093	0.57±0.094	<0.001	<0.001	0.000	1.00
LSTG	8.07±0.77	6.56±1.42	6.61±1.31	<0.001	<0.001	0.005	0.071
RSTG	10.86±0.96	7.94±1.47	8.10±1.34	<0.001	<0.001	0.000	1.00
LMTG	17.31±1.22	13.35±4.12	13.47±2.52	<0.001	<0.001	0.004	1.00
RMTG	16.29±1.31	12.54±3.5	12.64±2.49	<0.001	<0.001	0.002	1.00
LITG	10.8±0.8	7.92±1.65	8.05±1.8	<0.001	<0.001	0.000	1.00
RITG	12.66±0.82	9.10±1.49	9.2±1.69	<0.001	<0.001	0.000	1.00
LSTP	4.41±0.51	3.02±0.88	3.2±0.96	<0.001	<0.001	0.000	0.998
RSTP	3.95±0.47	2.59±0.81	2.94±0.69	<0.001	<0.001	0.000	0.412
LMTP	2.51±0.30	1.72±0.58	1.81±0.39	<0.001	<0.001	0.000	1.00
RMTP	3.32±0.50	2.21±0.62	2.51±0.52	<0.001	<0.001	0.001	0.356
Occipital Lobe							
LCL	7.25±0.74	6.27±1.28	6.28±0.63	0.001	0.002	0.039	1.00
RCL	5.98±0.627	6.05±0.36	5.3±0.74	<0.001	<0.001	0.789	0.5

IV.4.3 Relationship between Regional brain volume and Behavioural scores

In order to identify the relationship between regional brain volume measures and FrSBe subscores of A, D and E, linear regression analyses were performed and as expected, significant negative correlations were found. In fvFTD, apathy scores were negatively correlated with GM volume in LMFG (r^2 = 0.25, p = 0.003), RMFG (r^2 = **0.45**, p <0.001), RMOFG (r^2 = 0.22, p = 0.001), LSFG (r^2 = 0.27, p = 0.002), LSOFG (r^2 = 0.25, p = 0.003), RSOFG (r^2 = 0.24, p = 0.004), LIOFG (r^2 = 0.17, p = 0.02), RIOFG (r^2 = 0.24, p = 0.004), LMedOFG (r^2 =0.22, p = 0.006), RMedOFG (r^2 =**0.32**, p = 0.001), LRECG (r^2 = **0.29**, p = 0.002), RRECG (r^2 = 0.19, p = 0.011), LAC (r^2= 0.29, p =0.001), RAC (r^2=**0.33**, p = 0.006), LIN (r^2= 0.24, p = 0.004), RIN (r^2= 0.25, p = 0.01), LITG (r^2 = 0.24, p = 0.004), RSTG (r^2 = 0.21, p = 0.008), LMTG (r^2 = **0.29**, p = 0.001) and RMTG (r^2= **0.27**, p = 0.001), while disinhibition score was negatively correlated with GM volume in LHP (r^2 = 0.19, p = 0.01), RHP (r^2 = **0.32**, p = 0.001), LPHP (r^2 = 0.15, p = 0.02), RPHP (r^2 **= 0.37**, p < 0.001), RAMY (r^2 = **0.29**, p = 0.007), LAMY (r^2 = 0.16, p = 0.02), RSTG (r^2 = 0.26, p = 0.001), LMTG (r^2 = **0.28**, p = 0.002), RMTG (r^2= 0.25, p = 0.003), LMTP (r^2 = 0.15, p = 0.02) , RMTP (r^2= 0.27, p = 0.002), LSTP (r^2= 0.18, p = 0.01), RSTP (r^2 = 0.18, p = 0.01), and RIN (r^2 = 0.29, p = 0.001). In PPA, correlation analysis of apathy and disinhibition scores did not yield any significant areas of the association. However the executive dysfunction scores showed a significant negative correlation with LIFoperG (r^2 = 0.40, p = 0.01) and LIN (r^2 = 0.38, p = 0.02).

IV.5 DTI voxel-wise whole brain findings

TBSS analysis of white matter tract integrity in subtypes of FTD identified varying degrees of abnormalities in the corpous calosum (CC), anterior thalamic radiation and intra hemispheric association pathways in patients compared to controls.

IV.5.1 FvFTD versus healthy controls

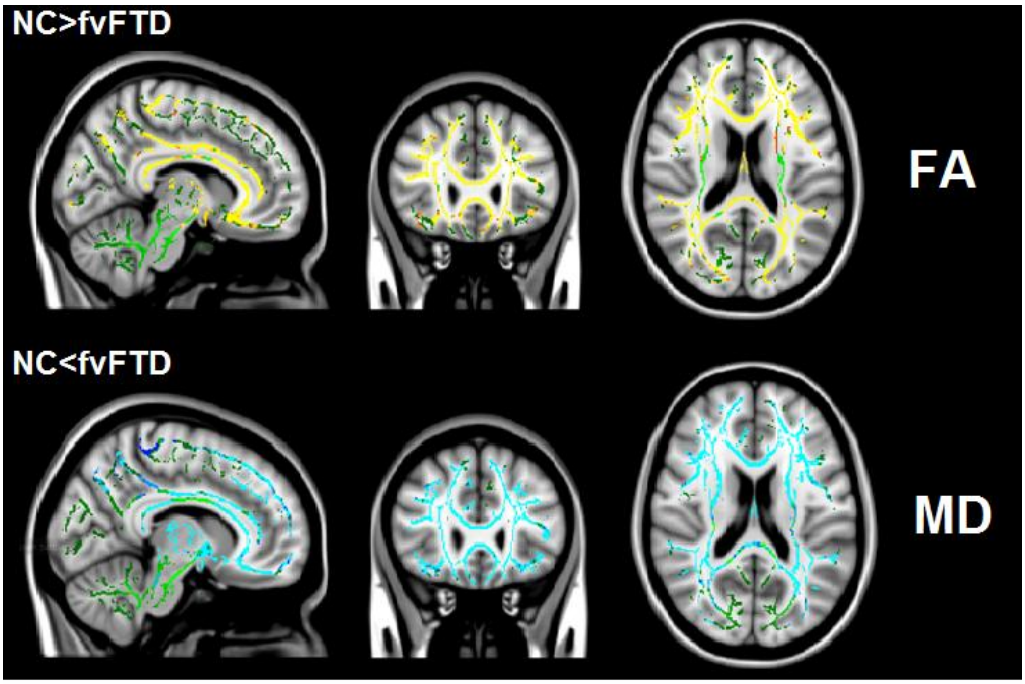

Figure 25: Patterns of white matter tract degeneration in fvFTD group compared with controls. TBSS voxel wise group differences (significance level of P<0.05, FWE corrected for multiple comparisons across space using threshold free cluster enhancement) are shown in red-yellow (FA) and blue-light blue (MD). The

mean FA skeleton is displayed as green. The results are overlaid on the MNI standard brain in radiological convention.

In comparison to controls, fvFTD patients showed widespread bilateral patterns of decreased FA values throughout the whole brain including the forceps minor, forceps major, IFOF, SLF, ILF, UF, cingulum and anterior thalamic radiation. Among these regions, the degeneration was more pronounced in forceps minor, IFOF, SLF, ILF and UF. Furthermore, fvFTD patients showed a wide spread patterns of increased MD in all those regions where FA change was detected (Figure 25).

IV.5.2 PPA versus healthy controls

In comparison to controls, PPA patients showed patterns of decreased FA in forceps minor, IFOF, ILF, anterior thalamic radiation, cingulate gyrus, UF, and SLF with more pronounced atrophy in left hemisphere. Among these regions, most significant atrophy was noted in forceps minor and temporal parts of ILF, IFOF and UF. PPA also showed increased MD in those regions with decreased FA (Figure 26).

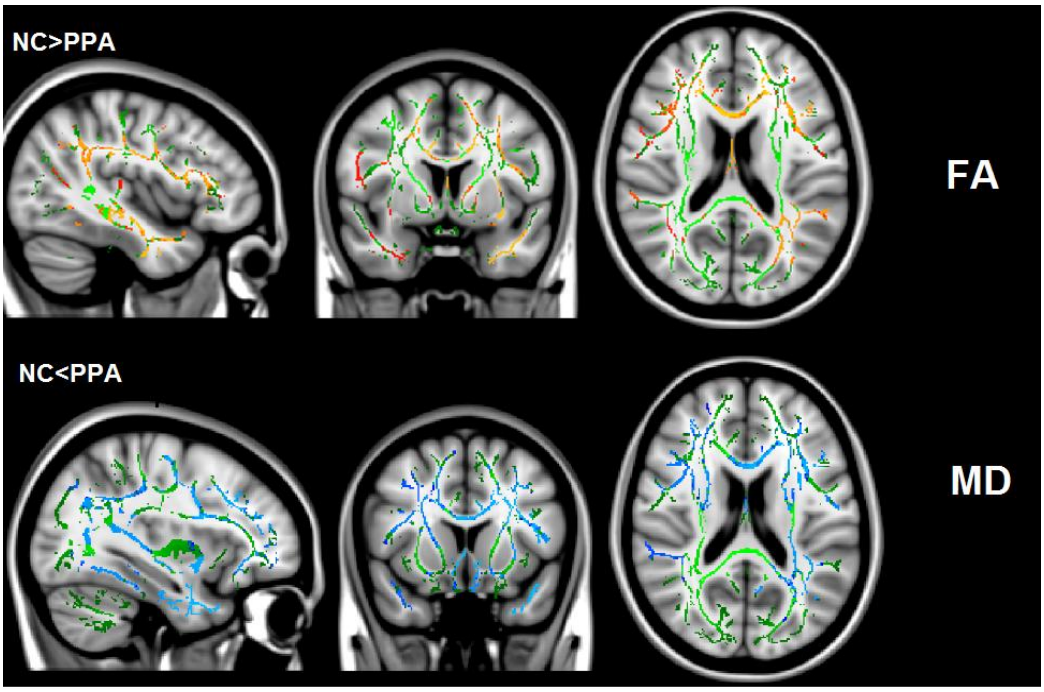

Figure 26: Patterns of white matter tract degeneration in PPA group compared with controls. TBSS voxel wise group differences (significance level of P<0.05, FWE corrected for multiple comparisons across space using threshold free cluster enhancement) are shown in red-yellow (FA) and blue-light blue (MD). The mean FA skeleton is displayed as green. The results are overlaid on the MNI standard brain in radiological convention.

IV.5.3 fvFTD versus PPA

A direct comparison between subtypes of FTD showed that in comparison to PPA, fvfTD had decreased FA solely in forceps minor and anterior parts of superior longitudinal fasiculus and inferior fronto occipital fasciculus. Increased MD values were also noted in regions with decreased FA in fvFTD. The opposite contrast failed to reveal any significant decrease in FA and increase in MD in PPA compared to fvFTD.

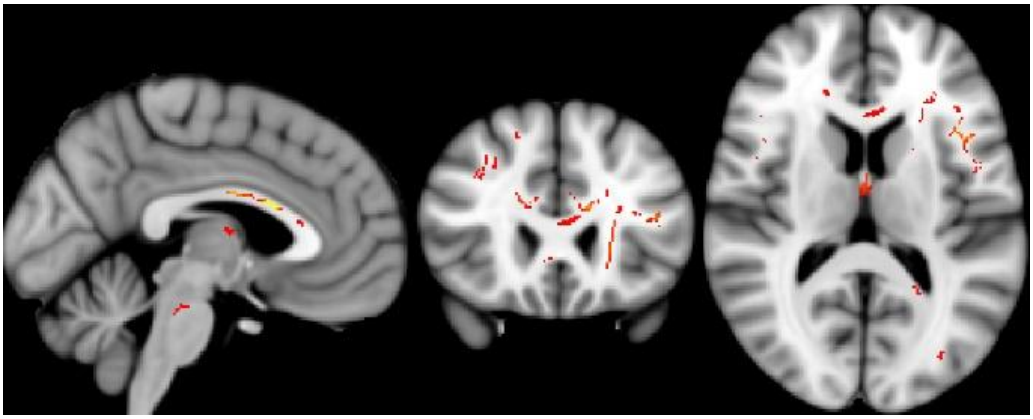

Figure 27: Patterns of white matter tract degeneration in fvfTD group compared with PPA. TBSS voxel wise group differences with a significance level set at P<0.05, FWE corrected. The results are overlaid on the MNI standard brain in radiological convention

IV.5.4 Diffusion Metrics of Major white matter tracts

The estimated means of the diffusion metrics from the studied WM tracts are summarized in Table 8. Compared with controls, FTD patients showed statistically significant white matter pathology across diffusivity metrics in several regions. When compared to controls, fvFTD patients showed decreased FA (P<0.005) and increased MD (P<0.001) in most of the analysed tracts except in CST. While in PPA, decreased FA was found in the left UF (P=0.004), bilateral IFOF (greater damage in leftside, P=0.004), left ILF and left SLF (0.03). Also, an increased MD was found in

the left UF (P=0.008), left ILF (0.04) and genu of corpous callosum (P=0.02) in PPA. The reverse contrasts in fvfTD and PPA compared to controls(decreased FA and increased MD in controls) did not reveal any significant WM damage. Conversely, compared with PPA, the fvfTD had most significant and prominent WM changes in DTI metrics of both FA and MD in left SLF (P=0.01), genu (P=0.03) and some what comparitively less prominent FA changes in right UF (P=.04) and left IFOF (P=0.034). Furthermore, the direct comparison showed a trend towards significance for MD values in RUF (P=0.08) and splenium (0.121).

IV.5.5 Relationship between DTI metrics and Behavioural scores

The DTI metrics showed a significant correlation with behaviorural scores. In fvFTD, the FA values of bilateral SLF were correlated with the severity of apathy scores (r^2=0.25, P=0.006 for right and r^2=0.17, P=0.02 for left), while FA values of RSLF were correlated with severity in disinhibition (r^2=0.21, P=0.008). In PPA, apathy and disinhibition scores failed to reveal any significant correlation with FA and MD values.

Table 8: DTI metrics of individual WM tracts in fvFTD, PPA and healthy controls.

WMT		MD [x10^{-3} mm^2 s^{-1}]			*P value	FA			*P value
		Controls	fvFTD	PPA		Controls	fvFTD	PPA	
Genu		0.88 ± 0.06	1.04 ± 0.1	1.0 ± 0.09	<0.001	0.51 ± 0.02	0.45± 0.05	0.48± 0.03	<0.001
Splenium		0.84 ± 0.06	0.99 ± 0.01	0.92 ± 0.04	<0.001	0.50 ± 0.03	0.48 ± 0.03	0.49± 0.03	0.02
Cingulum	L	0.88 ± 0.06	1.05 ± 0.10	0.97 ± 0.06	<0.001	0.44 ± 0.03	0.39 ± 0.05	0.40 ± 0.05	0.001
	R	0.87 ± 0.06	1.03 ± 0.1	0.96 ± 0.05	<0.001	0.44 ± 0.03	0.39 ± 0.05	0.40 ± 0.03	0.001
UF	L	1.54 ± 0.10	1.75 ± 0.17	1.63 ± 0.06	<0.001	0.39 ± 0.03	0.32 ± 0.04	0.33 ± 0.02	<0.001
	R	1.62 ± 0.12	1.90 ± 0.16	1.86 ± 0.14	<0.001	0.37 ± 0.02	0.31 ± 0.04	0.35± 0.01	<0.001
IFOF	L	0.80 ± 0.05	0.86 ± 0.08	0.88 ± 0.05	0.001	0.51± 0.04	0.44 ± 0.03	0.47 ± 0.04	<0.001
	R	0.82 ± 0.05	0.87 ± 0.09	0.92 ± 0.10	0.002	0.48 ± 0.03	0.42 ± 0.02	0.45 ± 0.06	<0.001
ILF	L	0.84 ± 0.05	1.03 ± 0.12	0.96 ± 0.04	<0.001	0.44 ± 0.02	0.39 ± 0.05	0.39 ± 0.04	<0.001

	R	0.85 ± 0.05	1.03 ± 0.13	0.96 ± 0.04	<0.001	0.44 ± 0.02	0.38 ± 0.05	0.39 ± 0.02	<0.001
SLF	L	0.86 ± 0.05	1.06 ± 0.10	0.92 ± 0.04	<0.001	0.45 ± 0.02	0.39± 0.05	0.41± 0.01	<0.001
	R	0.85 ± 0.05	0.98 ± 0.09	0.92 ± 0.04	<0.001	0.45 ± 0.02	0.40 ± 0.05	0.41± 0.02	0.007
CST	L	0.77 ± 0.03	0.78 ± 0.07	0.77 ± 0.01	1.00	0.54± 0.03	0.53 ± 0.03	0.52± 0.04	0.813
	R	0.76± 0.04	0.77 ± 0.07	0.77 ± 0.02	1.00	0.55 ± 0.03	0.53 ± 0.03	0.54 ± 0.01	0.818

* Bonferroni corrected P value

fvFTD= frontal variant frontotemporal dementia; PPA= primary progressive aphasia; CST= corticospinal tract; FA= fractional anisotropy; MD= mean diffusivity; ILF= inferior longitudinal fasciculus; IFOF= inferior fronto-occipital fasciculus; SLF= superior longitudinal fasciculus.L = left; R= right

IV.6 Quantitative measurements of brain iron content in patient with FTD

A very good inter- rater agreement (K= 0.88) was observed between the two raters in the quantitative measurement of iron values. The quantitative assessment of brain iron deposition (µg Fe/gm of tissue) in the various regions in FTD patients demonstrated significantly increased iron levels in bilateral SFG(P<0.001), bilateral TEMPG(P<0.001 for right and P=0.001 for left), bilateral AC(P=0.002 for right and P=0.036 for left), bilateral PUT(P=0.004 for right and P=0.037 for left), RPBMC(P=0.01), RIN(P=0.01),RHP(P=0.016), and RRN(P=0.02), in fvFTD compared to controls. Also a trend towards significance was noted in LPBMC (P=0.06), RFWM (P=0.067), and RDN (P=0.059). While patients with PPA, significant iron level was noted in LSTG (P=0.046) and a trend for significance in RSTG(P=0.073). The direct comparison between fvFTD and PPA showed an increased iron deposition in RSFG (P=0.031) in fvFTD. Furthermore, increased iron levels in RPUT (P=0.086) in fvFTD had a trend towards significance to discriminate from the PPA group.

IV.6.1 Relationship between cortical brain iron deposition and Behavioural scores

Linear regression analysis for examining the relationship between cortical iron deposition and FrSBe subscores, found significant positive correlation between the iron content in RSFG and the apathy score (r^2=0.31, P=0.005) and iron content in RPUT and disinhibition scores (r^2=0.21, P=0.02). The patients with PPA did not show any correlation with iron content and any of the behavioural scores.

Table 9: Iron content (µg Fe/gm of tissue) of each ROI in fvFTD, PPA and control group

Region	Controls	fvFTD	PPA	Bonferroni corrected P value		
				fvFTD vs Controls	PPA vs Controls	fvFTD vs PPA
LSFG	13.03±7.19	25.11±9.98	18.57±3.03	**<0.001**	0.53	0.12
RSFG	11.42±7.93	26.8±9.43	16.51±5.03	**<0.001**	0.65	**0.031**
LPBMC	32.14±12.39	40.78±9.97	37.45±10.71	0.06	0.954	1.00
RPBMC	30.94±14.79	41.89±7.26	36.32±10.86	**0.011**	0.932	0.82
LAC	16.56±5.67	21.57±6.24	19.9±4.43	**0.036**	0.719	0.98
RAC	14.72±7.3	23.68±7.81	18.34±4.62	**0.002**	0.923	0.358
LIN	11.40±5.96	16.22±10.11	15.76±5.27	0.249	0.842	1.00
RIN	10.18±6.77	18.3±9.46	14.0±1.31	**0.01**	0.97	0.737
LCAU	25.06±12.31	29.32±13.59	28.33±5.30	0.196	1.00	1.00
RCAU	24.40±13.3	32.18±13.79	27.63±10.16	0.573	1.00	1.00
LPUT	20.68±9.5	27.94±8.37	21.48±5.76	**0.037**	1.00	0.319
RPUT	20.08±8.52	30.57±10.59	20.81±5.58	**0.004**	1.00	0.086

LGP	27.81±9.91	30.63±10.38	28.29±8.5	1.00	1.00	1.00
RGP	26.03±9.53	34.18±13.96	28.22±8.54	0.128	1.00	0.851
LFWM	13.98±6.06	15.02±5.98	14.16±5.03	1.00	1.00	1.00
RFWM	13.98±6.06	18.39±6.19	14.55±4.35	0.067	1.00	0.475
LHP	13.07±6.98	16.27±6.88	16.95±4.43	0.443	0.531	1.000
RHP	11.5±6.84	19.07±9.25	14.79±3.89	**0.016**	0.735	1.00
LTEMPG	13.70±4.86	22.91±8.41	22.00±3.61	**0.001**	**0.046**	1.00
RTEMPG	13.01±5.89	23.72±7.77	20.48±2.19	**<0.001**	0.073	0.89
LRN	26.63±10.25	30.45±12.46	27.35±6.65	0.897	1.00	1.00
RRN	22.73±8.36	33.56±13.85	24.08±9.21	**0.020**	1.00	0.249
LSN	26.87±13.82	29.94±11.89	27.70±11.27	1.00	1.00	1.00
RSN	24.76±14.01	33.52±12.01	24.93±6.95	0.103	1.00	0.407
LDN	20.79±8.03	23.68±6.7	17.96±5.57	0.6**5**2	1.00	0.257
RDN	19.15±6.76	24.92±8.05	18.62±5.02	0.059	1.00	0.2

V DISCUSSION

The clinical subtypes of FTD are characterized by distinctive profiles of clinical and imaging features in its initial presentation. As the disease progresses, there is a considerable overlap, and the in vivo phenotypes characteristic can be identified by the joint assessment of clinical, behavioural, and imaging biomarkers. Earlier studies using imaging markers focused on either GM damage or WM alterations in the FTD subtypes. However, no study, to date, has evaluated combined radiological biomarkers such as brain volume, WM integrity, and iron deposition and the extent to which they contribute to clinical profiles in the FTD subtypes. The current study investigated the patterns of cortical and subcortical GM atrophy, loss of WM integrity and abnormal iron deposition between patients with fvFTD, PPA and controls. The study provides valuable insight into the similarities and differences in the patterns of GM and WM damage in fvFTD and PPA and is the first of its kind from South Asia. The study proposes iron as an additional biomarker which may be useful for the diagnostic work-up of this neurodegenerative disease.

The participant group was selected from the Memory clinic at SCTIMST. The clinical diagnosis of FTD was based on Lund Manchester consensus criteria and subsequently confirmed by neuroimaging examinations. The syndromic variants were identified by Rascovsky criteria for fvFTD and Mesulam criteria for PPA. Out of the FTD patients, 74% were of fvFTD, and 26% were of PPA (15% SD and 11% PNFA). The controls included in the study were comparable with the patient's in terms of age, education level. A slight male predominance (57%) was seen in the population (Ratnavalli et al., 2002).

V.1 VBM analysis of GM degeneration in FTD

The primary aim of the VBM study was to compare the distinct profiles of GM involvement in the clinical variants of FTD. The study confirmed the widespread pattern of atrophy in frontal and anterior temporal lobes in FTD patients as previously demonstrated by postmortem and other imaging studies. Eventhough there are considerable overlap in atrophic patterns in clinical subtypes, the changes were specific to each group. Consistent with the clinical profiles, whole brain and regional analysis in fvFTD showed significant bilateral damage in the medial, orbital, and dorsolateral frontal cortex, anterior insula and anterior cingulate as well as striatum, hippocampus, amygdala, and other temporal lobe structures thus corroborating previous findings (Table 3). Whereas PPA showed greater bilateral atrophy in anterior insula, anterior temporal regions including HP, AMY with extended atrophy in frontal, occipital and parietal regions (Table 4). A quantitative evaluation of regional brain volumes showed excellent agreement with the whole brain analysis. Furthermore, the fvFTD had more atrophy in the TH, middle, medial and SFG, and anterior, middle cingulate regions along with some more clusters in CAU, HP, PHP, and precuneus than PPA patients (Table 7). Though the pattern in certain brain areas are bilateral, atrophy was more specific to left hemisphere.

A large number of neuroimaging and pathological studies investigated the GM atrophy in fvFTD or PPA compared to controls. The results have shown areas of atrophy in the ventromedial and posterior OFC, AC, anterior insula, striatum, lateral

temporal cortices, TH, STG and AMY bilaterally in fvFTD (Rosen et al., 2002; Boccardi et al., 2005; Borroni et al., 2007; Rabinovici & Miller, 2010; Hornberger et al., 2011; Looi et al., 2012; Couto et al., 2013) and left perisylvian region, bilateral anterior temporal lobe and basal ganglia, IFG, IN and parietal cortex (Gorno-Tempini et al., 2004; Rogalski et al., 2011) in PPA. Most consistent atrophic regions reported in fvfTD involved mesial or orbitofrontal cortex and anterior insula (Rosen et al., 2002; Davies et al., 2006), which are found to be affected early in the course of disease (Seeley et al., 2008). Hence, our observations in fvFTD pathology are corroborate with these earlier reports and a meta-analysis conducted by Pan P et al (Pan et al., 2012). They compared 11 VBM studies with 237 fvFTD and 297 healthy controls and provided evidence of fronto-striatial-limbic atrophy, highlighted the anatomical changes in the fronto-insular-anterior cingulate cortex. In addition to these fronto-temporal and limbic areas, our study identified an involvement of parietal and occipital regions in fvFTD pathology (Whitwell et al., 2011).

The extended atrophic clusters in cerebellum are quite unusual which have been reported by pathological studies in association with *C9orf72* mutation carriers of FTD (Whitwell and Josephs, 2012; Mahoney et al., 2012; Irwin et al., 2013). Comparing the anatomical patterns in PPA patients with previous studies confirmed the involvement of left hemisphere structures responsible in speech and language processing. The atrophy of the bilateral anterior temporal lobe is inline with previous findings in SD (Hodges et al., 1999; Mummery et al., 2000 ; Rosen et al., 2002; Gorno-Tempini et al., 2004) whereas the atrophy of left anterior insula, premotor and

inferior frontal regions inline with findings in PNFA (Gorno-Tempini et al., 2004; Josephs et al., 2006; Wilson et al., 2009). The extended clusters in the right hemisphere of PPA patients may due to the nonverbal semantic deficits (Seeley et al., 2005) developed over time. These behavioural symptoms often cause spread between hemispheres with more posterior temporal and inferior frontal involvement (Brambati et al., 2009). Furthermore, Rohrer et al reported that the extended patterns in parietal, frontal, caudate, and the right precuneus or posterior cingulate areas associated with disease progression (Rohrer & Rosen, 2013). Consistent with other studies in PPA, we could not find any significant atrophy in PC.

We also found that fvFTD and PPA shared a common pattern of whole brain and regional atrophy especially greater GM loss in fvFTD. The shared patterns clearly indicate the behavioural abnormalities seen in PPA group. Since our pathological group contained more SD than PNFA, the findings from this study are concordant with the previous studies comparing fvFTD and SD. Rosen et al had observed GM tissue loss in orbito frontal, anterior cingulate and insula in both fvfTD and SD (Rosen et al., 2002). As in our study, Bozeat et al detected the involvement of a common network with ventral frontal region, temporal pole and amygdala in both groups, hence were behaviourally similar (Bozeat et al., 2000).

Besides these common regions affected in both variants, fvFTD patients presented greater damage to both bilateral frontal and temporal regions while PPA patients

exhibited greater damage in temporal structures and significant involvement of frontal language regions. In contrast to fvFTD, PPA failed to reveal atrophy in bilateral CM, TH, and CL in right hemisphere. Interestingly, both these groups could not find significant GM changes in PC regions. These findings sharply discriminated the patient groups and act as potentially important imaging biomarker for FTD subtypes.

The strength of our study is the divergent anatomical pattern of atrophy in these FTD syndromes. This is the first of its kind in Indian population and put forward some outstanding imaging findings. Although mounting evidences exist for the more right hemisphere involvement in fvFTD, our study highlights the moreover equal contribution of both hemispheres. This striking largely symmetrical bilateral frontal and temporal involvement encompassing the bilateral DLPFC, OFC, VMFC, extending to medial, lateral and anterior temporal lobes. The spread of atrophy in the right hemisphere in PPA in our study was well suited with a recent study by Kamminga et al (Kamminga et al., 2015). They displayed widespread atrophy in the medial and lateral temporal lobes with heavily affected right hemisphere than left in right hemispheric variant SD in comparison with fvFTD. They also investigated the neural correlates of emotion processing in the syndrome of right SD and found possible right temporal connections. Hence, our findings indicate the clinical presentation of behavioural and interpersonal disturbances in SD patients. Identification of severe impairement in the HG of both the groups by the whole brain and regional analysis is quite surprising. A previous VBM study to identify the

neural correlates of basic emotions in FTD revealed an association between fear recognition and HG atrophy along with planum temporal (PT), right HP, AMY, AC, medial and superior frontal gyrus, left lingual gyrus and occipital regions by caricature task (Kumfor et al., 2013). Also the highly disrupted language in FTD contributed to the atrophy in HG (Mitchell & Crow, 2005). Moreover, HG and PT are the key components in the STG associated with auditory and language processing respectively.

The shrinkage of FG and anterior temporal pole areas are implicated in the difficulty in perceiving and remembering the faces and social and emotional stimuli in our patient groups (Olson et al., 2007). Kumfor et al explored the anatomical correlation of face perception, face recognition and object recognition in 13 fvFTD and 1 SD patients (Kumfor et al., 2015) and revealed a common finding of face memory and face perception deficits in both groups. These observations indicate the need for strategies to improve face perception and memory that may improve both the quality of life and their interpersonal relationship with caregiver and their family members.

The results also highlight the fact that VBM may assist in the differential diagnosis of fvFTD and PPA with GM volume loss in SFG, MFG, TH, CAU, AC, and RECG, supporting the clinical diagnosis of fvFTD. Identification of the subcortical regions in addition to frontal might be more predictive than cortical, which often have been shown to overlap between diseases.

V.2 TBSS Analysis of WM degeneration in FTD

The primary aim of the DTI study was to evaluate the WM alterations that mirrored the GM atrophy in FTD. Several studies have been performed in FTD subtypes to investigate the WM structural integrity (Borroni et al., 2007; Matsuo et al., 2008; Zhang et al., 2009 ; Acosta-Cabronero et al., 2011; Agosta et al., 2011); Pan et al., 2012; Mahoney et al., 2013) and they found significant differences in regional severity depending on the DTI metrics used. To date, relatively few DTI studies have investigated the patterns of WM damage in variants of FTD with whole brain analysis. They have described the WM integrity differences between fvfTD and tvfTD (Borroni et al., 2007), as well as in fvfTD and PPA (Agosta et al., 2011). Agosta et al identified widespread bilateral injury in the major commissural and association tracts in fvfTD in comparison with PPA and controls. Further, they observed prefrontal and temporal damage is in consistent with the behavioural and neuropsychological symptoms of FTD (Boccardi et al., 2005)

The present study applied both the whole brain and regional WM measurements to identify the spatial pattern of WM abnormalities in the variants of FTD. In agreement with the distribution of pathology measured by neuroimaging (Pereira et al., 2009) and postmortem studies (Brun, 1987), TBSS revealed a significant and extensive bilateral pattern of diffusivity and FA abnormalities in WM tracts of FTD subtypes.

Our investigations in patients with fvFTD showed diffusion MRI alterations in tracts connecting frontal poles through the anterior corpous callosum, such as genu and forceps minor, bilateral WM tracts in frontal lobes such as SLF and cingulum, and

those passing through temporal lobes, such as the uncinate, ILF and in IFOF (Figure 25). The extensive atrophic patterns were observed in forceps major, and anterior thalamic radiations and hence the findings corroborated with previous studies (Borroni et al., 2007; Zhang et al., 2009; Whitwell et al., 2011; Federica Agosta et al., 2012a; Nguyen et al., 2013; Tovar-Moll et al., 2014). Conversely, a recent study failed to reveal any tract specific changes in the SLF of fvFTD patients compared to controls (Powers et al., 2014). They reported disruption of WM integrity in anterior potions of CC, bilateral UF, ILF, and IFOF in 11 fvFTD patients compared to controls. The involvement of posterior brain regions such as posterior corpous callosum and parietal and occipital WM either may due to the heterogenous pattern of atrophy in this condition (Whitwell et al., 2009a) or may due to the atrophy in the lateral and medial parietal regions in the later disease course (Brambati et al., 2009). On the other hand, patients with PPA showed significant and severe WM alterations in forceps minor and left ILF, left uncinate and bilateral IFOF, consistent with previous analyses (Borroni et al., 2007; Matsuo et al., 2008; Agosta et al., 2011; Whitwell et al., 2011). In addition, in PPA the left SLF, cingulum, and anterior thalamic radiation atrophic patterns were observed (Figure 26). The most severe left frontotemporal atrophy in PPA group suggest that damage of fronto-temporal-parietal network which plays an important role in the language deficits seen in these patients. The study also highlighted that both patient group share a common pattern of atrophy. Relative to PPA, fvFTD was associated with markedly reduced FA in frontal lobe regions, especially in the forceps minor and left hemisphere SLF and IFOF (Figure 27), and the finding is consistent with our GM results measured by VBM.

The WM vulnerability seen in fvFTD and PPA are most likely due to axonal degeneration associated with injury or death of neuronal cell bodies. However, these findings are in agreement with the previous histopathological evidence of tau or (Schofield et al., 2003) TDP-43 (Neumann et al., 2007) protein deposition in FTD. Notably, the FA reduction in the cingulum tract, which is considered as the major limbic fibre in the medial temporal lobe is consistent with prior structural findings of paralimbic network degeneration in FTD (Rabinovici & Miller, 2010; Seeley, 2008). The regional pattern of FA and MD alterations measured by means of DT MR metrics in fvFTD overlaps with the pattern of WM atrophy detected by TBSS. On the contrary, the diffusivity alterations investigated by DTI metrics in PPA was found significant in genu of CC and left hemisphere UF and ILF. While, the FA changes in PPA was found prominent in all language tracts. In line with previous studies, we could not find any prominent WM alterations in CST of FTD subtypes in comparison to controls (Zhang et al., 2009; F. Agosta et al., 2012b). Moreover, the most prominent FA reduction in SLF detected in the direct comparison coincide with the severe frontal lobe damage in frontal variant group. Furthermore, the consistent finding of UF damage in both group is likely to be responsible for the behavioural symptoms in FTD group (F. Agosta et al., 2012b), (Rohrer and Warren, 2010).

Our study had clinical implications because an association between OFC damage and behavioural manifestations has been shown in fvFTD (Borroni et al., 2007) and PPA(Rohrer & Warren, 2010). Although the role of UF in language processing is still debated, it has been suggested in the semantic memory and name retrieval

circuitory (Papagno et al., 2011). Moreover, the observation of severe ILF damage in PPA patients confirmed the language impairment (Borroni et al., 2007; Matsuo et al., 2008; Zhang et al., 2009; Whitwell et al., 2011; F. Agosta et al., 2012b). In summary, the whole brain and regional DTI alterations suggest that both fvFTD and PPA associated with characteristic distribution of WM degeneration. The results also implicate a greater vulnerablity of WM in fvFTD than in PPA. It may provide additional biomarker to distinguish fvfTD from PPA.

V.3 Measurement of Cortical Brain iron deposition using SWI

In this study, we quantified the extent of brain iron deposition in the cortical and subcortical regions in FTD patients in comparison with controls and correlated this with behavioural and neuropsychological test measures. To our knowledge, no other previous studies have performed the quantitative assessment of brain iron deposition in the FTD patients.

Iron (Fe) is an important element for normal brain function due to its critical role in oxidative metabolism, DNA synthesis and other enzymatic processes. Iron misregulation (Hallgren & Sourander, 1958) causes the abnormal elevation of iron, which might be modulated by genetic factors (Bartzokis et al., 2010). The relentless accumulation of iron promote spontaneous release of highly neurotoxic free iron which inturn produce highly reactive radical species, thus leading to oxidative stress (Gutteridge, 1992; Floyd, 1999). Such iron-mediated oxidative stress thought to promote the formation of cytotoxic protein aggregates which may trigger

neurodegeneration (Götz et al., 2004; Berg & Youdim, 2006). Still it is an open question whether iron accumulation is the cause or consequence of neurodegenerative process, but it is widely accepted that the monitoring the spatial distribution and the temporal dynamics of iron deposition may offer important insights into our understanding of pathogenesis of neurodegeneration (Schenck & Zimmerman, 2004; Zecca et al., 2004; Haacke et al., 2005) syndrome, NBIA-1), and aceruloplasminemia (Batista et al 2012) has been found to associate with excessive iron accumulation. Also, our previous study in ALS demonstrated abnormal brain iron deposition in the posterior bank of motor cortex, which proposed it as a potential biomarker in this patient group (Sheelakumari et al., 2015). Recently there has been an increasing urge for invivo quantitative estimation of non-heme iron and its importance in the pathophysiology of AD (Wang et al., 2013; Raven et al., 2013).

Several MRI methods including R2, R2*, magnetic field correlation (MFC), relaxation time mapping and Susceptibility Weighted Imaging (SWI) have been proposed for detection and quantification of tissue iron (Péran et al., 2007; Jensen et al., 2009; Bartzokis et al., 2007; Harder et al., 2008; Sheelakumari et al., 2015). SWI is a 3D velocity compensated gradient echo sequence that uses both magnitude and phase data separately or together to enhance information about any tissue or substance with different susceptibility in contrast. It has been shown to be an ideal invivo tool to quantify iron in the form of ferritin, hemosiderin and deoxyhemoglobin.

In the present study, we performed a quantitative assessment of brain iron deposition in the frontal, temporal and basal ganglia regions in the subtypes of FTD in comparison to controls. We found significant increase of iron levels in the bilateral anterior TEMG, AC and PUT along with right hemispheric IN, PBMC, HP, and RN of fvFTD patients in comparison to controls (Table 9). The patients with PPA only showed significant iron levels in the left hemisphere TEMG and a trend towards significance in the right hemisphere in comparison with controls. A direct comparison between fvFTD and PPA revealed significant iron deposition in the right hemisphere SFG in fvFTD patients, whereas, the iron content in the right hemisphere PUT of fvFTD reaches a level of significance compared to PPA.

Earlier studies proved significant grey and white matter degeneration in fronto-insular-striatial-temporal regions in fvfTD (Boccardi et al., 2005; Borroni et al., 2007; Zamboni et al., 2008; Bertoux et al., 2015) and more severe temporal atrophy in PPA (Borroni et al., 2007; Agosta et al., 2012b), however there is no quantitative comparison of iron deposition in FTD brain. Recently, Reuck et al analysed the post-mortem brains of patients with neurodegenerative and cerebrovascular disease and observed most significant iron deposition in the claustrum, CAU and PUT and comparatively lesser significant deposition in GP, TH and subthalamic nucleus in FTD compared with controls (De Reuck et al., 2014). These findings support our observation of increased iron deposition in basal ganglia regions. Moreover, our volumetric results in the same patient group showed characteristic atrophy patterns in the basal ganglia (unpublished data) similar to findings in previous study (Josephs,

2008). Notably, a prior tractography analysis in human brain demonstrated well established connections between fronto-striatial network (Leh et al., 2007). The significant iron deposition in the red nucleus of frontal variant group may be due to the strong functional coherence between red nucleus and prefrontal, insula, temporal, parietal, thalamic and hypothalamic regions (Nioche et al., 2009). This implicates the role of rubral circuit in cognition, especially in salience detection and executive control.

V.4 Association between radiological measures and behavioural scores

The neural correlates of measures of FrSBe such as apathy and disinhibition with GM atrophy and WM tract integrity still not clearly established. This prospective study investigated the relationship between FRSBe sub items and GM loss, WM atrophy as well as elevated iron levels.

V.4.1 Neural substrate of behavioural features in FTD using VBM

In this imaging study we observed relatively distinct anatomic distributions of GM loss in each behavior in patients with fvFTD. Apathy was found associated with DLPFC, medial PFC, OFC, limbic lobe especially AC, insula and right temporal regions, while disinhibition was associated with limbic regions (AMY, HP and PHP), temporal pole, IN and fusiform areas (Figure 23). We found an association of frontal damage only with apathy not with disinhibition. A few prior studies investigated the abnormal behaviours and anatomical correlation. Our study used both whole brain

and regional GM atrophy relationships to optimize the results and identified consistent findings in both case.

The atrophy of DLPFC is implicated in *cognitive inertia*, (Levy & Dubois, 2006), which leads to a deficit in executing goal directed behavior (GDB). Recent observations rely on the fact that apathy emanates from the difficulty in manipulating and integrating the various levels in a plan to execute an action (Eslinger et al., 2012). As DLPFC has an important role in planning, problem solving and rule finding (Goldman-Rakic, 1987; Miller & Cohen, 2001) our findings are compatible with these findings. Notably, our findings of an association between apathy and OFC damage corroborate with Massimo et al 2015, who reported a correlation between OFC damage and poor motivation (Massimo et al., 2015). The goal selection deficits in patients are highly linked to poor motivation, thereby making them disreactive to positive reward and negative *punishment* signals.

The role of ACC in initiating behavior has previously been implicated in healthy adults (Mulert et al., 2003), akinetic mute state (Mega & Cohenour, 1997), frontal lobe injury and fvFTD patients (Zamboni et al., 2008; Massimo et al., 2009). Hence, the extended atrophy of frontal to ACC networks consistent with previous literature regarding apathy in fvFTD (Zamboni et al., 2008; Massimo et al., 2009) and PD (Reijnders et al., 2010). In addition to frontal atrophy, insular damage was noted in our group, which is consistent with apathy findings in AD and PSP (Stanton et al.,

2013). In addition, we found that RECG and SMA are significantly correlated with apathy. Both these regions previously implicated in FTD patients in association with disinhibition and aberrant motor behavior respectively (Rosen et al., 2005; Peters et al., 2006). Our analysis also identified a significant correlation of apathy with atrophic changes in the inferiorparietal lobule. This extended evidence suggests the role of this region in mediating the integration of competing sources of situational data for the purpose of contextualizing and scene setting.

The severity of disinhibition significantly correlated with limbic regions (HP, AMY, and PHP), temporal cortices (STG,ITG,TP, FG) and right hemisphere insular cortex. Prior studies investigated the neural correlate of disinhibition by using carer based questionnaires. In contrast, they reported frontal-limbic damage in disinhibition (Rosen et al., 2005; Peters et al., 2006; Massimo et al., 2009; Hornberger et al., 2011). Rosen et al showed that the disinhibition score of the NPI covaried with subgenual cingulate gyrus atrophy (Rosen et al., 2005). Also, Hornberger et al identified OFC atrophy as a candidate marker of disinhibition by using both subjective NPI and objective Hayling test (Hornberger et al., 2011). They also found the involvement of temporal areas in disinhibition which is in accordance with the current findings. Furthermore, the same finding was replicated in a large sample of mixed dementia patients, including fvfTD using measures of cortical thickness measurement of OFC GM integrity (Krueger et al., 2011). In contrast, instead of OFC atrophy, another study (Zamboni et al., 2008) by employing FrSBe and VBM

established right hemisphere AMY, HP, MTG and nucleus accumbens atrophy. Hence, our study results corroborate with these findings.

The HP and AMY is involved in the behavioural inhibition system and have been found to correspond with fear conditioning (Baeuchl et al., 2015) and their relationship with temperament dimensions are quite complex and interdependent. The lesions and hypoperfusion in AMY leads to diminished fear response and weakened fear conditioning (moral-emotive deficit), on the other hand, hippocampal dysfunction leads to memory problems and behavioural control deficit (Sah et al., 2003). The investigation of multimodal system of emotions such as anger, fear, disgust, happiness, sadness and surprise in FTD showed the insula as a neural substrate for processing of disgust recognition (Kumfor et al., 2013) .

Prior reports in patients with temporal lesions or temporal lobe epilepsy clearly described the extensive behavioural symptoms, including mania, euphoria, and aggressive behaviours and it seems consistent with the GM loss in temporal structures. Moreover, these behavioural deficits often interpreted in terms of connected pathways, reflecting the connections between temporal lobe and orbitofrontal regions and not as a consequence of loss of specific functions in the temporal lobe. According to Cummings et al, temperolimbic structures are part of OFC, whose dysfunction leads to prominent disinhibitive syndromes (Cummings, 1995). Our study is the first in describing the relation between fusiform atrophy in

disinhibitive behavior. This discrepant finding may be due to the evolution of Capgras delusion which has been found to be associated with dementia and other neurodegenerative disorders (Butler & Zeman, 2005). Since our study could not find any correlation between disinhibition score and frontal areas, the results suggest that disinhibition may arise from impaired reward/punishment attribution mechanisms that seems independent from prefrontal cortex dysfunction. Hence our results implicate that it is important to integrate the prefrontal and temporal limbic structures to properly perform complex social behaviours.

V.4.2 Neural substrate of behavioural features in FTD using DTI

The DTI results of the study suggest that similar to GM involvement, WM alterations in specific brain regions are likely to be responsible for different clinical symptoms associated with fvFTD and PPA. Our study examined the WM changes associated with behavioural symptoms of apathy and disinhibition in FTD group. It has been suggested that the GM and WM structures in frontal and temporal parts of the brain comprise the critical components of a large scale network which is important in the regulating the GDB (Brown & Pluck, 2000). The role of orbital and medial regions of inferior temporal lobe in value and reward related information has been implicated in several studies (Kable and Glimcher, 2007; Grossman et al., 2010) . Thus, it is possible that the degeneration of these frontal WM projections to temporal areas may interfere with motivation and GDB. Previous studies in fvFTD described the WM association with disinhibition using different methods and revealed inconsistent findings. Our study demonstrated that damage in SLF correlated to apathy and disinhibition. The findings were corroborating with Borroni et al, who used an ROI

approach and reported an association between SLF damage and behavioural deficits measured by the FBI (Borroni et al., 2007). In contrast, Hornberger et al reported a correlation between FA changes in the UF, cingulum and forceps minor with disinhibition measured by Hayling test (Hornberger et al., 2011). Then it is important to notice that the disruption of distinct regions of WM in frontotemporal networks corresponds to goal directed behavior in fvFTD. The variability of results across studies either may due to the measures used to assess the behavioural symptoms or may due to the heterogeneity in clinical cohort. Future studies using whole brain techniques to characterize changes in functional network such as salience that has been implicated in affective cognition and behavioural disruptions could provide valuable information about the relative contribution of GM and WM to behavioural manifestations in FTD.

V.4.3 Neural substrate of behavioural features in FTD using SWI

The new biomarker of cortical iron deposition in fvFTD also revealed a significant association between increased iron content in SFG with apathetic profile, while the increased iron content in right PUT revealed an association with disinhibited profile (Eslinger et al., 2012; Halabi et al., 2013). This apathy correlation was consistent with volumetric findings and the role of PUT in disinhibition may be due to its afferent connections to the mediofrontal, dorsolateral prefrontal, and orbitofrontal regions as well as its link with prefrontal motor circuits(Macfarlane et al., 2015).

V.5 Limitations of the study

The present study had few limitations. Firstly, the study was carried out in a relatively limited number of subjects especially in the PPA group. Further studies with large samples are warranted to confirm our findings. Secondly, we considered our language variant patients as a single group because of the small sample size with less number of PNFA, while it is now clear that both SD and PNFA have specific distribution of pathology and clinical manifestations. Thirdly, all the subjects were unable to complete the neuropsychological tests due to more advanced stage of the disease. The absence of neuropsychological correlations may have lowered the power of analysis. Fourthly, in the analysis of brain iron deposition we could not include the ROIs such as IFG, MFG and OFC and other language regionsof temporal pole and ITG due to large susceptibility artifacts from skull-base, which also reduces the strength of the study. Finally, the lack of autopsy confirmation in all patients possibly is a minor limitation too. Hence further longitudinal studies involving large cohort with and pathological confirmation in relation with neuropsychological and behavioural correlation are needed to support our findings.

VI SUMMARY AND CONCLUSIONS

The study examined the patterns of GM and WM changes and abnormal iron deposition associated with the clinical variants of FTD compared to healthy controls. The study is the first of its kind in Indian population. This study confirmed the GM and WM changes associated with the diagnosis of FTD compared to healthy controls seen in previous work, but extend this by the demonstration of correlation between behavioural measures in both fvfTD and PPA. Estimations of subscales of FrSBe scores also showed significantly increased scores in frontal variant groups which differed from aphasic group in terms of disinhibition and executive dysfunction.

The analysis of GM degeneration using VBM demonstrated consistent findings of bilateral largely symmetrical patterns of frontal and temporal degeneration along with subcortical involvement in fvFTD. In addition, the parietal and occipital involvement was observed at lower thresholds. The PPA variants exhibited wide spread atrophy in the temporal regions with more spread in the right hemisphere. We found significant clusters in the left frontal regions and subcortical thalamus in the fvFTD patients compared to PPA. As expected, the opposite contrast failed to reveal any significant clusters. Inorder to validate the whole brain findings, ARV analysis was performed and confirmed the earlier results.

As most of the previous studies only investigated either the GM or WM differences in patients, our study aimed to improve the reliability by diagnosing and monitoring FTD variants by diffusion MRI by using TBSS whole brain analysis and by tract

specific measurements, which is considered to be novel in these patients. Both voxelwise analysis and DTI metrics measurements showed significant and extensive FA and MD changes in fvFTD and PPA that mirrored the GM abnormalities which offer additional biomarker for the diagnostic work of FTD patients. The direct comparison between patient groups described WM changes in terms of both metrics and clusters of FA and MD values in left SLF and genu with comparatively less significance in right UF and left IFOF. The findings speculate that WM changes observed are most likely arise due to the axonal degeneration associated with death of neuronal cell bodies.

The urge for a new biomarker in the form of advanced neuroimaging techniques leads to the application of SWI as a measure of cortical iron deposition to differentiate the variants of FTD subtypes. The study found significant elevated iron levels in the bilateral SFG and TEMG, AC, PUT, and right hemisphere PBMC, HP, IN and RN in fvFTD and only left hemisphere TEMG in PPA. These findings replicated the previous findings of greater GM and WM damage in the right hemisphere of fvFTD and left hemisphere in PPA. The greater iron deposition in the SFG of fvFTD compared to PPA converges with the findings of other imaging biomarkers.

Apart from these, the correlation analysis between GM, WM and iron content measures in the specific brain regions and behavioural assessment scores suggest that

disease in the fronto-temporal and limbic structures may contribute to behavioural profiles in FTD. The study confirmed that eventhough the variants have considerable overlap; the changes were specific to each group. The behavioural findings have important implications for the management of patients with fvFTD. Also the more spread in atrophy of the right hemisphere in PPA contribute to caregiver burden as observed in fvFTD.

The earlier onset of FTD compared to other dementias contributes to a greater caregiver burden. Recent investigations have focused on the brain-behaviour relationship in the FTD because the behavioural and personality changes can precede the cognitive symptoms. The association between neuropsychological performance and activities of daily living has been implicated previously. Although the researchers at several centers have explored the cognitive and behavioural changes associated with this degenerative dementia, it is important to provide multimodal imaging biomarkers that would help the clinicians to guide treatment recommendations. The results of this study demonstrate a multiparametric approach for classifying fvFTD and PPA. Based on these results we concluded that the above multimodal biomarkers can serve as a predictor of impending behavioural abnormalities in FTD. We suggest that future longitudinal studies targeting complex socio-emotional and cognitive processes may assist in the differential diagnosis of these syndromic variants of FTD.

VII BIBLIOGRAPHY

Acosta-Cabronero, J., Patterson, K., Fryer, T.D., Hodges, J.R., Pengas, G., Williams, G.B., Nestor, P.J., (2011). Atrophy, hypometabolism and white matter abnormalities in semantic dementia tell a coherent story. Brain J. Neurol. 134, 2025–2035. doi:10.1093/brain/awr119

Agosta, F., Canu, E., Sarro, L., Comi, G., Filippi, M., (2012a). Neuroimaging findings in frontotemporal lobar degeneration spectrum of disorders.Cortex J. DevotedStudyNerv.Syst.Behav.48,389–413.doi:10.1016/j.cortex.2011.04.012

Agosta, F., Scola, E., Canu, E., Marcone, A., Magnani, G., Sarro, L., Copetti, M., Caso, F., Cerami, C., Comi, G., Cappa, S.F., Falini, A., Filippi, M., (2012b). White matter damage in frontotemporal lobar degeneration spectrum. Cereb. Cortex N. Y. N 1991 22, 2705–2714. doi:10.1093/cercor/bhr288

Alexander, A.L., Lee, J.E., Lazar, M., Field, A.S., (2007). Diffusion Tensor Imaging of the Brain. Neurother. J. Am. Soc. Exp. Neurother. 4, 316–329. doi:10.1016/j.nurt.2007.05.011

Alladi, S., Mekala, S., Chadalawada, S.K., Jala, S., Mridula, R., Kaul, S., (2011). Subtypes of Dementia: A Study from a Memory Clinic in India. Dement. Geriatr. Cogn. Disord. 32, 32–38. doi:10.1159/000329862

Alzheimer, A., (1991). Über eigenartige Krankheitsfälle des späteren Alters (On certain peculiar diseases of old age. Hist. Psychiatry 2, 74–101. doi:10.1177/0957154X9100200506

Armitage, P. a., Bastin, M. e., (2001). Utilizing the diffusion-to-noise ratio to optimize magnetic resonance diffusion tensor acquisition strategies for improving measurements of diffusion anisotropy. Magn. Reson. Med. 45, 1056–1065. doi:10.1002/mrm.1140

Ashburner, J., Friston, K.J., (2001). Why voxel-based morphometry should be used. NeuroImage 14, 1238–1243. doi:10.1006/nimg.2001.0961

Ashburner, J., Friston, K.J., (2000). Voxel-based morphometry--the methods. NeuroImage 11, 805–821. doi:10.1006/nimg.2000.0582

Ashburner, J., Hutton, C., Frackowiak, R., Johnsrude, I., Price, C., Friston, K., 1998. Identifying global anatomical differences: deformation-based morphometry. Hum. Brain Mapp. 6, 348–357.

Baeuchl, C., Meyer, P., Hoppstädter, M., Diener, C., Flor, H., (2015). Contextual fear conditioning in humans using feature-identical contexts. Neurobiol. Learn. Mem. 121, 1–11. doi:10.1016/j.nlm.2015.03.001

Baker, M., Mackenzie, I.R., Pickering-Brown, S.M., Gass, J., Rademakers, R., Lindholm, C., Snowden, J., Adamson, J., Sadovnick, A.D., Rollinson, S., Cannon, A., Dwosh, E., Neary, D., Melquist, S., Richardson, A., Dickson, D., Berger, Z., Eriksen, J., Robinson, T., Zehr, C., Dickey, C.A., Crook, R., McGowan, E., Mann, D., Boeve, B., Feldman, H., Hutton, M., (2006). Mutations in progranulin cause tau-negative frontotemporal dementia linked to chromosome 17. Nature 442, 916–919. doi:10.1038/nature05016

Barber, R., Snowden, J.S., Craufurd, D., (1995). Frontotemporal dementia and Alzheimer's disease: retrospective differentiation using information from informants. J. Neurol. Neurosurg. Psychiatry 59, 61–70.

Bartzokis, G., Lu, P.H., Tishler, T.A., Peters, D.G., Kosenko, A., Barrall, K.A., Finn, J.P., Villablanca, P., Laub, G., Altshuler, L.L., Geschwind, D.H., Mintz, J., Neely, E., Connor, J.R., (2010). Prevalent iron metabolism gene variants associated with increased brain ferritin iron in healthy older men. J. Alzheimers Dis. JAD 20, 333–341. doi:10.3233/JAD-2010-1368

Bartzokis, G., Tishler, T.A., Lu, P.H., Villablanca, P., Altshuler, L.L., Carter, M., Huang, D., Edwards, N., Mintz, J., (2007). Brain ferritin iron may influence age- and gender-related risks of neurodegeneration. Neurobiol. Aging 28, 414–423. doi:10.1016/j.neurobiolaging.2006.02.005

Basser, P.J., Mattiello, J., LeBihan, D., (1994). MR diffusion tensor spectroscopy and imaging. Biophys. J. 66, 259–267. doi:10.1016/S0006-3495(94)80775-1

Basser, P.J., Pierpaoli, C., (1996). Microstructural and physiological features of tissues elucidated by quantitative-diffusion-tensor MRI. J. Magn. Reson. B 111, 209–219.

Beaulieu, C., 2002. The basis of anisotropic water diffusion in the nervous system - a technical review. NMR Biomed. 15, 435–455. doi:10.1002/nbm.782

Berg, D., Youdim, M.B.H., 2006. Role of iron in neurodegenerative disorders. Top. Magn.Reson.ImagingTMRI17,5–17. doi:10.1097/01.rmr.0000245461.90406.ad

Bertoux, M., O'Callaghan, C., Flanagan, E., Hodges, J.R., Hornberger, M., (2015). Fronto-Striatal Atrophy in Behavioral Variant Frontotemporal Dementia and Alzheimer's Disease. Front. Neurol. 6. doi:10.3389/fneur.2015.00147

Bitar, R., Leung, G., Perng, R., Tadros, S., Moody, A.R., Sarrazin, J., McGregor, C., Christakis, M., Symons, S., Nelson, A., Roberts, T.P., (2006). MR Pulse Sequences: What Every Radiologist Wants to Know but Is Afraid to Ask. RadioGraphics 26, 513–537. doi:10.1148/rg.262055063

Bloch,F.,(1946).NuclearInduction.Phys.Rev.70,460–474.doi:10.1103/PhysRev .70.460

Boccardi, M., Sabattoli, F., Laakso, M.P., Testa, C., Rossi, R., Beltramello, A., Soininen, H., Frisoni, G.B., (2005a). Frontotemporal dementia as a neural system disease. Neurobiol. Aging 26, 37–44. doi:10.1016/j.neurobiolaging.2004.02.019

Boccardi, M., Sabattoli, F., Testa, C., Beltramello, A., Soininen, H., Frisoni, G.B., (2004). APOE and modulation of Alzheimer's and frontotemporal dementia. Neurosci. Lett. 356, 167–170. doi:10.1016/j.neulet.2003.11.042

Borroni, B., Brambati, S.M., Agosti, C., Gipponi, S., Bellelli, G., Gasparotti, R., Garibotto, V., Di Luca, M., Scifo, P., Perani, D., Padovani, A., (2007). Evidence of white matter changes on diffusion tensor imaging in frontotemporal dementia. Arch. Neurol. 64, 246–251. doi:10.1001/archneur.64.2.246

Borroni, B., Alberici, A., Grassi, M., Rozzini, L., Turla, M., Zanetti, O., Bianchetti, A., Gilberti, N., Bonvicini, C., Volta, G.D., Rozzini, R., Padovani, A., 2011. Prevalence and demographic features of early-onset neurodegenerative dementia in Brescia County, Italy. Alzheimer Dis. Assoc. Disord. 25, 341–344. doi:10.1097/WAD.0b013e3182147f80.

Borroni, B., Ferrari, F., Galimberti, D., Nacmias, B., Barone, C., Bagnoli, S., Fenoglio, C., Piaceri, I., Archetti, S., Bonvicini, C., Gennarelli, M., Turla, M., Scarpini, E., Sorbi, S., Padovani, A., 2014. Heterozygous TREM2 mutations in frontotemporal dementia. Neurobiol. Aging 35, 934.e7–10. doi:10.1016/j.neurobiolaging.2013.09.017

Bozeat, S., Gregory, C.A., Ralph, M.A., Hodges, J.R., (2000). Which neuropsychiatric and behavioural features distinguish frontal and temporal variants of frontotemporal dementia from Alzheimer's disease? J. Neurol. Neurosurg. Psychiatry 69, 178–186.

Brambati, S.M., Rankin, K.P., Narvid, J., Seeley, W.W., Dean, D., Rosen, H.J., Miller, B.L., Ashburner, J., Gorno-Tempini, M.L., (2009). Atrophy progression in semantic dementia with asymmetric temporal involvement: a tensor-based morphometry study. Neurobiol. Aging 30, 103–111. doi:10.1016/j.neurobiolaging.2007.05.014

Brodaty, H., Seeher, K., Gibson, L., (2012). Dementia time to death: a systematic literature review on survival time and years of life lost in people with dementia. Int. Psychogeriatr. IPA 24, 1034–1045. doi:10.1017/S1041610211002924

Brown, R.G., Pluck, G., (2000). Negative symptoms: the "pathology" of motivation and goal-directed behaviour. Trends Neurosci. 23, 412–417.

Brun,A.,(1987). Frontal lobe degeneration of non-Alzheimer type. I. Neuropathology. Arch. Gerontol. Geriatr. 6, 193–208.

Butler, C., Zeman, A.Z.J., (2005). Neurological syndromes which can be mistaken for psychiatric conditions. J. Neurol. Neurosurg. Psychiatry 76, i31–i38. doi:10.1136/jnnp.2004.060459

Catani, M., Howard, R.J., Pajevic, S., Jones, D.K., (2002). Virtual in vivo interactive dissection of white matter fasciculi in the human brain. NeuroImage 17, 77–94.

Chan, D., Fox, N.C., Jenkins, R., Scahill, R.I., Crum, W.R., Rossor, M.N., (2001). Rates of global and regional cerebral atrophy in AD and frontotemporal dementia. Neurology 57, 1756–1763.

Chow, T.W., Miller, B.L., Boone, K., Mishkin, F., Cummings, J.L., (2002). Frontotemporal dementia classification and neuropsychiatry. The Neurologist 8, 263–269.

Chow, T.W., Hodges, J.R., Dawson, K.E., Miller, B.L., Smith, V., Mendez, M.F., Lipton, A.M., 2005. Referral Patterns for Syndromes Associated With

Frontotemporal Lobar Degeneration. Alzheimer Dis. Assoc. Disord. 19, 17–19.

Clinical and neuropathological criteria for frontotemporal dementia. The Lund and Manchester Groups., (1994) . J. Neurol. Neurosurg. Psychiatry 57, 416–418.

Constantinidis, J., Richard, J., Tissot, R., (1974). Pick's disease. Histological and clinical correlations. Eur. Neurol. 11, 208–217.

Couto, B., Manes, F., Montañés, P., Matallana, D., Reyes, P., Velasquez, M., Yoris, A., Baez, S., Ibáñez, A., (2013). Structural neuroimaging of social cognition in progressive non-fluent aphasia and behavioral variant of frontotemporal dementia. Front. Hum. Neurosci. 7. doi:10.3389/fnhum.2013.00467

Cummings, J.L., (1997). The Neuropsychiatric Inventory: assessing psychopathology in dementia patients. Neurology 48, S10–16.

Cummings, J.L., (1995). Anatomic and behavioral aspects of frontal-subcortical circuits. Ann. N. Y. Acad. Sci. 769, 1–13.

Das, S., Ghosal, M., Pal, S., (2012). Dementia: Indian scenario. Neurol. India 60, 618. doi:10.4103/0028-3886.105197

Davatzikos, C., Genc, A., Xu, D., Resnick, S.M., (2001). Voxel-based morphometry using the RAVENS maps: methods and validation using simulated longitudinal atrophy. NeuroImage 14, 1361–1369. doi:10.1006/nimg.2001.0937

Davatzikos, C., Resnick, S.M., Wu, X., Parmpi, P., Clark, C.M., (2008). Individual patient diagnosis of AD and FTD via high-dimensional pattern classification of MRI. NeuroImage 41, 1220–1227. doi:10.1016/j.neuroimage.2008.03.050

Davies, R.R., Hodges, J.R., Kril, J.J., Patterson, K., Halliday, G.M., Xuereb, J.H., (2005). The pathological basis of semantic dementia. Brain J. Neurol. 128, 1984–1995. doi:10.1093/brain/awh582

Davies, R.R., Kipps, C.M., Mitchell, J., Kril, J.J., Halliday, G.M., Hodges, J.R., (2006). Progression in frontotemporal dementia: identifying a benign behavioral variant by magnetic resonance imaging. Arch. Neurol. 63, 1627–1631. doi:10.1001/archneur.63.11.1627

DeJesus-Hernandez, M., Mackenzie, I.R., Boeve, B.F., Boxer, A.L., Baker, M., Rutherford, N.J., Nicholson, A.M., Finch, N.A., Flynn, H., Adamson, J., Kouri, N., Wojtas, A., Sengdy, P., Hsiung, G.-Y.R., Karydas, A., Seeley, W.W., Josephs, K.A., Coppola, G., Geschwind, D.H., Wszolek, Z.K., Feldman, H., Knopman, D.S., Petersen, R.C., Miller, B.L., Dickson, D.W., Boylan, K.B., Graff-Radford, N.R., Rademakers, R., (2011). Expanded GGGGCC hexanucleotide repeat in noncoding region of C9ORF72 causes chromosome 9p-linked FTD and ALS. Neuron 72, 245–256. doi:10.1016/j.neuron.2011.09.011

De Reuck, J.L., Deramecourt, V., Auger, F., Durieux, N., Cordonnier, C., Devos, D., Defebvre, L., Moreau, C., Caparros-Lefebvre, D., Leys, D., Maurage, C.A., Pasquier, F., Bordet, R., (2014). Iron deposits in post-mortem brains of patients with neurodegenerative and cerebrovascular diseases: a semi-quantitative 7.0 T magnetic resonance imaging study. Eur. J. Neurol. 21, 1026–1031. doi:10.1111/ene.12432

Diehl, J., Grimmer, T., Drzezga, A., Riemenschneider, M., Förstl, H., Kurz, A., (2004). Cerebral metabolic patterns at early stages of frontotemporal dementia and semantic dementia. A PET study. Neurobiol. Aging 25, 1051–1056. doi:10.1016/j.neurobiolaging.2003.10.007

Duara, R., Barker, W., Luis, C.A., (1999). Frontotemporal dementia and Alzheimer's disease: differential diagnosis. Dement. Geriatr. Cogn. Disord. 10 Suppl 1, 37–42. doi:51210

Du, A.-T., Schuff, N., Kramer, J.H., Rosen, H.J., Gorno-Tempini, M.L., Rankin, K., Miller, B.L., Weiner, M.W., (2007). Different regional patterns of cortical thinning in Alzheimer's disease and frontotemporal dementia. Brain J. Neurol. 130, 1159–1166. doi:10.1093/brain/awm016

Einstein A. Investigations on the Theory of the Brownian Movement. Dover Publications, Inc; 1956. p. 17

Ehmann, W.D., Alauddin, M., Hossain, T.I., Markesbery, W.R., (1984). Brain trace elements in Pick's disease. Ann. Neurol. 15, 102–104. doi:10.1002/ana.410150119

Eslinger, P.J., Moore, P., Antani, S., Anderson, C., Grossman, M., (2012). Apathy in frontotemporal dementia: behavioral and neuroimaging correlates. Behav. Neurol. 25, 127–136. doi:10.3233/BEN-2011-0351

Filley, C.M., Cullum, C.M., (1993). Early detection of fronto-temporal degeneration by clinical evaluation. Arch. Clin. Neuropsychol. 8, 359–367. doi:10.1093/arclin/8.4.359

Floyd, R.A., (1999). Antioxidants, oxidative stress, and degenerative neurological disorders. Proc. Soc. Exp. Biol. Med. Soc. Exp. Biol. Med. N. Y. N 222, 236–245.

Folstein, M.F., Folstein, S.E., McHugh, P.R., (1975). "Mini-mental state". A practical method for grading the cognitive state of patients for the clinician. J. Psychiatr. Res. 12, 189–198.

Friston, K.J., Frith, C.D., Liddle, P.F., Frackowiak, R.S., (1993). Functional connectivity: the principal-component analysis of large (PET) data sets. J. Cereb. Blood Flow Metab. Off. J. Int. Soc. Cereb. Blood Flow Metab. 13, 5–14. doi:10.1038/jcbfm.1993.4

Galantucci, S., Tartaglia, M.C., Wilson, S.M., Henry, M.L., Filippi, M., Agosta, F., Dronkers, N.F., Henry, R.G., Ogar, J.M., Miller, B.L., Gorno-Tempini, M.L., (2011). White matter damage in primary progressive aphasias: a diffusion tensor tractography study. Brain J. Neurol. 134, 3011–3029. doi:10.1093/brain/awr099

Galimberti, D., Scarpini, E., (2012). Genetics of Frontotemporal Lobar Degeneration. Front. Neurol. 3. doi:10.3389/fneur.2012.00052

Gislason, T.B., Sjögren, M., Larsson, L., Skoog, I., (2003). The prevalence of frontal variant frontotemporal dementia and the frontal lobe syndrome in a population based sample of 85 year olds. J. Neurol. Neurosurg. Psychiatry 74, 867–871. doi:10.1136/jnnp.74.7.867

Goedert, M., Ghetti, B., Spillantini, M.G., (2012). Frontotemporal dementia: implications for understanding Alzheimer disease. Cold Spring Harb. Perspect. Med. 2, a006254. doi:10.1101/cshperspect.a006254

Goldman-Rakic, P.S., (1987). Development of Cortical Circuitry and Cognitive Function. Child Dev. 58, 601–622. doi:10.2307/1130201

Good, C.D., Johnsrude, I.S., Ashburner, J., Henson, R.N., Friston, K.J., Frackowiak, R.S., (2001). A voxel-based morphometric study of ageing in 465 normal adult human brains. NeuroImage 14, 21–36. doi:10.1006/nimg.2001.0786

Good, C.D., Scahill, R.I., Fox, N.C., Ashburner, J., Friston, K.J., Chan, D., Crum, W.R., Rossor, M.N., Frackowiak, R.S.J., (2002). Automatic differentiation of anatomical patterns in the human brain: validation with studies of degenerative dementias. NeuroImage 17, 29–46.

Gorno-Tempini, M.L., Brambati, S.M., Ginex, V., Ogar, J., Dronkers, N.F., Marcone, A., Perani, D., Garibotto, V., Cappa, S.F., Miller, B.L.,(2008). The logopenic/phonological variant of primary progressive aphasia. Neurology 71, 1227–1234. doi:10.1212/01.wnl.0000320506.79811.da

Gorno-Tempini, M.L., Dronkers, N.F., Rankin, K.P., Ogar, J.M., Phengrasamy, L., Rosen, H.J., Johnson, J.K., Weiner, M.W., Miller, B.L., (2004). Cognition and anatomy in three variants of primary progressive aphasia. Ann. Neurol. 55, 335–346. doi:10.1002/ana.10825

Gorno-Tempini, M.L., Hillis, A.E., Weintraub, S., Kertesz, A., Mendez, M., Cappa, S.F., Ogar, J.M., Rohrer, J.D., Black, S., Boeve, B.F., Manes, F., Dronkers, N.F., Vandenberghe, R., Rascovsky, K., Patterson, K., Miller, B.L., Knopman, D.S., Hodges, J.R., Mesulam, M.M., Grossman, M., (2011). Classification of primary progressive aphasia and its variants. Neurology 76, 1006–1014. doi:10.1212/WNL.0b013e31821103e6

Götz, M.E., Double, K., Gerlach, M., Youdim, M.B.H., Riederer, P., (2004). The relevance of iron in the pathogenesis of Parkinson's disease. Ann. N. Y. Acad. Sci. 1012, 193–208.

Gregory, C.A., Serra-Mestres, J., Hodges, J.R., (1999). Early diagnosis of the frontal variant of frontotemporal dementia: how sensitive are standard neuroimaging and neuropsychologic tests? Neuropsychiatry. Neuropsychol. Behav. Neurol. 12, 128–135.

Grossman, M., Eslinger, P.J., Troiani, V., Anderson, C., Avants, B., Gee, J.C., McMillan, C., Massimo, L., Khan, A., Antani, S., (2010). The role of ventral medial prefrontal cortex in social decisions: converging evidence from fMRI

and frontotemporal lobar degeneration. Neuropsychologia 48, 3505–3512. doi:10.1016/j.neuropsychologia.2010.07.036

Grossman, M., McMillan, C., Moore, P., Ding, L., Glosser, G., Work, M., Gee, J., (2004). What's in a name: voxel-based morphometric analyses of MRI and naming difficulty in Alzheimer's disease, frontotemporal dementia and corticobasal degeneration. Brain J. Neurol. 127, 628–649. doi:10.1093/brain/awh075

Gutteridge, J.M., (1992). Iron and oxygen radicals in brain. Ann. Neurol. 32 Suppl, S16–21.

Haacke, E.M., Ayaz, M., Khan, A., Manova, E.S., Krishnamurthy, B., Gollapalli, L., Ciulla, C., Kim, I., Petersen, F., Kirsch, W., (2007). Establishing a baseline phase behavior in magnetic resonance imaging to determine normal vs. abnormal iron content in the brain. J. Magn. Reson. Imaging JMRI 26, 256–264. doi:10.1002/jmri.22987

Haacke, E.M., Cheng, N.Y.C., House, M.J., Liu, Q., Neelavalli, J., Ogg, R.J., Khan, A., Ayaz, M., Kirsch, W., Obenaus, A., (2005). Imaging iron stores in the brain using magnetic resonance imaging. Magn. Reson. Imaging 23, 1–25. doi:10.1016/j.mri.2004.10.001

Haacke, E.M., Makki, M., Ge, Y., Maheshwari, M., Sehgal, V., Hu, J., Selvan, M., Wu, Z., Latif, Z., Xuan, Y., Khan, O., Garbern, J., Grossman, R.I., (2009a). Characterizing iron deposition in multiple sclerosis lesions using susceptibility weighted imaging. J. Magn. Reson. Imaging JMRI 29, 537–544. doi:10.1002/jmri.21676

Haacke, E.M., Mittal, S., Wu, Z., Neelavalli, J., Cheng, Y.-C.N., (2009b). Susceptibility-Weighted Imaging: Technical Aspects and Clinical Applications, Part 1. Am. J. Neuroradiol. 30, 19–30. doi:10.3174/ajnr.A1400

Haacke, E.M., Xu, Y., Cheng, Y.-C.N., Reichenbach, J.R., (2004). Susceptibility weighted imaging (SWI). Magn. Reson. Med. 52, 612–618. doi:10.1002/mrm.20198

Halabi, C., Halabi, A., Dean, D.L., Wang, P.-N., Boxer, A.L., Trojanowski, J.Q., DeArmond, S.J., Miller, B.L., Kramer, J.H., Seeley, W.W., (2013). Patterns

of striatal degeneration in frontotemporal dementia. Alzheimer Dis. Assoc. Disord. 27, 74–83. doi:10.1097/WAD.0b013e31824a7df4

Hallgren, B., Sourander, P., (1958). The effect of age on the non-haemin iron in the human brain. J. Neurochem. 3, 41–51.

Hanyu, H., Asano, T., Sakurai, H., Imon, Y., Iwamoto, T., Takasaki, M., Shindo, H., Abe, K., (1999). Diffusion-weighted and magnetization transfer imaging of the corpus callosum in Alzheimer's disease. J. Neurol. Sci. 167, 37–44.

Harder, S.L., Hopp, K.M., Ward, H., Neglio, H., Gitlin, J., Kido, D., (2008). Mineralization of the deep gray matter with age: a retrospective review with susceptibility-weighted MR imaging. AJNR Am. J. Neuroradiol. 29, 176–183. doi:10.3174/ajnr.A0770

Harvey, R.J., Skelton-Robinson, M., Rossor, M.N., (2003). The prevalence and causes of dementia in people under the age of 65 years. J. Neurol. Neurosurg. Psychiatry 74, 1206–1209.

Hodges, J.R., Davies, R., Xuereb, J., Kril, J., Halliday, G., (2003). Survival in frontotemporal dementia. Neurology 61, 349–354.

Hodges, J.R., Patterson, K., (2007). Semantic dementia: a unique clinicopathological syndrome. Lancet Neurol. 6, 1004–1014. doi:10.1016/S1474-4422(07)70266-1

Hodges, J.R., Patterson, K., (1996). Nonfluent progressive aphasia and semantic dementia: a comparative neuropsychological study. J. Int. Neuropsychol. Soc. JINS 2, 511–524.

Hodges, J.R., Patterson, K., Oxbury, S., Funnell, E., (1992). Semantic dementia. Progressive fluent aphasia with temporal lobe atrophy. Brain J. Neurol. 115 (Pt 6), 1783–1806.

Hodges, J.R., Patterson, K., Ward, R., Garrard, P., Bak, T., Perry, R., Gregory, C., (1999). The differentiation of semantic dementia and frontal lobe dementia (temporal and frontal variants of frontotemporal dementia) from early Alzheimer's disease: a comparative neuropsychological study. Neuropsychology 13, 31–40.

Hokoishi, K., Ikeda, M., Maki, N., Nebu, A., Komori, K., Tanabe, H., (1999). [Two cases of fronto-temporal dementia without remarkable lobar atrophy]. Nō Shinkei Brain Nerve 51, 641–645.

Hornberger, M., Geng, J., Hodges, J.R., (2011). Convergent grey and white matter evidence of orbitofrontal cortex changes related to disinhibition in behavioural variant frontotemporal dementia. Brain J. Neurol. 134, 2502–2512. doi:10.1093/brain/awr173

Hughes, C.P., Berg, L., Danziger, W.L., Coben, L.A., Martin, R.L., (1982). A new clinical scale for the staging of dementia. Br. J. Psychiatry J. Ment. Sci. 140, 566–572.

Hutton, M., Lendon, C.L., Rizzu, P., Baker, M., Froelich, S., Houlden, H., Pickering-Brown, S., Chakraverty, S., Isaacs, A., Grover, A., Hackett, J., Adamson, J., Lincoln, S., Dickson, D., Davies, P., Petersen, R.C., Stevens, M., de Graaff, E., Wauters, E., van Baren, J., Hillebrand, M., Joosse, M., Kwon, J.M., Nowotny, P., Che, L.K., Norton, J., Morris, J.C., Reed, L.A., Trojanowski, J., Basun, H., Lannfelt, L., Neystat, M., Fahn, S., Dark, F., Tannenberg, T., Dodd, P.R., Hayward, N., Kwok, J.B., Schofield, P.R., Andreadis, A., Snowden, J., Craufurd, D., Neary, D., Owen, F., Oostra, B.A., Hardy, J., Goate, A., van Swieten, J., Mann, D., Lynch, T., Heutink, P., (1998). Association of missense and 5'-splice-site mutations in tau with the inherited dementia FTDP-17. Nature 393, 702–705. doi:10.1038/31508

Ioannidis, P., Konstantinopoulou, E., Maiovis, P., Karacostas, D., 2012. The frontotemporal dementias in a tertiary referral center: classification and demographic characteristics in a series of 232 cases. J. Neurol. Sci. 318, 171–173. doi:10.1016/j.jns.2012.04.002

Ibañez, A., Manes, F., (2012). Contextual social cognition and the behavioral variant of frontotemporal dementia. Neurology 78, 1354–1362. doi:10.1212/WNL.0b013e3182518375

Ikeda, M., Ishikawa, T., Tanabe, H., (2004). Epidemiology of frontotemporal lobar degeneration. Dement. Geriatr. Cogn. Disord. 17, 265–268. doi:10.1159/000077151

Irwin, D.J., McMillan, C.T., Brettschneider, J., Libon, D.J., Powers, J., Rascovsky, K., Toledo, J.B., Boller, A., Bekisz, J., Chandrasekaran, K., Wood, E.M., Shaw, L.M., Woo, J.H., Cook, P.A., Wolk, D.A., Arnold, S.E., Van Deerlin, V.M., McCluskey, L.F., Elman, L., Lee, V.M.-Y., Trojanowski, J.Q., Grossman, M., (2013). Cognitive decline and reduced survival in C9orf72 expansion frontotemporal degeneration and amyotrophic lateral sclerosis. J. Neurol. Neurosurg. Psychiatry 84, 163–169. doi:10.1136/jnnp-2012-303507

Ishii, K., Sakamoto, S., Sasaki, M., Kitagaki, H., Yamaji, S., Hashimoto, M., Imamura, T., Shimomura, T., Hirono, N., Mori, E., (1998). Cerebral glucose metabolism in patients with frontotemporal dementia. J. Nucl. Med. Off. Publ. Soc. Nucl. Med. 39, 1875–1878.

Jenkinson, M., Beckmann, C.F., Behrens, T.E.J., Woolrich, M.W., Smith, S.M., (2012).FSL.NeuroImage 62, 782–790. doi:10.1016/j.neuroimage.2011.09.015

Jensen, J.H., Szulc, K., Hu, C., Ramani, A., Lu, H., Xuan, L., Falangola, M.F., Chandra, R., Knopp, E.A., Schenck, J., Zimmerman, E.A., Helpren, J.A., (2009). Magnetic Field Correlation as a Measure of Iron-Generated Magnetic Field Inhomogeneities in the Brain. Magn. Reson. Med. Off. J. Soc. Magn. Reson. Med. Soc. Magn. Reson. Med. 61, 481–485. doi:10.1002/mrm.21823

Josephs, K.A., (2008). Frontotemporal dementia and related disorders: deciphering the enigma. Ann. Neurol. 64, 4–14. doi:10.1002/ana.21426

Josephs, K.A., Duffy, J.R., Strand, E.A., Whitwell, J.L., Layton, K.F., Parisi, J.E., Hauser, M.F., Witte, R.J., Boeve, B.F., Knopman, D.S., Dickson, D.W., Jack, C.R., Petersen, R.C., 2006. Clinicopathologic and Imaging Correlates of Progressive Aphasia and Apraxia of Speech. Brain J. Neurol. 129, 1385–1398. doi:10.1093/brain/awl078

Kable, J.W., Glimcher, P.W., (2007). The neural correlates of subjective value during intertemporal choice. Nat. Neurosci. 10, 1625–1633. doi:10.1038/nn2007

Kalkonde, Y.V., Jawaid, A., Qureshi, S.U., Shirani, P., Wheaton, M., Pinto-Patarroyo, G.P., Schulz, P.E., (2012). Medical and environmental risk factors associated with frontotemporal dementia: a case-control study in a veteran

population. Alzheimers Dement. J. Alzheimers Assoc. 8, 204–210. doi:10.1016/j.jalz.2011.03.011

Kamminga, J., Kumfor, F., Burrell, J.R., Piguet, O., Hodges, J.R., Irish, M., (2015). Differentiating between right-lateralised semantic dementia and behavioural-variant frontotemporal dementia: an examination of clinical characteristics and emotion processing. J. Neurol. Neurosurg. Psychiatry 86, 1082–1088. doi:10.1136/jnnp-2014-309120

Kertesz, A., Blair, M., McMonagle, P., Munoz, D.G., (2007). The diagnosis and course of frontotemporal dementia. Alzheimer Dis. Assoc. Disord. 21, 155–163. doi:10.1097/WAD.0b013e31806547eb

Kertesz, A., Davidson, W., Fox, H., (1997). Frontal behavioral inventory: diagnostic criteria for frontal lobe dementia. Can. J. Neurol. Sci. J. Can. Sci. Neurol. 24, 29–36.

Kertesz, A., Davidson, W., McCabe, P., Munoz, D., (2003). Behavioral quantitation is more sensitive than cognitive testing in frontotemporal dementia. Alzheimer Dis. Assoc. Disord. 17, 223–229.

Kertesz, A., Munoz, D.G., 2002. Frontotemporal dementia. Med. Clin. North Am. 86, 501–518, vi.

Kertesz, A., Nadkarni, N., Davidson, W., Thomas, A.W., (2000). The Frontal Behavioral Inventory in the differential diagnosis of frontotemporal dementia. J. Int. Neuropsychol. Soc. JINS 6, 460–468.

Kesavadas, C., Fiorelli, M., Gupta, A.K., Pantano, P., Bozzao, L., Kapilamoorthy, T.R., (2003). Diffusion weighted magnetic resonance imaging in acute ischemic stroke. Indian J. Radiol. Imaging 13, 433.

Kitagaki, H., Mori, E., Yamaji, S., Ishii, K., Hirono, N., Kobashi, S., Hata, Y., (1998). Frontotemporal dementia and Alzheimer disease: evaluation of cortical atrophy with automated hemispheric surface display generated with MR images. Radiology 208, 431–439. doi:10.1148/radiology.208.2.9680572

Knopman, D.S., Boeve, B.F., Parisi, J.E., Dickson, D.W., Smith, G.E., Ivnik, R.J., Josephs, K.A., Petersen, R.C., (2005). Antemortem diagnosis of frontotemporal lobar degeneration. Ann. Neurol. 57, 480–488. doi:10.1002/ana.20425

Krueger, C.E., Laluz, V., Rosen, H.J., Neuhaus, J.M., Miller, B.L., Kramer, J.H., (2011). Double dissociation in the anatomy of socioemotional disinhibition and executive functioning in dementia. Neuropsychology 25, 249–259. doi:10.1037/a0021681

Kumfor, F., Hutchings, R., Irish, M., Hodges, J.R., Rhodes, G., Palermo, R., Piguet, O., (2015). Do I know you? Examining face and object memory in frontotemporal dementia. Neuropsychologia 71, 101–111. doi:10.1016/j.neuropsychologia.2015.03.020

Kumfor, F., Irish, M., Hodges, J.R., Piguet, O., (2013). Discrete Neural Correlates for the Recognition of Negative Emotions: Insights from Frontotemporal Dementia. PLOS ONE 8, e67457. doi:10.1371/journal.pone.0067457

Lauterbur PC. Image formation by induced local interactions: examples of employing nuclear magnetic resonance. Nature (1973);242:190–1

Lansberg, M.G., Thijs, V.N., O'Brien, M.W., Ali, J.O., de Crespigny, A.J., Tong, D.C., Moseley, M.E., Albers, G.W., (2001). Evolution of apparent diffusion coefficient, diffusion-weighted, and T2-weighted signal intensity of acute stroke. AJNR Am. J. Neuroradiol. 22, 637–644.

Le Bihan, D., Mangin, J.F., Poupon, C., Clark, C.A., Pappata, S., Molko, N., Chabriat, H., (2001). Diffusion tensor imaging: concepts and applications. J. Magn. Reson. Imaging JMRI 13, 534–546.

Leh, S.E., Ptito, A., Chakravarty, M.M., Strafella, A.P., (2007). Fronto-striatal connections in the human brain: a probabilistic diffusion tractography study. Neurosci. Lett. 419, 113–118. doi:10.1016/j.neulet.2007.04.049

Levy, R., Dubois, B., (2006). Apathy and the Functional Anatomy of the Prefrontal Cortex–Basal Ganglia Circuits. Cereb. Cortex 16, 916–928. doi:10.1093/cercor/bhj043

Looi, J.C.L., Walterfang, M., Velakoulis, D., Macfarlane, M.D., Svensson, L.A., Wahlund, L.-O., (2012). Frontotemporal dementia as a frontostriatal disorder: neostriatal morphology as a biomarker and structural basis for an endophenotype. Aust. N. Z. J. Psychiatry 46, 422–434. doi:10.1177/0004867411432076

Macfarlane, M.D., Jakabek, D., Walterfang, M., Vestberg, S., Velakoulis, D., Wilkes, F.A., Nilsson, C., Westen, D. van, Looi, J.C.L., Santillo, A.F., (2015). Striatal Atrophy in the Behavioural Variant of Frontotemporal Dementia: Correlation with Diagnosis, Negative Symptoms and Disease Severity. PLOS ONE 10, e0129692. doi:10.1371/journal.pone.0129692

Mackenzie, I.R.A., Foti, D., Woulfe, J., Hurwitz, T.A., (2008). Atypical frontotemporal lobar degeneration with ubiquitin-positive, TDP-43-negative neuronal inclusions. Brain J. Neurol. 131, 1282–1293. doi:10.1093/brain/awn061

Mackenzie, I.R., Rademakers, R., Neumann, M., (2010). TDP-43 and FUS in amyotrophic lateral sclerosis and frontotemporal dementia. Lancet Neurol. 9, 995–1007. doi:10.1016/S1474-4422(10)70195-2

Mahoney, C.J., Beck, J., Rohrer, J.D., Lashley, T., Mok, K., Shakespeare, T., Yeatman, T., Warrington, E.K., Schott, J.M., Fox, N.C., Rossor, M.N., Hardy, J., Collinge, J., Revesz, T., Mead, S., Warren, J.D., (2012). Frontotemporal dementia with the C9ORF72 hexanucleotide repeat expansion: clinical, neuroanatomical and neuropathological features. Brain 135, 736–750. doi:10.1093/brain/awr361

Mahoney, C.J., Malone, I.B., Ridgway, G.R., Buckley, A.H., Downey, L.E., Golden, H.L., Ryan, N.S., Ourselin, S., Schott, J.M., Rossor, M.N., Fox, N.C., Warren, J.D., (2013). White matter tract signatures of the progressive aphasias. Neurobiol. Aging 34, 1687–1699. doi:10.1016/j.neurobiolaging.2012.12.002

Malloy, P., Tremont, G., Grace, J., Frakey, L., (2007). The Frontal Systems Behavior Scale discriminates frontotemporal dementia from Alzheimer's disease. Alzheimers Dement. J. Alzheimers Assoc. 3, 200–203. doi:10.1016/j.jalz.2007.04.374

Mann, D.M., South, P.W., Snowden, J.S., Neary, D., (1993). Dementia of frontal lobe type: neuropathology and immunohistochemistry. J. Neurol. Neurosurg. Psychiatry 56, 605–614.

Mansfield, P., (1977). Multi-planar image formation using NMR spin echoes. J. Phys. C Solid State Phys. 10, L55. doi:10.1088/0022-3719/10/3/004

Marczinski, C.A., Davidson, W., Kertesz, A., (2004). A longitudinal study of behavior in frontotemporal dementia and primary progressive aphasia. Cogn. Behav. Neurol. Off. J. Soc. Behav. Cogn. Neurol. 17, 185–190.

Massimo, L., Powers, C., Moore, P., Vesely, L., Avants, B., Gee, J., Libon, D.J., Grossman, M., (2009). Neuroanatomy of apathy and disinhibition in frontotemporal lobar degeneration. Dement. Geriatr. Cogn. Disord. 27, 96–104. doi:10.1159/000194658

Massimo, L., Powers, J.P., Evans, L.K., McMillan, C.T., Rascovsky, K., Eslinger, P., Ersek, M., Irwin, D.J., Grossman, M., (2015). Apathy in Frontotemporal Degeneration: Neuroanatomical Evidence of Impaired Goal-directed Behavior. Front. Hum. Neurosci. 9. doi:10.3389/fnhum.2015.00611

Mathuranath, P., George, A., (2005). Primary progressive aphasia: A comparative study of progressive nonfluent aphasia and semantic dementia. Neurol. India 53, 162. doi:10.4103/0028-3886.16398

Mathuranath, P.S., Hodges, J.R., Mathew, R., Cherian, P.J., George, A., Bak, T.H., (2004). Adaptation of the ACE for a Malayalam speaking population in southern India. Int. J. Geriatr. Psychiatry 19, 1188–1194. doi:10.1002/gps.1239

Matsuo, K., Mizuno, T., Yamada, K., Akazawa, K., Kasai, T., Kondo, M., Mori, S., Nishimura, T., Nakagawa, M., (2008). Cerebral white matter damage in frontotemporal dementia assessed by diffusion tensor tractography. Neuroradiology 50, 605–611. doi:10.1007/s00234-008-0379-5

Mega, M.S., Cohenour, R.C., (1997). Akinetic mutism: disconnection of frontal-subcortical circuits. Neuropsychiatry. Neuropsychol. Behav. Neurol. 10, 254–259.

Mendez, M.F., Shapira, J.S., McMurtray, A., Licht, E., Miller, B.L., (2007). Accuracy of the clinical evaluation for frontotemporal dementia. Arch. Neurol. 64, 830–835. doi:10.1001/archneur.64.6.830

Mendez, M.F., Shapira, J.S., Woods, R.J., Licht, E.A., Saul, R.E., (2008). Psychotic symptoms in frontotemporal dementia: prevalence and review. Dement. Geriatr. Cogn. Disord. 25, 206–211. doi:10.1159/000113418

Mesulam, M.M., 2001. Primary progressive aphasia. Ann. Neurol. 49, 425–432.

Mesulam, M.-M., (2003). Primary Progressive Aphasia — A Language-Based Dementia. N. Engl. J. Med. 349, 1535–1542. doi:10.1056/NEJMra022435

Mesulam, M.M., 1982. Slowly progressive aphasia without generalized dementia. Ann. Neurol. 11, 592–598. doi:10.1002/ana.410110607

Mickanin, J., Grossman, M., Onishi, K., Auriacombe, S., Clark, C., (1994). Verbal and nonverbal fluency in patients with probable Alzheimer's disease. Neuropsychology 8, 385–394. doi:10.1037/0894-4105.8.3.385

Miller, B.L., Gearhart, R., (1999). Neuroimaging in the diagnosis of frontotemporal dementia. Dement. Geriatr. Cogn. Disord. 10 Suppl 1, 71–74. doi:51217

Miller, E.K., Cohen, J.D., (2001). An integrative theory of prefrontal cortex function. Annu. Rev. Neurosci. 24, 167–202. doi:10.1146/annurev.neuro.24.1.167

Mioshi, E., Hsieh, S., Savage, S., Hornberger, M., Hodges, J.R., (2010). Clinical staging and disease progression in frontotemporal dementia. Neurology 74, 1591–1597. doi:10.1212/WNL.0b013e3181e04070

Mitchell, R.L.C., Crow, T.J., (2005). Right hemisphere language functions and schizophrenia: the forgotten hemisphere? Brain J. Neurol. 128, 963–978. doi:10.1093/brain/awh466

Mori, S., Crain, B.J., Chacko, V.P., Van Zijl, P.C.M., (1999). Three-dimensional tracking of axonal projections in the brain by magnetic resonance imaging. Ann. Neurol. 45, 265–269. doi:10.1002/1531-8249(199902)45:2<265::AID-ANA21>3.0.CO;2-3

Moseley, M.E., Cohen, Y., Kucharczyk, J., Mintorovitch, J., Asgari, H.S., Wendland, M.F., Tsuruda, J., Norman, D., (1990). Diffusion-weighted MR imaging of anisotropic water diffusion in cat central nervous system. Radiology 176, 439–445. doi:10.1148/radiology.176.2.2367658

Mulert, C., Gallinat, J., Dorn, H., Herrmann, W.M., Winterer, G., (2003). The relationship between reaction time, error rate and anterior cingulate cortex activity. Int. J. Psychophysiol. Off. J. Int. Organ. Psychophysiol. 47, 175–183.

Mummery, C.J., Patterson, K., Price, C.J., Ashburner, J., Frackowiak, R.S., Hodges, J.R., (2000). A voxel-based morphometry study of semantic dementia:

relationship between temporal lobe atrophy and semantic memory. Ann. Neurol. 47, 36–45.

Neary, D., Snowden, J.S., Gustafson, L., Passant, U., Stuss, D., Black, S., Freedman, M., Kertesz, A., Robert, P.H., Albert, M., Boone, K., Miller, B.L., Cummings, J., Benson, D.F., (1998). Frontotemporal lobar degeneration: a consensus on clinical diagnostic criteria. Neurology 51, 1546–1554.

Neumann, M., Kwong, L.K., Truax, A.C., Vanmassenhove, B., Kretzschmar, H.A., Van Deerlin, V.M., Clark, C.M., Grossman, M., Miller, B.L., Trojanowski, J.Q., Lee, V.M.-Y., (2007). TDP-43-positive white matter pathology in frontotemporal lobar degeneration with ubiquitin-positive inclusions. J. Neuropathol.Exp.Neurol.66,177–183. doi:10.1097/01.jnen.0000248554.45456.58

Neumann, M., Rademakers, R., Roeber, S., Baker, M., Kretzschmar, H.A., Mackenzie, I.R.A., (2009). A new subtype of frontotemporal lobar degeneration with FUS pathology. Brain J. Neurol. 132, 2922–2931. doi:10.1093/brain/awp214

Nguyen, T., Bertoux, M., O'Callaghan, C., Ahmed, S., Hodges, J.R., Hornberger, M., (2013). Grey and white matter brain network changes in frontotemporal dementia subtypes. Transl. Neurosci. 4, 410–418. doi:10.2478/s13380-013-0141-2

Nichols, T.E., Holmes, A.P., (2002). Nonparametric permutation tests for functional neuroimaging: a primer with examples. Hum. Brain Mapp. 15, 1–25.

Nioche, C., Cabanis, E.A., Habas, C.,(2009). Functional Connectivity of the Human Red Nucleus in the Brain Resting State at 3T. Am. J. Neuroradiol. 30, 396–403. doi:10.3174/ajnr.A1375

Olson, I.R., Plotzker, A., Ezzyat, Y., (2007). The Enigmatic temporal pole: a review of findings on social and emotional processing. Brain J. Neurol. 130, 1718–1731. doi:10.1093/brain/awm052

Onari, K., Spatz, H., (1926). Anatomische Beiträge zur Lehre von der Pickschen umschriebenen Großhirnrinden-Atrophie („Picksche Krankheit"), in: Heidelberg, S.-V.B. (Ed.), Arbeiten aus der Deutschen Forschungsanstalt für

Psychiatrie in München (Kaiser-Wilhelm-Institut). Springer Berlin Heidelberg, pp. 546–587.

Onyike, C.U., Diehl-Schmid, J., (2013). The Epidemiology of Frontotemporal Dementia. Int. Rev. Psychiatry Abingdon Engl. 25, 130–137. doi:10.3109/09540261.2013.776523

Pan, P.L., Song, W., Yang, J., Huang, R., Chen, K., Gong, Q.Y., Zhong, J.G., Shi, H.C., Shang, H.F., (2012). Gray matter atrophy in behavioral variant frontotemporal dementia: a meta-analysis of voxel-based morphometry studies. Dement. Geriatr. Cogn. Disord. 33, 141–148. doi:10.1159/000338176

Papagno, C., Miracapillo, C., Casarotti, A., Romero Lauro, L.J., Castellano, A., Falini, A., Casaceli, G., Fava, E., Bello, L., (2011). What is the role of the uncinate fasciculus? Surgical removal and proper name retrieval. Brain J. Neurol. 134, 405–414. doi:10.1093/brain/awq283

Parker, G.J.M., Haroon, H.A., Wheeler-Kingshott, C.A.M., (2003). A framework for a streamline-based probabilistic index of connectivity (PICo) using a structural interpretation of MRI diffusion measurements. J. Magn. Reson. Imaging JMRI 18, 242–254. doi:10.1002/jmri.10350

Péran, P., Hagberg, G., Luccichenti, G., Cherubini, A., Brainovich, V., Celsis, P., Caltagirone, C., Sabatini, U., (2007). Voxel-based analysis of R2* maps in the healthy human brain. J. Magn. Reson. Imaging JMRI 26, 1413–1420. doi:10.1002/jmri.21204

Pereira, J.M.S., Williams, G.B., Acosta-Cabronero, J., Pengas, G., Spillantini, M.G., Xuereb, J.H., Hodges, J.R., Nestor, P.J., (2009). Atrophy patterns in histologic vs clinical groupings of frontotemporal lobar degeneration. Neurology 72, 1653–1660. doi:10.1212/WNL.0b013e3181a55fa2

Perry, R.J., Hodges, J.R., (2000). Differentiating frontal and temporal variant frontotemporal dementia from Alzheimer's disease. Neurology 54, 2277–2284.

Peters, F., Perani, D., Herholz, K., Holthoff, V., Beuthien-Baumann, B., Sorbi, S., Pupi, A., Degueldre, C., Lemaire, C., Collette, F., Salmon, E., (2006). Orbitofrontal dysfunction related to both apathy and disinhibition in

frontotemporal dementia. Dement. Geriatr. Cogn. Disord. 21, 373–379. doi:10.1159/000091898

Pick, A. (1892). Über die Beziehungen der senilen Hirnatrophie zur Aphasie. *Prager medicinische Wochenschrift, 17*: 165-167.

Piguet, O., Brooks, W.S., Halliday, G.M., Schofield, P.R., Stanford, P.M., Kwok, J.B.J., Spillantini, M.-G., Yancopoulou, D., Nestor, P.J., Broe, G.A., Hodges, J.R., 2004. Similar early clinical presentations in familial and non-familial frontotemporal dementia. J. Neurol. Neurosurg. Psychiatry 75, 1743–1745. doi:10.1136/jnnp.2003.031948

Piguet, O., Hornberger, M., Mioshi, E., Hodges, J.R., 2011. Behavioural-variant frontotemporal dementia: diagnosis, clinical staging, and management. Lancet Neurol. 10, 162–172. doi:10.1016/S1474-4422(10)70299-4

Pikkarainen, M., Hartikainen, P., Alafuzoff, I., (2008). Neuropathologic features of frontotemporal lobar degeneration with ubiquitin-positive inclusions visualized with ubiquitin-binding protein p62 immunohistochemistry. J. Neuropathol. Exp. Neurol. 67, 280–298. doi:10.1097/NEN.0b013e31816a1da2

Powers, J.P., Massimo, L., McMillan, C.T., Yushkevich, P.A., Zhang, H., Gee, J.C., Grossman, M., (2014). White Matter Disease Contributes to Apathy and Disinhibition in Behavioral Variant Frontotemporal Dementia. Cogn. Behav. Neurol. Off. J. Soc. Behav. Cogn. Neurol. 27, 206–214. doi:10.1097/WNN.0000000000000044

Premi, E., Padovani, A., Borroni, B., (2012). Frontotemporal Lobar Degeneration. Adv. Exp. Med. Biol. 724, 114–127. doi:10.1007/978-1-4614-0653-2_9

Rabinovici, G.D., Miller, B.L., (2010). Frontotemporal lobar degeneration: epidemiology, pathophysiology, diagnosis and management. CNS Drugs 24, 375–398. doi:10.2165/11533100-000000000-00000

Rascovsky, K., Hodges, J.R., Kipps, C.M., Johnson, J.K., Seeley, W.W., Mendez, M.F., Knopman, D., Kertesz, A., Mesulam, M., Salmon, D.P., Galasko, D., Chow, T.W., Decarli, C., Hillis, A., Josephs, K., Kramer, J.H., Weintraub, S., Grossman, M., Gorno-Tempini, M.-L., Miller, B.M., (2007). Diagnostic

criteria for the behavioral variant of frontotemporal dementia (bvFTD): current limitations and future directions. Alzheimer Dis. Assoc. Disord. 21, S14–18. doi:10.1097/WAD.0b013e31815c3445

Rascovsky, K., Hodges, J.R., Knopman, D., Mendez, M.F., Kramer, J.H., Neuhaus, J., van Swieten, J.C., Seelaar, H., Dopper, E.G.P., Onyike, C.U., Hillis, A.E., Josephs, K.A., Boeve, B.F., Kertesz, A., Seeley, W.W., Rankin, K.P., Johnson, J.K., Gorno-Tempini, M.-L., Rosen, H., Prioleau-Latham, C.E., Lee, A., Kipps, C.M., Lillo, P., Piguet, O., Rohrer, J.D., Rossor, M.N., Warren, J.D., Fox, N.C., Galasko, D., Salmon, D.P., Black, S.E., Mesulam, M., Weintraub, S., Dickerson, B.C., Diehl-Schmid, J., Pasquier, F., Deramecourt, V., Lebert, F., Pijnenburg, Y., Chow, T.W., Manes, F., Grafman, J., Cappa, S.F., Freedman, M., Grossman, M., Miller, B.L., (2011). Sensitivity of revised diagnostic criteria for the behavioural variant of frontotemporal dementia. Brain 134, 2456–2477. doi:10.1093/brain/awr179

Ratnavalli, E., Brayne, C., Dawson, K., Hodges, J.R., (2002). The prevalence of frontotemporal dementia. Neurology 58, 1615–1621.

Raven, E.P., Lu, P.H., Tishler, T.A., Heydari, P., Bartzokis, G., 2013. Increased iron levels and decreased tissue integrity in hippocampus of Alzheimer's disease detected in vivo with magnetic resonance imaging. J. Alzheimers Dis. JAD 37, 127–136. doi:10.3233/JAD-130209

Reichenbach, J.R., Venkatesan, R., Schillinger, D.J., Kido, D.K., Haacke, E.M., (1997). Small vessels in the human brain: MR venography with deoxyhemoglobin as an intrinsic contrast agent. Radiology 204, 272–277. doi:10.1148/radiology.204.1.9205259

Reijnders, J.S.A.M., Scholtissen, B., Weber, W.E.J., Aalten, P., Verhey, F.R.J., Leentjens, A.F.G., (2010). Neuroanatomical correlates of apathy in Parkinson's disease: A magnetic resonance imaging study using voxel-based morphometry. Mov. Disord. 25, 2318–2325. doi:10.1002/mds.23268

Reitan, R.M., (1958). Validity of the Trail Making Test as an Indicator of Organic Brain Damage. Percept. Mot. Skills 8, 271–276. doi:10.2466/pms.1958.8.3.271

Reichenbach, J.R., Venkatesan, R., Yablonskiy, D.A., Thompson, M.R., Lai, S., Haacke, E.M., 1997. Theory and application of static field inhomogeneity effects in gradient-echo imaging. J. Magn. Reson. Imaging JMRI 7, 266–279.

Renton, A.E., Majounie, E., Waite, A., Simón-Sánchez, J., Rollinson, S., Gibbs, J.R., Schymick, J.C., Laaksovirta, H., van Swieten, J.C., Myllykangas, L., Kalimo, H., Paetau, A., Abramzon, Y., Remes, A.M., Kaganovich, A., Scholz, S.W., Duckworth, J., Ding, J., Harmer, D.W., Hernandez, D.G., Johnson, J.O., Mok, K., Ryten, M., Trabzuni, D., Guerreiro, R.J., Orrell, R.W., Neal, J., Murray, A., Pearson, J., Jansen, I.E., Sondervan, D., Seelaar, H., Blake, D., Young, K., Halliwell, N., Callister, J.B., Toulson, G., Richardson, A., Gerhard, A., Snowden, J., Mann, D., Neary, D., Nalls, M.A., Peuralinna, T., Jansson, L., Isoviita, V.-M., Kaivorinne, A.-L., Hölttä-Vuori, M., Ikonen, E., Sulkava, R., Benatar, M., Wuu, J., Chiò, A., Restagno, G., Borghero, G., Sabatelli, M., ITALSGEN Consortium, Heckerman, D., Rogaeva, E., Zinman, L., Rothstein, J.D., Sendtner, M., Drepper, C., Eichler, E.E., Alkan, C., Abdullaev, Z., Pack, S.D., Dutra, A., Pak, E., Hardy, J., Singleton, A., Williams, N.M., Heutink, P., Pickering-Brown, S., Morris, H.R., Tienari, P.J., Traynor, B.J., (2011). A hexanucleotide repeat expansion in C9ORF72 is the cause of chromosome 9p21-linked ALS-FTD. Neuron 72, 257–268. doi:10.1016/j.neuron.2011.09.010

Roberson, E.D., Hesse, J.H., Rose, K.D., Slama, H., Johnson, J.K., Yaffe, K., Forman, M.S., Miller, C.A., Trojanowski, J.Q., Kramer, J.H., Miller, B.L., (2005). Frontotemporal dementia progresses to death faster than Alzheimer disease. Neurology 65, 719–725. doi:10.1212/01.wnl.0000173837.82820.9f

Rogalski, E., Cobia, D., Harrison, T.M., Wieneke, C., Thompson, C.K., Weintraub, S., Mesulam, M.-M., (2011). Anatomy of language impairments in primary progressive aphasia. J. Neurosci. Off. J. Soc. Neurosci. 31, 3344–3350. doi:10.1523/JNEUROSCI.5544-10.2011

Rohrer, J.D., Rosen, H.J., (2013). Neuroimaging in frontotemporal dementia. Int. Rev. Psychiatry Abingdon Engl. 25, 221–229. doi:10.3109/09540261.2013.778822

Rohrer, J.D., Warren, J.D., (2011). Phenotypic signatures of genetic frontotemporal dementia. Curr. Opin. Neurol. 24, 542–549. doi:10.1097/WCO.0b013e32834cd442

Rohrer, J.D., Warren, J.D., (2010). Phenomenology and anatomy of abnormal behaviours in primary progressive aphasia. J. Neurol. Sci. 293, 35–38. doi:10.1016/j.jns.2010.03.012

Rosen, H.J., Allison, S.C., Schauer, G.F., Gorno-Tempini, M.L., Weiner, M.W., Miller, B.L., (2005). Neuroanatomical correlates of behavioural disorders in dementia. Brain J. Neurol. 128, 2612–2625. doi:10.1093/brain/awh628

Rosen, H.J., Gorno-Tempini, M.L., Goldman, W.P., Perry, R.J., Schuff, N., Weiner, M., Feiwell, R., Kramer, J.H., Miller, B.L., (2002). Patterns of brain atrophy in frontotemporal dementia and semantic dementia. Neurology 58, 198–208.

Rossor, M.N., Fox, N.C., Mummery, C.J., Schott, J.M., Warren, J.D., (2010). The diagnosis of young-onset dementia. Lancet Neurol. 9, 793–806. doi:10.1016/S1474-4422(10)70159-9

Rosso, S.M., Donker Kaat, L., Baks, T., Joosse, M., de Koning, I., Pijnenburg, Y., de Jong, D., Dooijes, D., Kamphorst, W., Ravid, R., Niermeijer, M.F., Verheij, F., Kremer, H.P., Scheltens, P., van Duijn, C.M., Heutink, P., van Swieten, J.C., (2003). Frontotemporal dementia in The Netherlands: patient characteristics and prevalence estimates from a population-based study. Brain J. Neurol. 126, 2016–2022. doi:10.1093/brain/awg204

Sah, P., Faber, E.S.L., Lopez De Armentia, M., Power, J., (2003). The amygdaloid complex: anatomy and physiology. Physiol. Rev. 83, 803–834. doi:10.1152/physrev.00002.2003

Salmond, C.H., Ashburner, J., Vargha-Khadem, F., Connelly, A., Gadian, D.G., Friston, K.J., (2002). Distributional assumptions in voxel-based morphometry. NeuroImage 17, 1027–1030.

Santillo, A.F., Skoglund, L., Lindau, M., Eeg-Olofsson, K.E., Tovi, M., Engler, H., Brundin, R.-M., Ingvast, S., Lannfelt, L., Glaser, A., Kilander, L., (2009). Frontotemporal dementia-amyotrophic lateral sclerosis complex is simulated by neurodegeneration with brain iron accumulation. Alzheimer Dis. Assoc. Disord. 23, 298–300. doi:10.1097/WAD.0b013e3181a2b76b

Schenck, J.F., Zimmerman, E.A., (2004). High-field magnetic resonance imaging of brain iron: birth of a biomarker? NMR Biomed. 17, 433–445. doi:10.1002/nbm.922

Schneider, Dr., C., (1927). Über Picksche Krankheit. pp. 230–252. Eur. Neurol. 65, 230–252. doi:10.1159/000166080

Schofield, E., Kersaitis, C., Shepherd, C.E., Kril, J.J., Halliday, G.M., (2003). Severity of gliosis in Pick's disease and frontotemporal lobar degeneration: tau-positive glia differentiate these disorders. Brain J. Neurol. 126, 827–840.

Seelaar, H., Kamphorst, W., Rosso, S.M., Azmani, A., Masdjedi, R., de Koning, I., Maat-Kievit, J.A., Anar, B., Donker Kaat, L., Breedveld, G.J., Dooijes, D., Rozemuller, J.M., Bronner, I.F., Rizzu, P., van Swieten, J.C., (2008). Distinct genetic forms of frontotemporal dementia. Neurology 71, 1220–1226. doi:10.1212/01.wnl.0000319702.37497.72

Seelaar, H., Rohrer, J.D., Pijnenburg, Y.A.L., Fox, N.C., van Swieten, J.C., (2011). Clinical, genetic and pathological heterogeneity of frontotemporal dementia: a review. J. Neurol. Neurosurg. Psychiatry 82, 476–486. doi:10.1136/jnnp.2010.212225

Seeley, W.W., (2008). Selective functional, regional, and neuronal vulnerability in frontotemporal dementia. Curr. Opin. Neurol. 21, 701–707. doi:10.1097/WCO.0b013e3283168e2d

Seeley, W.W., Bauer, A.M., Miller, B.L., Gorno-Tempini, M.L., Kramer, J.H., Weiner, M., Rosen, H.J., (2005). The natural history of temporal variant frontotemporal dementia. Neurology 64, 1384–1390. doi:10.1212/01.WNL.0000158425.46019.5C

Shankar P Nandi, Atanu Biswas, Sandip Pal, Sagar Basu, Asit K Senapati, & Das, S. K. (2008). Clinical profile of young-onset dementia: A study from Eastern India. Neurology Asia, 13: 103-108.

Sheelakumari, R., Madhusoodanan, M., Radhakrishnan, A., Ranjith, G., Thomas, B., 2015. A Potential Biomarker in Amyotrophic Lateral Sclerosis: Can Assessment of Brain Iron Deposition with SWI and Corticospinal Tract Degeneration with DTI Help? Am. J. Neuroradiol. doi:10.3174/ajnr.A4524

Skibinski, G., Parkinson, N.J., Brown, J.M., Chakrabarti, L., Lloyd, S.L., Hummerich, H., Nielsen, J.E., Hodges, J.R., Spillantini, M.G., Thusgaard, T., Brandner, S., Brun, A., Rossor, M.N., Gade, A., Johannsen, P., Sørensen, S.A., Gydesen, S., Fisher, E.M.C., Collinge, J., (2005). Mutations in the endosomal ESCRTIII-complex subunit CHMP2B in frontotemporal dementia. Nat. Genet. 37, 806–808. doi:10.1038/ng1609

Smith, S.M., (2002). Fast robust automated brain extraction. Hum. Brain Mapp. 17, 143–155. doi:10.1002/hbm.10062

Smith, S.M., Jenkinson, M., Johansen-Berg, H., Rueckert, D., Nichols, T.E., Mackay, C.E., Watkins, K.E., Ciccarelli, O., Cader, M.Z., Matthews, P.M., Behrens, T.E.J., (2006). Tract-based spatial statistics: voxelwise analysis of multi-subject diffusion data. NeuroImage 31, 1487–1505. doi:10.1016/j.neuroimage.2006.02.024

Snowden, J., Neary, D., Mann, D., (2007). Frontotemporal lobar degeneration: clinical and pathological relationships. Acta Neuropathol. (Berl.) 114, 31–38. doi:10.1007/s00401-007-0236-3

Snowden, J.S., Bathgate, D., Varma, A., Blackshaw, A., Gibbons, Z.C., Neary, D., (2001). Distinct behavioural profiles in frontotemporal dementia and semantic dementia. J. Neurol. Neurosurg. Psychiatry 70, 323–332. doi:10.1136/jnnp.70.3.323

Stanton, B.R., Leigh, P.N., Howard, R.J., Barker, G.J., Brown, R.G., (2013). Behavioural and emotional symptoms of apathy are associated with distinct patterns of brain atrophy in neurodegenerative disorders. J. Neurol. 260, 2481–2490. doi:10.1007/s00415-013-6989-9

Stehling, M.K., Turner, R., Mansfield, P., (1991). Echo-planar imaging: magnetic resonance imaging in a fraction of a second. Science 254, 43–50.

Stout, J.C., Ready, R.E., Grace, J., Malloy, P.F., Paulsen, J.S., (2003). Factor Analysis of the Frontal Systems Behavior Scale (FrSBe). Assessment 10, 79–85. doi:10.1177/1073191102250339

Thomas, B., Somasundaram, S., Thamburaj, K., Kesavadas, C., Gupta, A.K., Bodhey, N.K., Kapilamoorthy, T.R., (2007). Clinical applications of

susceptibility weighted MR imaging of the brain – a pictorial review. Neuroradiology 50, 105–116. doi:10.1007/s00234-007-0316-z

Timmann, D., Konczak, J., Ilg, W., Donchin, O., Hermsdörfer, J., Gizewski, E.R., Schoch, B., (2009). Current advances in lesion-symptom mapping of the human cerebellum. Neuroscience 162, 836–851. doi:10.1016/j.neuroscience.2009.01.040

Tovar-Moll, F., Oliveira-Souza, R. de, Bramati, I.E., Zahn, R., Cavanagh, A., Tierney, M., Moll, J., Grafman, J., (2014). White Matter Tract Damage in the Behavioral Variant of Frontotemporal and Corticobasal Dementia Syndromes. PLOS ONE 9, e102656. doi:10.1371/journal.pone.0102656

Twieg, D.B., (1983). The k-trajectory formulation of the NMR imaging process with applications in analysis and synthesis of imaging methods. Med. Phys. 10, 610–621. doi:10.1118/1.595331

Tzourio-Mazoyer, N., Landeau, B., Papathanassiou, D., Crivello, F., Etard, O., Delcroix, N., Mazoyer, B., Joliot, M., (2002). Automated anatomical labeling of activations in SPM using a macroscopic anatomical parcellation of the MNI MRI single-subject brain. NeuroImage 15, 273–289. doi:10.1006/nimg.2001.0978

Velakoulis, D., Walterfang, M., Mocellin, R., Pantelis, C., McLean, C., (2009). Frontotemporal dementia presenting as schizophrenia-like psychosis in young people: clinicopathological series and review of cases. Br. J. Psychiatry J. Ment. Sci. 194, 298–305. doi:10.1192/bjp.bp.108.057034

Wakana, S., Caprihan, A., Panzenboeck, M.M., Fallon, J.H., Perry, M., Gollub, R.L., Hua, K., Zhang, J., Jiang, H., Dubey, P., Blitz, A., van Zijl, P., Mori, S., (2007). Reproducibility of quantitative tractography methods applied to cerebral white matter. NeuroImage 36, 630–644. doi:10.1016/j.neuroimage.2007.02.049

Wang, D., Zhu, D., Wei, X.-E., Li, Y.-H., Li, W.-B., (2013). Using susceptibility-weighted images to quantify iron deposition differences in amnestic mild cognitive impairment and Alzheimer's disease. Neurol. India 61, 26–34. doi:10.4103/0028-3886.107924

Warren, J.D., Rohrer, J.D., Rossor, M.N., 2013. Frontotemporal dementia. BMJ 347, f4827. doi:10.1136/bmj.f4827

Warrington, E.K., Shallice, T., (1984). Category specific semantic impairments. Brain J. Neurol. 107 (Pt 3), 829–854

Watts, G.D.J., Wymer, J., Kovach, M.J., Mehta, S.G., Mumm, S., Darvish, D., Pestronk, A., Whyte, M.P., Kimonis, V.E. ,(2004). Inclusion body myopathy associated with Paget disease of bone and frontotemporal dementia is caused by mutant valosin-containing protein. Nat. Genet. 36, 377–381. doi:10.1038/ng1332

Wechsler, D., (1981). WAIS-R: manual : Wechsler adult intelligence scale--revised. Harcourt Brace Jovanovich [for] Psychological Corp., New York, NY.

Weintraub S, Rubin NP, Mesulam M, (1990). Primary progressive aphasia: Longitudinal course, neuropsychological profile, and language features. Arch. Neurol. 47, 1329–1335. doi:10.1001/archneur.1990.00530120075013

Whitwell, J.L., Avula, R., Senjem, M.L., Kantarci, K., Weigand, S.D., Samikoglu, A., Edmonson, H.A., Vemuri, P., Knopman, D.S., Boeve, B.F., Petersen, R.C., Josephs, K.A., Jack, C.R., (2010). Gray and white matter water diffusion in the syndromic variants of frontotemporal dementia. Neurology 74, 1279–1287. doi:10.1212/WNL.0b013e3181d9edde

Whitwell, J.L., Jack, C.R., Parisi, J.E., Knopman, D.S., Boeve, B.F., Petersen, R.C., Dickson, D.W., Josephs, K.A., (2011). Imaging signatures of molecular pathology in behavioral variant frontotemporal dementia. J. Mol. Neurosci. MN 45, 372–378. doi:10.1007/s12031-011-9533-3

Whitwell, J.L., Josephs, K.A., (2012). Recent Advances in the Imaging of Frontotemporal Dementia. Curr. Neurol. Neurosci. Rep. 12, 715–723. doi:10.1007/s11910-012-0317-0

Whitwell, J.L., Przybelski, S.A., Weigand, S.D., Ivnik, R.J., Vemuri, P., Gunter, J.L., Senjem, M.L., Shiung, M.M., Boeve, B.F., Knopman, D.S., Parisi, J.E., Dickson, D.W., Petersen, R.C., Jack, C.R., Josephs, K.A., (2009). Distinct anatomical subtypes of the behavioural variant of frontotemporal dementia: a cluster analysis study. Brain J. Neurol. 132, 2932–2946. doi:10.1093/brain/awp232

Williams, G.B., Nestor, P.J., Hodges, J.R., (2005). Neural correlates of semantic and behavioural deficits in frontotemporal dementia. NeuroImage 24, 1042–1051. doi:10.1016/j.neuroimage.2004.10.023

Wilson, S.M., Galantucci, S., Tartaglia, M.C., Rising, K., Patterson, D.K., Henry, M.L., Ogar, J.M., DeLeon, J., Miller, B.L., Gorno-Tempini, M.L., (2011). Syntactic processing depends on dorsal language tracts. Neuron 72, 397–403. doi:10.1016/j.neuron.2011.09.014

Wilson, S.M., Ogar, J.M., Laluz, V., Growdon, M., Jang, J., Glenn, S., Miller, B.L., Weiner, M.W., Gorno-Tempini, M.L., (2009). Automated MRI-based classification of primary progressive aphasia variants. NeuroImage 47, 1558–1567. doi:10.1016/j.neuroimage.2009.05.085

World Alzheimer Report (2015), The Global Impact of Dementia: An analysis of prevalence, incidence, cost and trends - WorldAlzheimerReport2015.pdf, n.d.

Zamboni, G., Huey, E.D., Krueger, F., Nichelli, P.F., Grafman, J., (2008). Apathy and disinhibition in frontotemporal dementia: Insights into their neural correlates.Neurology 71, 736–742. doi:10.1212/01.wnl.0000324920.96835.95

Zecca, L., Youdim, M.B.H., Riederer, P., Connor, J.R., Crichton, R.R., (2004). Iron, brain ageing and neurodegenerative disorders. Nat. Rev. Neurosci. 5, 863–873. doi:10.1038/nrn1537

Zhang, Y., Schuff, N., Du, A.-T., Rosen, H.J., Kramer, J.H., Gorno-Tempini, M.L., Miller, B.L., Weiner, M.W., (2009). White matter damage in frontotemporal dementia and Alzheimer's disease measured by diffusion MRI. Brain J. Neurol. 132, 2579–2592. doi:10.1093/brain/awp071

Zigmond, A.S., Snaith, R.P., (1983). The hospital anxiety and depression scale. Acta Psychiatr. Scand. 67, 361–370.

APPENDIX I

Diagnostic criteria for fvFTD, SD and PNFA

Syndrome	fvFTD	PPA	
		SD	PNFA
Core criteria	Shows progressive deterioration of behaviorand/or cognition	Prominent feature of difficulty with language that cause the impaired daily living activities, and aphasia should be the most prominent deficit at symptom onset and for the initial phases of the disease	
Possible FTD/Clinical Diagnosis	At least three of the following features must be present A. Early behavioural disinhibition B. Early apathy or inertia C. Early loss of sympathy or empathy D. Early perseverative, stereotyped or compulsive/ritualistic behavior E. Hyperorality and dietary changes F. Neuropsychological profile: executive/generation deficits with relative sparing of memory and visuospatial functions	Both of following features must be present A. Impaired confrontation naming B. Impaired single-word comprehension At least 3 of the following must be present:ct knowledge A. Surface dyslexia or dysgraphia B. Spared repetition C. Spared speech Production	At least one of the following features must be present A. Agrammatism in Language production B. Effortful, halting Speech(apraxia of speech) At least 2 of the following must be present: A. Impaired comprehension of syntactically complex B. sentences C. Spared singleword comprehension D. Spared object knowledge
Probable **Supported Diagnosis**	Possible diagnosis of fvFTD, plus A and/imaging – B: A.Significant functional decline B. Frontal and/or anterior temporal atrophy	Clinical diagnosis of SD, plus A or B: A. Predominant anterior temporal lobe atrophy on MRI B. Predominant anterior temporal lobe hypoperfusion or hypometabolism on PET/SPECT	Clinical diagnosis of PNFA, plus A or B: A. Predominant atrophy on MRI left posterior frontoinsular B. Predominant left posterior frontoinsular hypoperfusion or hypometabolism on PET/SPECT

APPENDIX II

.List of Publications

- **Sheelakumari. R**, M. Madhusoodanan, A. Radhakrishnan, G. Ranjith, and B. Thomas. A Potential Biomarker in Amyotrophic Lateral Sclerosis: Can Assessment of Brain Iron Deposition with SWI and Corticospinal Tract Degeneration with DTI help?. AJNR Am J Neuroradiol. 2016 Feb; 37(2):252-8.
- **Sheelakumari. R**, C. Kesavadas, Lekha V.S, Sunitha Justus, P.Sankara Sarma, Ramshekhar Menon. Structural correlates of Mild Cognitive Impairment - A clinico-volumetric study. Neurology India, 2016, (Article in Press)
- **Sheela Kumari R,** C. Kesavadas, Tinu Varghese, Ruma Madhu Sreedharan, Bejoy Thomas, Joe Verghese, P.S. Mathuranath . Quantitative Measurement of Iron deposition in Frontotemporal Dementia by Susceptibility Weighted Imaging. Under Review in American Journal of Neuroradiology.
- **Sheela kumari R**, Venkateswaran Rajagopalan, Anuvitha C, Tinu Varghese, et al, Quantitative analysis of grey matter degeneration in FTD patients using fractal dimension analysis. Under Review in Brain Imaging and Behaviour.
- **Brief Communication**: P.M Aswathy, P.S. Jairani, **Sheela kumari R**, Joe Varghese, Srinivas Gopala, Priya Srinivas, P.S. Mathuranath. Progranulin mutation analysis: identification of one novel mutation in exon 12 associated with frontotemporal dementia. Neurobiology of Ageing 2016; 39: 218e1-218e3.
- Jija S. James, **Sheela Kumari R**, RM Sreedharan, B.Thomas, A. Radhakrishnan, C. Kesavadas. Analyzing functional, structural, and anatomical correlation of hemispheric language lateralization in healthy subjects using functional MRI, diffusion tensor imaging, and voxel-based morphometry. Neurol India. 2015 Jan-Feb;63(1):49-57

Review Article

- Tinu Varghese, **Sheela Kumari R**, Mathuranath.P.S. "A review of neuroimaging biomarkers of Alzheimer's disease". Neurology Asia 2013; 18(3): 239 – 248

Conference Proceedings

- **Sheela Kumari R**, Tinu Varghese, C.Kesavadas, Albertsingh N, Mathuranath.P.S. "Longitudinal Evalution of Structural changes in frontotemporal dementia Using Artificial Neural Networks". Paper published in Springer AISC, pp.169-172, 2014.
- **Sheela Kumari R**, Tinu Varghese, C.Kesavadas, Albertsingh N, Mathuranath.P.S."A Genetic algorithm Optimized Artificial Neural Networks for the segmentation of MR images in Frontotemporal Dementia". Paper published in Springer LNCS 8298, pp 268-276, 2013
- **Sheela Kumari R**, Tinu Varghese, Mathuranath.P.S, C.Kesavadas. "Segmentation of MR Brain Images Using FCM Technique in Frontotemporal Dementia". Paper published in IEEE digital explorer, pp 1-4, E-ISBN: 978-1-84919-797-7.